Time-series analysis to estimate aquifer parameters, recharge, and changes in the groundwater regime

Obergfell, Christophe

DOI
10.4233/uuid:40454512-e67c-41c5-963b-5862a1b94ac3

Publication date
2019

Document Version
Final published version

Citation (APA)
Obergfell, C. (2019). *Time-series analysis to estimate aquifer parameters, recharge, and changes in the groundwater regime.* [Dissertation (TU Delft), Delft University of Technology]. https://doi.org/10.4233/uuid:40454512-e67c-41c5-963b-5862a1b94ac3

Important note
To cite this publication, please use the final published version (if applicable).
Please check the document version above.

Time series analysis to estimate aquifer parameters, recharge, and changes in the groundwater regime

Time-series analysis to estimate aquifer parameters, recharge, and changes in the groundwater regime

Dissertation

for the purpose of obtaining the degree of doctor
at Delft University of Technology,
by the authority of the Rector Magnificus, prof. dr. ir. T.H.J.J. van der Hagen,
chair of the Board for Doctorates,
to be defended publicly on
Tuesday, 7 January 2020 at 12:30

by

Christophe Charles Augustin OBERGFELL,
Master of Science in Hydrology,
VU Amsterdam, the Netherlands,
born in Strasbourg, France.

This dissertation has been approved by the promotor.

Composition of the doctoral committee:
Rector Magnificus, chairperson
Prof. dr. ir. M. Bakker, Delft University of Technology, promotor

Independent members:
Prof. dr. ir. H.H.G. Savenije, Delft University of Technology
Prof. dr. ir. M.F.P. Bierkens, Utrecht University
Prof. dr. J.P.M. Witte, VU Amsterdam
Dr. M.O. Cuthbert, Cardiff University, United Kingdom
Dr. J.R. von Asmuth, Trefoil Hydrology
Prof. dr. ir. N.C. van de Giesen, Delft University of Technology, reserve member

Other member:
Dr. ir. C. Maas, Maas Geohydrologisch Advies

Dr. ir. C. Maas has contributed greatly to the preparation of this dissertation.

Keywords: time-series analysis, groundwater modeling, parameter estimation, response function, seasonal harmonic, groundwater regime

Printed by: Ipskamp printing

Front: 'A woman at a well' (In Dutch: 'Een vrouw bij een waterput'), oil on canvas, painted originally by Jacobus Johannes Lauwers in 1799, with permission of the Rijksmuseum, Amsterdam.

e-mail: christophe.obergfell@gmail.com
ISBN: 978-94-028-1859-8
An electronic version of this dissertation is available at
http://repository.tudelft.nl/.

Contents

Preface

In 2000, Professor Co de Vries (at that time head of the Hydrology department of the VU University in Amsterdam), published a paper entitled 'Groundwater level fluctuations - the pulse of the aquifer' at the occasion of a symposium on the evaluation and protection of groundwater resources [*de Vries*, 2000]. That paper was the first to raise my curiosity about the subject of time series analysis in groundwater hydrology: the pulse of the aquifer as a metaphor for groundwater level fluctuations suggested the possibility of time series analysis of groundwater levels to physically characterize and interpret groundwater level fluctuations.

When I started working as a free-lance groundwater hydrologist in 2004, the need to determine consistent groundwater model calibration targets (from measured groundwater level time series) led me again towards time series analysis. The combination of time series analysis and groundwater modeling was not a common practice at that time (and it still is not at the publication time of this thesis) but the complementarity of these two modeling approaches was clear to me. Later, Jos von Asmuth, the main author of the time series modeling software Menyanthes, tipped me about a PhD position to investigate how groundwater model parameters can be derived from time series analysis. I grabbed that chance and applied for it at the end of 2008. The position was partly at KWR (Kiwa Watercycle Research institute) and partly at the Technical University of Delft, in the Netherlands.

The interview with Mark Bakker made me even more enthusiastic about this research project: the subject and the supervising were promising. Mark confirmed my appointment for the position sometime later, with a mail starting with 'Welcome on-board Christophe'. Research can indeed be reminiscent to a sail journey where your position needs to be updated continuously. In a research project, the route is updated based on experimental results, which consisted here on the results of new models. Fortunately, my supervisors have been excellent pilots, allowing me the freedom to explore while intervening from time to time to adjust the course. This thesis is a distillate of the findings of the journey.

Financial support, data supply and reviewers

This thesis, especially the Chapters 2 & 3, was partly conducted in the TTIW-cooperation framework of Wetsus, centre for sustainable water technology (http://www.wetsus.nl/). Wetsus is funded by the Dutch Ministry of Economic Affairs. The author thanks the participants of the research theme 'Underground water functions and well management' for their comments and their financial support.

The study presented in Chapter 2 was supported by Water supply company Brabant Water. The author is grateful for their help and hopes that Brabant Water will benefit from the results of this research. In particular, the data provided by Harry Boukes were highly appreciated.

The study presented in Chapter 3 is based on data provided by consulting company Artesia and the Water Board Aa & Maas. Many thanks in particular to Frans Schaars, Wouter Beekman, Marco van Baar (Artesia) and Jos Moorman (Water Board Aa & Maas) for making this study possible.

The studies presented in chapters 4 and 5 are based on data and information about the groundwater system provided by Jan Hoogendoorn (Drinking Water Supply Company Vitens) , Thomas de Meij and Huub Verressen (Province of Overijssel), Chris Griffioen (Water Board Drents Overijsselse Delta), Prof. Pieter Stuyfzand (TU Delft), Dr. Elke Buis and Dr. Ronald Hoogerbrugge (Dutch National Institute for Public Health and the Environment), Johan Ten Dam (City of Hellendoorn), Jan Rikus Limbeek, Ben Ordelmans, Maarten Zonderdijk and Linda van der Toorn (Water Board Vechtsromen). For these two studies, the expertise of Dr. Miriam Coenders (TU Delft), Prof. Flip Witte (KWR Water Research), Prof. Pieter Stuyfzand (TU Delft), Dr. Randal Barnes (reviewer of the University of Minnesota) and three anonymous reviewers were very helpful.

Summary

The objective of this thesis is twofold: to develop time series analysis methods for the estimation of aquifer parameters and recharge to be used in groundwater models and to develop time series analysis methods for the identification and quantification of a regime change.

In Chapter 2, a pumping test is replaced by time series analysis of heads measured in the vicinity of a well field with a strongly varying pumping regime. The step response function obtained with time series analysis provides an estimate of the steady response to pumping that would be achieved if the pumping rate was constant. The resulting virtual steady state cone of depression of the well field allows for a straightforward calibration of a regular groundwater model to estimate aquifer parameters. In addition, time series analysis can be used to determine the type of reaction, phreatic or semi-confined, in the different monitoring wells.

In Chapter 3, stream-aquifer interaction is analyzed with a time series model using a response function that is a solution to the groundwater flow equation. Head fluctuations in the vicinity of a river are analyzed, which result directly in estimates of aquifer parameters, including the resistance to flow at the interface between the stream and the aquifer. For the study site, the resistance to flow between the stream and the aquifer can be explained by stream line contraction rather than by the presence of a semi-pervious layer at the bottom of the river.

In Chapter 4, time-averaged groundwater recharge is estimated from time series models of groundwater heads that are fitted under an additional constraint that aims at better identifying the influence of evaporation. The constraint is that the seasonal harmonic of the observed head is reproduced as the response of the seasonal harmonics of precipitation, evaporation, and pumping. Better identification of the influence of evaporation results in more reliable recharge estimates to be used in regular groundwater flow models.

In Chapter 5, time series analysis is applied to identify and analyze a transition in the groundwater regime of an aquifer. The groundwater regime is defined as the range of head variations of a time series throughout the seasons. A new time series modeling approach is proposed to simulate the transition from an initial regime to an altered regime. In the case study, the estimated timing and magnitude of the transition provides strong evidence that the transition is the result of dredging works in the main river draining the aquifer. The existence of the transition of the groundwater regime had gone unnoticed, despite intensive groundwater monitoring.

This thesis showed how time series analysis can be applied to estimate the magnitude of groundwater model parameters or recharge and be applied as a tool to gain insight in the functioning of groundwater systems.

A crucial issue when estimating aquifer parameters or recharge from time series models is the uncertainty of the estimates. A modified Gauss Newton approach was used in this thesis. This approach converges quickly and provides an estimate

of confidence intervals of the estimated parameters. The systematic comparison of different estimation procedures, including Markov Chain Monte Carlo, is recommended for future study.

Groundwater modeling is based on a conceptual model of a groundwater system to simulate groundwater flow, while time series analysis can be used to estimate groundwater model parameters and identify possible changes in regimes for use in groundwater models. Both modeling approaches are complementary and it is recommended that they be applied together in a systematic fashion.

Chapter 1 General introduction

1.1 Time series analysis of groundwater levels

The topic of this thesis is the physical interpretation of time series analysis of groundwater levels measured in one or more monitoring wells. The most straightforward analysis of a time series of measured groundwater levels (which will be further referred to as groundwater heads, or simply as 'heads') is to calculate its mean, standard deviation and the 0.05 and 0.95 quantiles. These statistical characteristics are useful as a first description of the groundwater regime over a given period of time; groundwater regime is defined here as the range of groundwater levels measured over the seasons. The mean groundwater flow direction can be estimated if these statistics are known at different positions in the aquifer over the same period of time. Additional information can be drawn from a time series of heads by explaining the head fluctuations as a result of external stresses such as precipitation, evaporation, pumping, or river stage variations, for example using transfer function noise (TFN) modeling [*Box and Jenkins*, 1969]. In TFN models, the head at a certain time is simulated as the sum of autoregressive terms and a weighted average of past heads and past precipitation, evaporation, or other stresses. TFN models have been widely applied since the 1980s in groundwater hydrology in the Netherlands [e.g. , *Baggelaar*, 1988; *Van Geer et al.*, 1988]. TFN models can be attributed a physical meaning by deriving the model coefficients from difference equations that approximate simple groundwater flow solutions [e.g., *Bierkens*, 1998; *Berendrecht et al.*, 2006].

Alternatively, head measurements can be explained using a weighted average of past stresses only. In such a simplified TFN model, the influence of the stresses is traced back as far as detectable in the past and the auto-regressive terms are omitted. Mathematically, such an approach is the convolution of a time series of a stress with the impulse response function for this stress. The impulse response function for a stress describes how the groundwater head reacts to an impulse of that stress [e.g. ,*Von Asmuth et al.*, 2002]. This approach of time series modeling is adopted in the present thesis because it relies completely on response functions (estimated for each stresses), which, play a key role in the physical interpretation of time series models and in the interplay between time series models and groundwater flow models.

1.2 Objectives and scope of the research

In current groundwater hydrology practice, groundwater flow modeling is used for a variety of tasks, including to dimension pumping activity, simulate hydro chemical mass transport, or answer questions regarding the groundwater

balance. On the other hand, time series modeling is used to characterize groundwater regimes and to relate head fluctuations to stresses such as precipitation and evaporation. Groundwater flow modeling and time series modeling are often considered as two different tools, that can be used for two different types of problems.

Advances in groundwater flow modeling and time series analysis are to be expected from a synergy between both modeling approaches. An important step in this direction was the development of a theoretical framework for groundwater flow model calibration based on the results of time series models [*Bakker et al.*, 2008]. The topic of this thesis is to further explore the complementarity of time series modeling.

The objective of this thesis is twofold: develop time series analysis methods for the estimation of aquifer parameters and recharge to be used in groundwater models, and develop time series analysis methods for the identification and quantification of a regime change.

A common thread in the investigations presented in this thesis is that the focus is on the quantification of model parameters or on a better understanding of groundwater systems function, instead of a focus on the forecasting of groundwater heads.

1.3 Methodology

In this thesis, groundwater heads are simulated as weighted averages of the past stresses on the groundwater system. Two main stresses (sometimes also referred to as forcings) are precipitation, evaporation. Other possible stresses include pumping and river stage variations. The weighted average of a past stress is computed as the convolution integral of the stress time series with a corresponding impulse response function, where the impulse response function acts as the weighing function.

In physical terms, the impulse response function of a stress describes the reaction of the groundwater head in response to an impulse of unit magnitude of this stress. An important assumption of this approach is that the groundwater heads react approximately linearly to the impulses of stresses.

The method of time series modeling used here was developed by von Asmuth et al. [2002], which in turn was initiated by the study of convolutional processes by *Maas* [1994]. Interestingly, *Besbes and de Marsily* [1984] applied similar convolution techniques in the context of groundwater flow modeling to model the delayed reaction of the water table to precipitation as a result of the passage through the unsaturated zone.

1.4 Thesis outline

Chapters 2 to 5 are adapted from four peer reviewed papers published in international journals. As such, there is some overlap as the method of time series

is explained in each chapter. In Chapters 2 and 3, groundwater flow model parameters are derived from the response functions of time series models, in a way reminiscent to pumping tests (Chapter 2) or flood wave tests (Chapter 3). In Chapter 4, time series analysis is applied to estimate groundwater recharge to be used in groundwater flow models. In Chapter 5, a change in groundwater regime is identified and explained; such a regime change typically goes unnoticed in a groundwater flow modeling project. Finally, a synthesis is presented in the last chapter.

Chapter 2 Deriving hydrogeological parameters through time series analysis of groundwater head fluctuations around well fields

Abstract
A method is presented by which time series analysis is applied to support groundwater system conceptualization and provide calibration targets for a steady groundwater model. The method is illustrated for heads measured in the vicinity of a drinking-water well field. The estimated steady response to pumping was used to classify the monitoring wells as semi-confined or phreatic. Based on this conceptualization, the aquifer system was represented by two layers separated by a leaky bed, which represents the resistance to vertical flow of the layers. The model could be calibrated satisfactorily using the drawdowns estimated by time series analysis. This approach was more successful than deriving the aquifer parameters directly from the analytical well function of Hantush, which was successful for a limited number of monitoring wells only and required the a-priory choice of the elevation of a confining layer which was not clear from bore logs. This study illustrates how time series analysis can lead to qualitative and quantitative insights regarding the local hydrogeology, providing complementary information to available bore logs to design a conceptual groundwater model. Time series analysis provides a cost-effective alternative to pumping tests when measured head fluctuations influenced by pumping wells are available.

Adapted from C. Obergfell, M. Bakker, W.J. Zaadnoordijk, and K. Maas, Deriving hydrogeological parameters through time series analysis of groundwater head fluctuations around well fields, Hydrogeology Journal, Volume 21, Issue 5, pp 987–999 , doi: 10.1007/s10040-013-0973-4, 2013.

2.1 Introduction

Pumping tests, also referred to as aquifer tests, are a standard approach to estimate pumping influences and aquifer parameters [*Kruseman and de Ridder*, 1970]. Aquifer parameters are needed to quantify groundwater flow and well capacities, and to facilitate the quantification of groundwater recharge [*Ferris et al.*, 1962]. Basically, a pumping test consists of withdrawing groundwater in a controlled way, usually during a few days, while measuring the groundwater head in monitoring wells. The observed head variations are subsequently matched with an analytical model, or with a numerical model when the conceptual model is too complex to be described by a mathematical expression [*Lebbe et al.*, 1992]. Pumping tests are expensive and usually only justified in cases where exploitation of the aquifer is considered [*Freeze and Cherry*, 1979].

As an alternative, *Van Geer et al.* [1988] and *Baggelaar* [1988] showed how pumping influences can be derived from time series analysis. Using Box-Jenkins transfer function noise models [*Box and Jenkins*, 1969], they separated long term groundwater fluctuations caused by pumping from other stresses like precipitation and evaporation. In turn, they used the transfer function of the time series model, which describes the response to pumping, to estimate the steady drawdowns at the locations of monitoring wells. The steady drawdown is defined as the drawdown that results from application of a stress (in this case pumping) at a constant rate for an infinitely long time. Drawdowns were estimated within relatively large confidence intervals, probably due to the coarse time resolution of pumping data. *Von Asmuth et al.* [2002] developed a time series analysis method that is able to deal with variable measurement time steps. The method is based on predefined impulse response functions which can be seen as continuous equivalents of the Box-Jenkins transfer functions. *Von Asmuth et al.* [2008] applied this method to estimate pumping influences around a well field using the well function of Hantush as a response function. More recently, *Harp and Vesselinov* [2011] presented a method closely related to time series analysis to estimate regional values of aquifer transmissivity and storativity. They estimated the influences of individual wells of a well field using the well function of Theis as a response function. They worked with time series of daily head measurements and daily pumped volumes. Regional values of aquifer transmissivity and storativity were obtained directly from the fitted response functions. As this assumes that the simple hydrogeological schematization and boundary conditions used for the derivation of the formula of Theis applies to the aquifer, the obtained aquifer parameters are indicative values [*Harp and Vesselinov*, 2011].

In order to derive optimum parameters for a groundwater model, *Bakker et al.* [2008] proposed to calibrate groundwater models on temporal moments of impulse response functions inferred from time series analysis. The method was presented with groundwater fluctuations caused by variations in areal recharge and canal stages using synthetic data.

Based on the same principle, the objective of this study is to illustrate how time series analysis of groundwater heads measured in the vicinity of a well field 1) can be used to support the conceptualization of a groundwater model, and 2) provide estimates of steady drawdowns for the calibration of the groundwater model; the method is presented through application to a case study. The proposed method can be seen as an alternative for pumping tests; model parameters are not derived directly from a well function, but indirectly, by applying time series analysis to compute calibration targets for a groundwater model.

This chapter is organized as follows. First, the application of time series analysis to estimate steady pumping drawdowns is presented. Next, the hydrogeological setting and groundwater model of the case study are described. Results of time series analysis are presented, followed by an interpretation of the estimated steady pumping drawdowns and their application as groundwater model calibration targets. Issues regarding the significance of the estimated parameters are discussed towards the end.

2.2 Time series analysis

2.2.1 Convolution of stress time series with response functions

Time series analysis is performed by the method of predefined impulse response functions, developed by von Asmuth et al. (2002). In this method, an impulse response function $\theta(t)$, depending on a few shape parameters, is defined for each stress. The groundwater head fluctuation $h(t)$, at time t, resulting from a time varying stress $N(t)$ is calculated by convoluting $N(t)$ with $\theta(t)$ [*Besbes and de Marsily*, 1984; *Maas*, 1995; *Von Asmuth et al.*, 2002]

$$h(t) = \int_0^t N(\tau)\theta(t-\tau)d\tau \qquad (2.1)$$

In practice, stress intensities are commonly measured for a certain period of time Δt. The fluctuation $h(t)$ resulting from a stress of intensity N applied between time $\tau = 0$ and $\tau = \Delta t$ is given by:

$$h(t) = N\left(\int_0^t \theta(t-\tau)d\tau - \int_{\Delta t}^t \theta(t-\tau)d\tau\right) \text{ for } t \geq \Delta t \qquad (2.2)$$

In equation (2.2), the integral $S(t) = \int_0^t \theta(t-\tau)d\tau$ is called the step response and describes the response of groundwater head to a unit step input beginning at time $\tau = 0$.

The parameters of the impulse response functions are optimized to obtain the best fit with the observed fluctuations. It is a linear method similar in many ways to the unit hydrograph in surface water hydrology. Although the linearity of the method might appear restrictive in the view of non-linear phenomena like groundwater recharge, experience strongly suggests that it results in many cases in a good approximation of the observed head variations [*Von Asmuth et al.*, 2008; *Manzione et al.*, 2012]

2.2.2 Signal decomposition

The method of time series analysis by predefined impulse response functions attempts to decompose the measured head fluctuations into partial fluctuation series, each of which is caused by one of the applied stresses [*Von Asmuth et al.*, 2008]. The sum of the partial fluctuations and a constant called the 'drainage base' form the deterministic part of the time series model. The drainage base is the head reached when all stresses are set to zero. The difference between the time series of observed heads and the time series computed with the deterministic model forms a residual time series. The decomposition of a time series of observed heads $h_o(t)$ can be summarized as follows:

$$h_o(t) = d + \sum_i h_i(t) + n(t) \tag{2.3}$$

where d is the drainage base, $h_i(t)$ represents the fluctuations explained by stress i, and $n(t)$ represents the residual time series of differences between observed heads and heads calculated by the deterministic model [*Von Asmuth et al.*, 2008]. If the characteristics of the residual time series substantially depart from white noise, modeling the residual time series might be necessary [*Von Asmuth and Bierkens*, 2005]

2.2.3 Predefined response functions

Response functions are predefined for each stress to simulate their specific influence on the head. In this study, the response functions for precipitation and evaporation proposed by *Von Asmuth et al.* [2008] are used. These functions are also implemented in the computer program Menyanthes [*von Asmuth et al.*, 2012]. The impulse response function $\theta_p(t)$ describing the influence of precipitation is a scaled gamma density function:

$$\theta_P(t) = A\frac{a^n t^{n-1} e^{-at}}{\Gamma(n)} \tag{2.4}$$

where A is a scaling factor, a and n define the shape of the function, t denotes time, and $\Gamma(n)$ is the gamma function of n. The corresponding step response is a scaled incomplete gamma function:

$$S_p(t) = \frac{A}{\Gamma(n)}\int_0^t a^n \tau^{n-1} e^{-a\tau} d\tau \tag{2.5}$$

which may be written as

$$S_p(t) = \frac{A}{\Gamma(n)}\int_0^{at} \tau^{n-1} e^{-\tau} d\tau = \frac{A}{\Gamma(n)}\Gamma(n, at) \tag{2.6}$$

where $\Gamma(n, at)$ is the lower incomplete gamma function of n at time at. To limit the number of parameters to fit, parameters a and n are the same for the precipitation response and evaporation response.

The impulse response function $\theta_w(t)$ describing the response to pumping is chosen as:

$$\theta_w(t) = -\frac{\alpha}{t}\exp(-\frac{\beta*}{\gamma t} - \gamma t) \tag{2.7}$$

where α is a scaling factor, and β^* and γ define the shape of the function. The corresponding step function is given by:

$$S_w(t) = \int_0^t -\frac{\alpha}{t}\exp(-\frac{\beta^*}{\gamma t} - \gamma t)dt \tag{2.8}$$

This choice is inspired by Hantush's well function. To limit the number of parameters, α and γ are attributed the same value for all pumping wells and parameter β^* is taken as $\beta^* = \frac{\beta^2 r^2}{4}$, where r is the distance between the pumping well and the monitoring well, and β is a shape parameter that is the same for all pumping wells.

$$S_w(t) = \int_0^t -\frac{\alpha}{t}\exp(-\frac{\beta^2 r^2}{4\gamma t} - \gamma t)dt \tag{2.9}$$

Integral (2.9) can be transformed into a form reminiscent to the well function of Hantush which can be evaluated efficiently by a method proposed by *Veling and Maas* [2010] (see Appendix).

2.2.4 Steady state drawdown

The area under the impulse response function $\theta(t)$ is referred to as the moment of order zero and denoted M_0:

$$M_0 = \int_0^\infty \theta(\tau) d\tau \tag{2.10}$$

M_0 represents the steady effect of a continuous unit stress at a given monitoring well. For groundwater withdrawal, the moment of order zero, denoted M_0^w, is the steady drawdown resulting from a constant unit pumping rate, as shown in Figure 2-1.

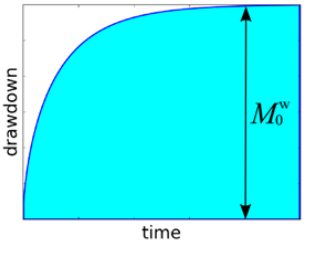

Figure 2-1: M_0^w interpreted as steady drawdown at a monitoring well resulting from of a constant unit pumping rate

In this study, M_0^w is obtained by taking the limit to infinity of equation (2.9) [*Gradshteyn and Ryzhik*, 1965, equation 3.471-9]:

$$M_0^w = 2\alpha \mathrm{K}_0(r\beta) \tag{2.11}$$

where K_0 denotes the modified Bessel function of the second kind and of order zero. The steady drawdown s corresponding to a constant pumping rate Q is given by the product

$$s = QM_0^w = 2Q\alpha \mathrm{K}_0(r\beta) \tag{2.12}$$

2.2.5 Parameter estimation of time series models

Model parameters need to be estimated for each monitoring well by fitting the time series model to the observed groundwater heads. All parameters are log-transformed during optimization to ensure parameter values remain positive, with the exception of the drainage base, which can take negative values. The sum of squares of the residuals is minimized through application of a modified Gauss-Newton algorithm [*Hill*, 1998].

Under the assumption that time series model residuals are normally distributed, homoscedastic, uncorrelated, and that the time series model can be linearized around the optimal parameters, the covariance matrix C_p of the optimized parameters can be calculated as [*Hill*, 1998]

$$C_p = \sigma_r^2 \left(J^T J \right)^{-1} \tag{2.13}$$

where σ_r^2 is the variance of the residuals of the time series model and J is the Jacobian matrix of the derivatives of calculated heads with respect to the parameters. The elements of the Jacobian matrix are:

$$J_{ij} = \frac{dh_i}{d(\ln p_j)} \tag{2.14}$$

for log-transformed parameters p_j and

$$J_{ij} = \frac{dh_i}{dp_j} \tag{2.15}$$

for non-transformed parameters p_j.

Confidence intervals of optimized parameters are estimated assuming a normal distribution around the optimum, scaled by the variance of the parameter as given by the covariance matrix. For an optimal value $\ln(p_i)$ of log-transformed parameter i, the lower and upper limits of the 95% confidence interval are:

$$\ln(p_i) \pm 1.96\sigma_{\ln(p_i)} \tag{2.16}$$

while for the drainage base, which is not transformed, the lower and upper limits of the 95% confidence interval are:

$$d \pm 1.96\sigma_d \tag{2.17}$$

The confidence intervals of the back-transformed parameters are obtained by taking the exponential of the lower and upper bounds of the log-transformed parameters.

Equation (2.12) gives the relation between time series model parameters and the estimated steady drawdown for pumping rate Q. The confidence interval of the estimated drawdown is computed using Monte-Carlo simulations; parameters α and β are drawn from a multi-normal distribution located at the optimal parameter values and scaled by the covariance matrix of the log-transformed parameters. The estimated drawdowns are used as calibration targets in a numerical groundwater model, as illustrated in the following case study.

2.3 Site description

2.3.1 Hydrogeology

The presented approach is applied to a well field of the drinking water supply company Brabant Water. The well field is situated in Waalwijk, a little city in the province of North-Brabant, in the south of the Netherlands. Geologically, Waalwijk is situated in the southeast-northwest oriented Dutch Central Graben. The graben is separated at the west from the Massif of Brabant by the Gilze Rijen fault zone and at the east from the Peel horst by the Peel border fault zone. The graben has been subsiding since the beginning of the Tertiary resulting in deposits of thick sediment layers [*Lekahena*, 1983]. At the end of the Pliocene, the area became an estuary for the river Rhine. The corresponding sediments are referred to as the formation of Peize-Waalre for its lowest part and Waalre for its upper part. The lower 20 m of the formation are mainly composed of sand. Between approximately 80 and 50 m below ground level (bgl), the formation of Waalre takes the form of a thick clay layer. From the available data, this clay layer appears over the whole surface of the study area and can be considered as the hydrological basis of the groundwater model. Above this clay layer, the Rhine deposited mainly sand over approximately 30-40 m corresponding to the formation of Sterksel, or locally to the formation of Kreftenheye. Drinking water is pumped from the aquifer formed by the formation of Sterksel at a depth of approximately 25m bgl. A borehole near the well field reveals the presence of a clay layer at about 20 m bgl. This layer, further referred to as the clay layer of Sterksel, is expected to constitute an aquitard above the well field. During the Pleistocene glaciations, aeolian fine sands with local silt sub-layers were deposited over approximately 10-15m and constitute the formation of Boxtel. The hydrogeological situation is summarized in Table 2-1.

Table 2-1: Site stratigraphy

Formation name	Age**	Depth (m bgl)*	Lithology

Boxtel	Middle Pleistocene to Lower Holocene (0.6-0.01Ma)	0-10	Middle coarse sand with local interspersed silt sub-layers
Sterksel***	Lower to Middle Pleistocene (1.0-0.6 Ma)	10-40	Fluvial coarse sand with one main interspersed clay sub-layers
Waalre****	Lower Pleistocene (1.8-1.0 Ma)	40-80	Fluvial clay

* bgl = below ground level, with ground level at about 2.5mNAP (NAP is the Amsterdam Ordnance Datum)
** 1Ma=one million years
*** Formation of the drinking water wells
**** Groundwater model hydrological basis

2.3.2 Observed time series

The well field is composed of seven wells with screens at depths of 25-30 m bgl. Heads in monitoring boreholes around the well field and in pumping wells were registered with automatic pressure transducers from May 2009 until April 2010 with a time interval of 5 min. The locations and depths of the monitoring wells are given in Figure 2-2 together with the location of the seven pumping wells. Time-series simulations were performed with a time-step of one hour. The dataset was reduced to one measurement per hour by taking the nearest measurement to each hour. Calibration points for time series analysis were selected by taking the lowest and highest head measured within time intervals of one and a half days.

Precipitation and potential evaporation series are obtained from stations of the Royal Dutch Meteorological Institute, respectively in Giersbergen, 5 km from the site, and Eindhoven, 40 km from the site.

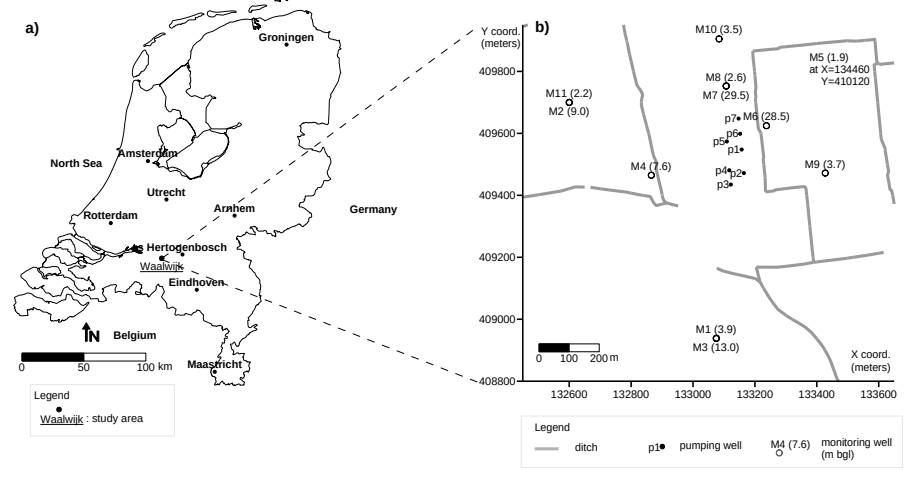

Figure 2-2: Locations and depths of monitoring wells and pumping wells

2.4 Groundwater flow model

2.4.1 Schematization of aquifers

Based on the geological description of the site, it is expected that some monitoring wells react as semi-confined, and some react as phreatic. The groundwater model has to account for these two responses, which means that at least a two-layer model is needed. Although the Sterksel clay layer 20m bgl is expected to cause most of the resistance to vertical flow, its extent is uncertain. In addition, more shallow silt sub-layers, interspersed in the top formation of Boxtel, can locally contribute to the resistance to vertical flow. It follows from these considerations that the Sterksel clay cannot be considered as the boundary between semi-confined and unconfined flow. Instead, a quasi-three dimensional two-layer model is used. The two layers are defined by their transmissivity and are separated by an abstract aquitard with zero thickness representing the vertical flow between the two layers. To limit the number of parameters to optimize, the same horizontal conductivity was used for both model layers. The pumping wells are screened in the semi-confined layer.

The head fluctuations in the monitoring wells were analyzed with time series analysis as described above. Steady state drawdowns (calibration targets) were estimated based on the parameters of the well response function following equation (2.12). Monitoring wells were assigned based on their reaction to pumping which can be semi-confined or phreatic as determined by time series analysis.

2.4.2 Numerical model

The well field lies at the transition between an infiltration area to the south consisting of the Holocene sand dunes of Loon and Drunen and an artificially drained region along the river Maas to the north. Drainage ditches are present around the well field within a radius of a few kilometers and constitute a head-dependent top boundary. The steady form of the calculated cone of depression depends on the choice of the boundary conditions. Given the presence of the dense network of ditches, it is assumed that leakage from surface water mainly determines the steady cone of depression and that no fixed head needs to be used at the model boundary. The objective of the model is to simulate drawdowns resulting from pumping, so that no recharge from precipitation needs to be entered. Furthermore, the drawdown at the head dependent boundaries is zero.

The model extent was determined by considering the drawdown caused by steady pumping in a semi-confined aquifer of infinite extent which was first derived by de Glee [*de Glee*, 1930]:

$$s = \frac{Q}{2\pi T} \mathrm{K}_0(\frac{r}{\lambda}) \quad (2.18)$$

where T [L^2/T] is the aquifer transmissivity, λ [L] is the leakage factor defined as $\sqrt{Tc}$, and c [T] is the hydraulic resistance of the aquitard.

Drawdown is negligible at a distance of approximately 3λ. At the site, an upper limit for the leakage factor is 1500m. Model boundaries are consequently chosen at least 5000m from the well field. The hydrogeological situation and the corresponding conceptual model are presented in Figure 2-3.

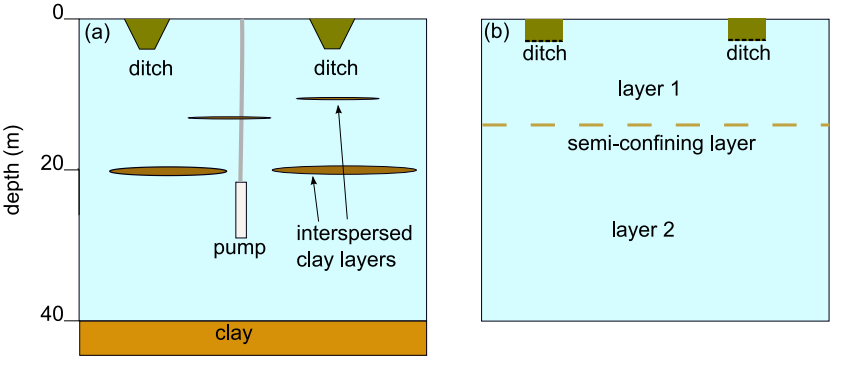

Figure 2-3: a) Hydrogeological setting, and b) conceptual model

The conceptual model was implemented in a finite difference model using MODFLOW-2000 [*Harbaugh et al.*, 2000], with Groundwater Vistas [*Rumbaugh and Rumbaugh*, 1996] as interface. The model covers a domain of 10,000x10,000 m around the well field with a uniform grid spacing of 25m. Ditches were imported as general head boundaries based on a shape file, with zero fixed head.

2.5 Results

2.5.1 Simulation of groundwater head fluctuations

Pumping influence is strongest in the closest and deepest monitoring wells M6 and M7, and becomes weaker with increasing distance from the well field and decreasing depth. This is shown in Figure 2-4 for monitoring well M7 for which pumping influence is strong, and in Figure 2-5 for monitoring well M11 for which pumping influence is weak. The simulated time series are shown for October 2009, together with the observed heads and the points used to optimize the parameters of the time series models. The decomposed responses to precipitation, evaporation, and the seven pumping wells are shown in Figure 2-4 for monitoring well M7, with the observed and simulated heads in the lower panel. Green bars represent stress intensities (values on right vertical axis) and lines represent groundwater heads (values on left vertical axis). The deviation

between modeled and observed heads is likely due to the difference between precipitation at the well field and the values measured at the weather station 5km from the site.

2.5.2 Goodness of fit

Visually, the time series models result in good fits for all monitoring wells. The percentage of explained variance, also referred to as coefficient of determination or Nash-Sutcliffe coefficient, is more than 90% for all monitoring wells. The statistical aspects of the residuals are analyzed in three ways. First, the normality of the distribution of the residuals is evaluated. Applying the Shapiro-Wilk test, the hypothesis that the residuals are normally distributed can be rejected with more than 95% confidence in all time series models. However, comparison of a histogram of the residuals to the closest normal distribution suggests that departure from normality is moderate (Figures 2-6a and 2-7a). Second, the residuals are plotted against the groundwater head fluctuation for a visual assessment of dependence of residual variance on fluctuation amplitude (Figures 2-6b and 2-7b). The magnitude of the residuals increases only moderately with the amplitude of the fluctuations, suggesting that the assumption of homoscedasticity is reasonable: the variance of the residuals is approximately the same at all measurement points of the time series. Finally, correlation of the residuals in time is evaluated using the experimental autocorrelation plots. All time series models indicate a moderate degree of autocorrelation (Figures 2-6c and 2-7c), but remain mostly within the 5% upper and lower confidence bands of a time independent random process.

2.5.3 Time series parameter uncertainty

The confidence intervals of the time series model parameters are computed following standard regression theory, as given in the methodology section, even though the assumptions of normality, homoscedasticity and independence of the residuals are only moderately satisfied. An alternative and possibly better method to estimate parameter variance and confidence intervals is discussed later and leads to comparable results.

For all time series models, the coefficient of correlation between parameters of the pumping response and parameters of the responses to precipitation and evaporation, and the drainage base were smaller than 0.5, indicating the absence of correlation between the parameters of the response to pumping and other time series model parameters. Consequently, uncertainty and correlation of the parameters of the response to precipitation and evaporation and the drainage base do not have to be taken into account to estimate pumping drawdowns. Correlation coefficients for the parameters of the well response function exceed 0.9, and confidence intervals are large for parameters of all time series models with the exception of the two closest and deepest wells M6 and M7. Pumping response parameters, associated 95% confidence intervals and correlation coefficients are given in Table 2-2 for monitoring wells M7, M3 and

M11, representing monitoring wells with strong, moderate and weak responses to pumping, respectively. An explanation for the inaccurate parameter estimation in most pumping response functions is the relatively small effect of pumping in most

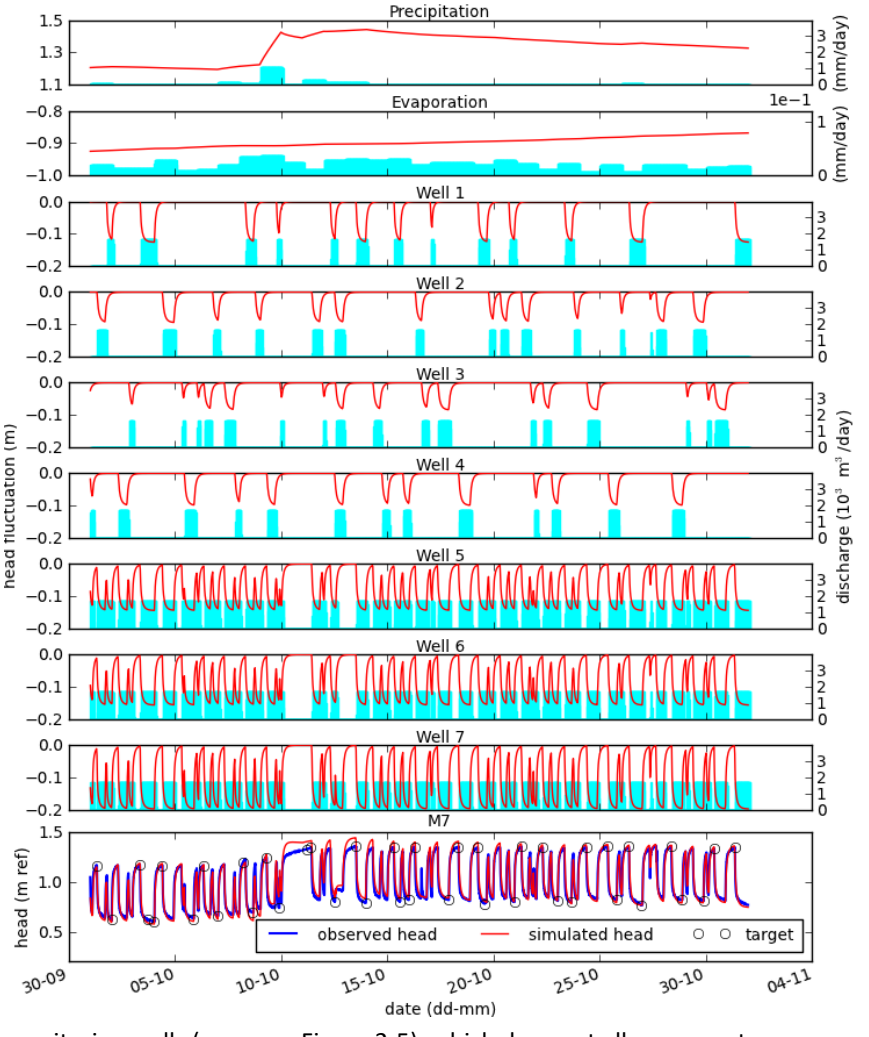

monitoring wells (see, e.g., Figure 2-5), which does not allow accurate determination of the shape of the response function. However, the confidence intervals of estimated steady drawdowns, computed with equation (2.12), are reasonable as shown in the next section.

Figure 2-4: Decomposition of groundwater heads for monitoring well M7 in October 2009. Green bars represent stress intensities (discharge; values on right vertical axis) and lines represent groundwater heads (values on left vertical axis). 'ref' means relative to NAP

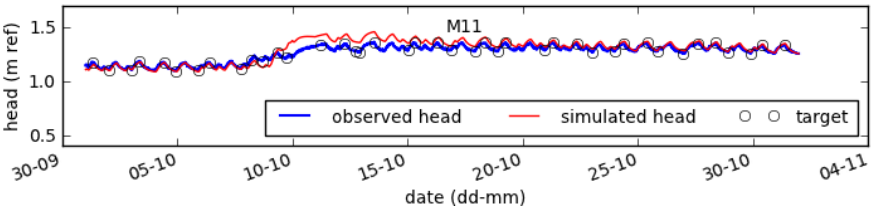

Figure 2-5: Observed and simulated groundwater heads for monitoring well M11 in October 2009

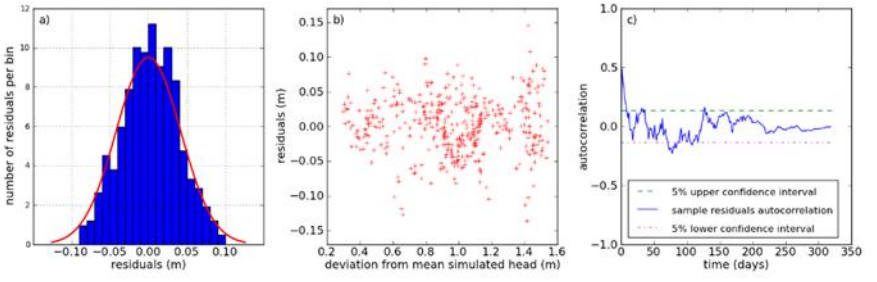

Figure 2-6: a) Residuals distribution, b) residuals versus deviation from mean groundwater head, and c) experimental residual autocorrelation, for time-series model M7

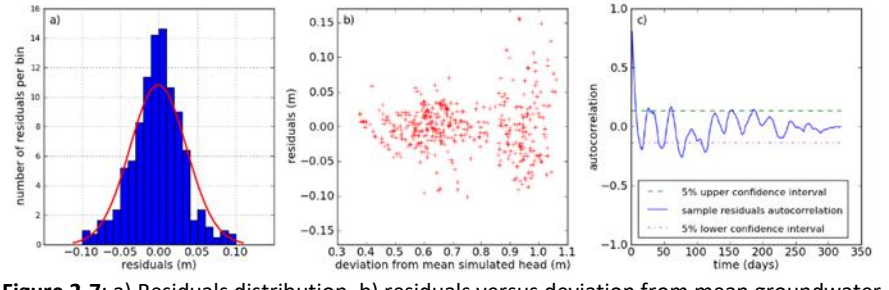

Figure 2-7: a) Residuals distribution, b) residuals versus deviation from mean groundwater level and c) experimental residuals autocorrelation, for time-series model M11

Table 2-2: Optimal pumping response parameters with corresponding 95% confidence interval and correlation coefficients of the log-transformed parameters for monitoring wells M7, M3 and M11

monitoring well	α	β	γ	correl. α / β	correl. α / γ	correl. β / γ
M7	3.6e-5 [3.2e-5, 4.1e-5]	2.1e-3 [1.9e-3, 2.4e-3]	6.4 [6.2, 8.9]	0.86	0.52	0.03
M3	5.6e-5 [3.2e-5, 9.9e-5]	1.9e-3 [1.4e-3, 2.4e-3]	3.7 [2.8, 4.9]	0.99	0.93	0.89
M11	3.2e-5 [3.2e-6, 3.1e-4]	2.1e-3 [8.4e-4, 5.4e-3]	2.3 [9.1e-1, 5.9]	>0.99	0.98	0.98

2.5.4 Virtual steady pumping tests

As stated in the methodology section, equation (2.12) may be used to compute the steady drawdown of any monitoring well. This constitutes, in essence, a virtual pumping test. Applying this idea, the drawdowns are calculated for seven virtual pumping tests. For each test, 100m^3/h is pumped from one of the seven wells. The resulting drawdowns are computed with (2.12) at each monitoring well. Confidence intervals are calculated by a Monte-Carlo procedure as explained in the methodology section. The lower bound of the confidence interval is strongest impacted by the uncertainty in response parameters.

Drawdowns at monitoring wells are plotted versus the distance from the pumping well (e.g., Figure 2.8). Examination of these plots reveals that the largest drawdowns are found in monitoring wells M3, M4, M6 and M7. For these four monitoring wells, the drawdown curves are typical for semi-confined aquifers, while all other monitoring wells exhibit a smaller steady drawdown suggesting phreatic response. The formula of the well function of de Glee for steady drawdown in a semi-confined aquifer is fitted to the computed drawdowns in monitoring wells M3, M4, M6 and M7; the plot of computed drawdowns versus distance between monitoring well and pumping well 6 is given in Figure 2.8. Square markers are used for the apparently semi-confined monitoring wells M3, M4, M6 and M7 whereas circles are used for other monitoring wells. The drawdown in well screen M5 is too small to identify it as semi-confined or phreatic, but it is considered phreatic as its depth is only 1.9 m. The dotted line is the best fit of the formula of de Glee to semi-confined monitoring wells. The transmissivity and vertical resistance from the best fit of the well function of de Glee are given for each virtual pumping test in Table 2-3.

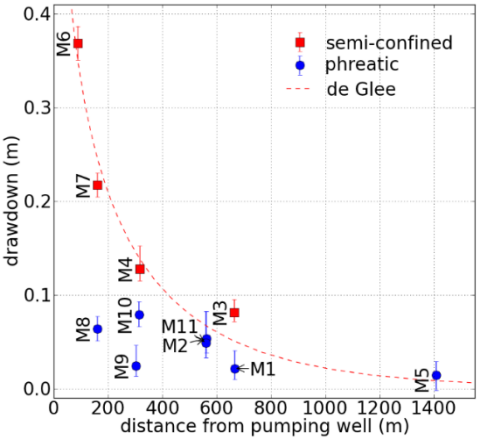

Figure 2-8: Estimated drawdown versus distance to pumping well with 95% confidence intervals for virtual pumping test from pumping well 6. Square markers are the semi-confined monitoring wells M3, M4, M6 and M7 and circles are the other monitoring wells. The dotted line is the de Glee best-fit through monitoring wells M3, M4, M6 and M7

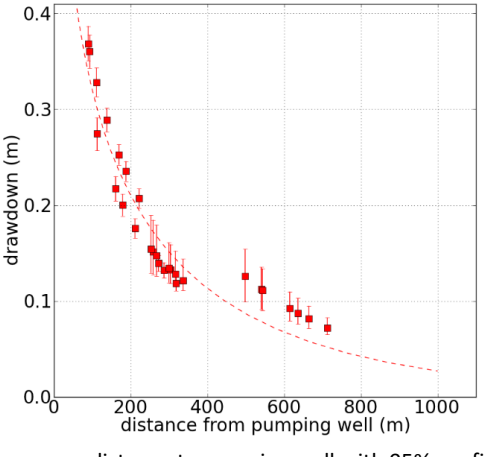

Figure 2-9: Drawdown versus distance to pumping well with 95% confidence intervals for monitoring wells M3, M4, M6 and M7 for all virtual pumping tests; dotted line is best-fit of de Glee

The seven pumping wells result in different aquifer parameters but all confidence intervals overlap over a range of [1610, 2880] for the transmissivity, and over a range of [66,250] for the hydraulic resistance. The differences in parameter values between the seven virtual pumping tests can be explained by the different relative position of the monitoring wells with respect to the pumping well which constrains the interpretation of the form of the cone of depression. For example, in the case of virtual pumping tests 2, 3 and 4, which exhibit the highest parameter uncertainty, the distance between the monitoring wells and

the pumping well range from 200m to 500m, while in the four other cases, the distances range from 150 to more than 600m.

Table 2-3: optimal transmissivity and vertical resistance of the fit of the well function of de Glee to the assumed semi-confined monitoring wells M3, M4, M6 and M7; 95% confidence interval given between square brackets

Pumped well	T (m²/day)	c (days)
Well 1	2070 [1370,3130]	128 [60,270]
Well 2	2440 [1230,4820]	167 [57,4940]
Well 3	3980 [1390,11390]	401 [30,5170]
Well 4	3130 [1440,6810]	252 [51,1240]
Well 5	2450 [1470,4090]	167 [60,460]
Well 6	2040 [1450,2880]	123 [60,250]
Well 7	2230 [1610,3080]	145 [66,316]

In Figure 2-9, a plot is shown of the drawdown versus distance to the pumping well for all semi-confined monitoring wells as determined by the seven virtual pumping tests. Again, the dotted line gives the best fit by the well function of de Glee. The seven points on the right of the figure are all above the fitted line of de Glee. These points correspond to monitoring well M3 for which the schematization of de Glee appears more approximate than for monitoring wells M4, M6 and M7.

The transmissivity and vertical resistance corresponding to the fit shown in Figure 2-9 are T =2260 m²/d and c =148 d. The 95% confidence intervals are [1916, 2667] and [109, 201], respectively, both overlapping the intervals found by fitting the drawdowns of the four semi-confined monitoring wells for each virtual pumping test separately (Table 2-3).

2.5.5 Groundwater model calibration

The drawdowns computed in the virtual pumping test from pumping well 6 are used as calibration targets for the numerical groundwater model. The drawdowns for monitoring wells 3, 4, 6 and 7 are assigned to the semi-confined model layer, while the drawdowns for the other monitoring wells are assigned to the phreatic layer. The discharge of well 6 is set to 100 m³/h and all other wells are inactive. Three parameters are optimized: the horizontal hydraulic conductivity K_h of layers 1 and 2, the vertical hydraulic conductivity K_v of layers 1 and 2, and the conductance C of the bottom of the ditches. The horizontal conductivity is the same for both layers based on available hydrogeological data. The transmissivity of layer 2 is approximated as three times as high as the transmissivity of layer 1, which is entered in the model by setting the thicknesses H_1 and H_2 of layers 1 and 2 to 10m and 30m, respectively. In the presentation of the calibrated parameters,

K_h is expressed as transmissivity of layer 2, $T = K_h H_2$. The vertical hydraulic conductivity is expressed as resistance between the layers $c = (H_1 + H_2)/(2K_v)$.

Parameter estimation was performed using MODFLOW-2000 [*Harbaugh et al.*, 2000]. Drawdowns calculated for the phreatic and semi-confined layers with the calibrated groundwater model are shown in Figure 2-10. Each calibration point is shown together with the monitoring well depth and the residual. The residual is the target (drawdown estimated with time series analysis) minus the simulated drawdown.

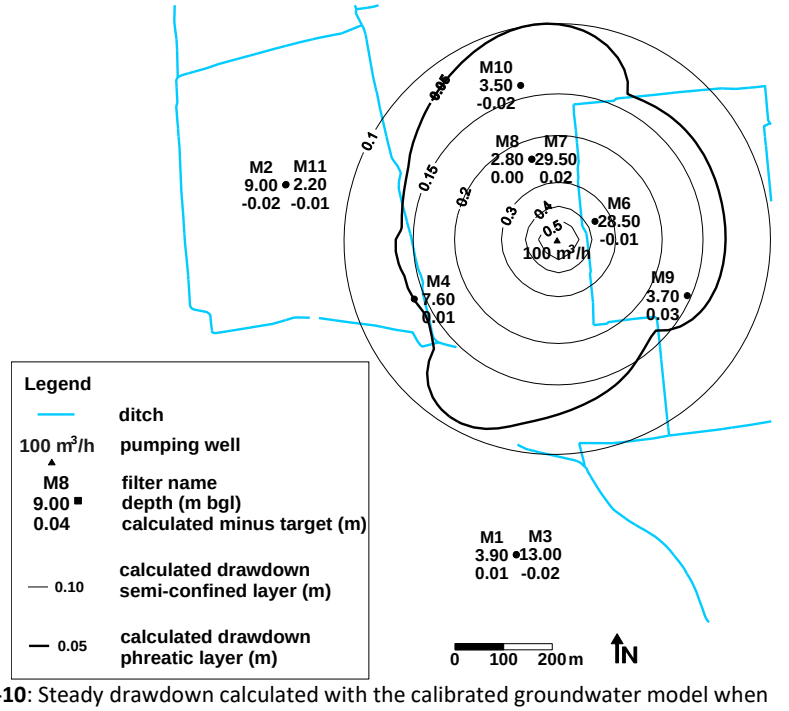

Figure 2-10: Steady drawdown calculated with the calibrated groundwater model when pumping 100m³/h from pumping well P6

A plot of the drawdowns calculated with the groundwater model versus the calibration targets derived from time series analysis, with their confidence intervals, is shown in Figure 2-11.

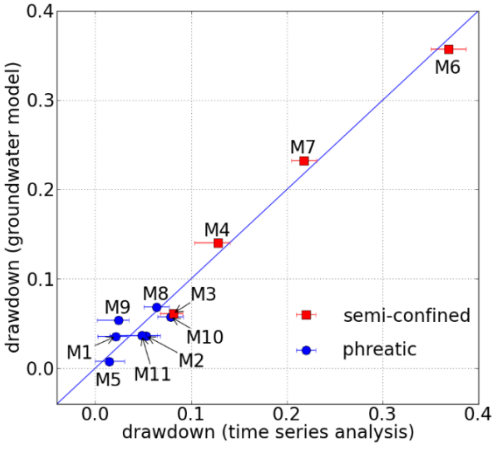

Figure 2-11: Drawdown (in meters) calculated with the groundwater model versus drawdown derived from time series analysis with their respective 95% confidence interval

The root mean square error of the calibrated model is 0.017m, while the maximum drawdown in the model is 0.84m. The calibrated model parameters are (with the 95% confidence interval given in brackets):

- Transmissivity of semi-confined layer T : 2120 m^2/day [1570-2870]
- Vertical resistance c : 130 days [70-260]
- Bottom conductance of ditches C : 195 m^2/day [60-620]

The correlation between the groundwater model parameters is given in Table 2-4.

Table 2-4: Correlation coefficient of groundwater flow model parameters

	T	c	C
T	1	0.80	0.77
c		1	0.54
C			1

The calibrated transmissivity of layer 2 and vertical resistance are in good agreement with the values found with the well function of de Glee.

2.6 Discussion

2.6.1 Groundwater model transmissivity values

In the calibration of the groundwater model, the same horizontal and vertical hydraulic conductivity is used for the two model layers, while the thicknesses of

the layers are fixed to approximate values. Fixing layer thicknesses while calibrating hydraulic conductivities is equivalent to calibrating transmissivities and vertical resistance. Calibration of the horizontal conductivities for the two layers separately resulted in over-parameterization: the hydraulic conductivity of the upper layer was highly correlated with the bottom conductance of the ditches. The horizontal conductivity of the lower layer has little correlation with other parameters. The horizontal conductivity of the top layer was set equal to the horizontal conductivity of the bottom layer, which means, for this case, that the transmissivity of the top layer is one third the transmissivity of the bottom layer.

2.6.2 Hydrogeological insights

Time series analysis of the observed heads combined with the use of the steady well function for semi-confined aquifers provides qualitative insight into the hydrogeological system.
It was shown that monitoring wells M3 and M4, at depths of 13.0 and 7.6 m bgl, respectively, have a semi-confined response. This indicates that the clay layer of Sterksel at a depth of about 20m bgl is not a semi-confining layer for the whole model area as first expected. The silty sub-layers interspersed in the formation of Boxtel appear to play a semi-confining role locally. The fact that monitoring well M4, at a depth of 7.6 m bgl, has a semi-confined response while monitoring well M2, at a depth of 9m bgl, does not, highlights the spatial variability of these silty sub-layers.

2.6.3 Validity of the confidence intervals

The efficient modified Gauss-Newton algorithm used to minimize the sum of the squares of the residuals may not result in accurate confidence intervals of the estimated parameters. The calculated confidence intervals are reasonable when the first-order approximation of the time series model is valid [*Vrugt and Bouten*, 2002] and when the residuals are uncorrelated, homoscedastic and Gaussian distributed [*Schoups and Vrugt*, 2010]. As illustrated in Figures 5 and 6, the latter assumptions are moderately satisfied.

More robust confidence intervals can be obtained with a Monte Carlo Markov Chain (MCMC) optimization algorithm [*Vrugt and Bouten*, 2002] but at significant computational costs [*Keating et al.*, 2010], as the model needs to be run tens of thousand of times to reach stationary Markov chains. As a test, the optimal parameters and their covariance obtained with the Gauss-Newton algorithm for monitoring well M7 are compared to those found with SCEM-UA (Shuffled Complex Evolution Metropolis-University of Arizona) , a MCMC algorithm [*Vrugt et al.*, 2003]. SCEM-UA does not require linearization of the model and explores the whole parameter space avoiding confinement in local minima. The optimal model parameters and associated covariance found by the modified Gauss Newton method and SCEM-UA were in good agreement.

2.6.4 Deriving aquifer parameters directly from the pumping response function

In the presented method, groundwater model parameters are derived from time series models in an indirect way. Time series models provide estimations of steady drawdowns that are used as calibration targets for the groundwater model. Alternatively, aquifer parameters can be derived directly from the pumping response function of the time series model, in a way similar to interpretation of pumping tests. The step response (2.9) can be replaced by the Hantush well function [*Hantush and Jacob*, 1955]:

$$W(\frac{r^2 S}{4Tt}, \frac{r}{\sqrt{Tc}}) = \frac{1}{4\pi T} \int_{\frac{r^2 S}{4Tt}}^{\infty} \frac{1}{u} \exp(-u - \frac{r^2}{4Tcu}) du \qquad (2.19)$$

This is achieved by replacing parameters α, β and γ by the following combination of aquifer parameters T, c and S:

$$\begin{aligned} \alpha &= \frac{1}{4\pi T} \\ \beta &= \frac{1}{\sqrt{Tc}} \\ \gamma &= \frac{1}{cS} \end{aligned} \qquad (2.20)$$

where S represents aquifer storativity.

Time series analysis was repeated using the Hantush well function as pumping response function and the optimal parameters are given in Table 2-5. The transmissivity and resistance found for monitoring wells M6 and M7 are in good agreement with the values found with the groundwater model. These two monitoring wells can adequately be represented by the conceptual model of Hantush and exhibit the most pronounced response to pumping. Parameters of the two other semi-confined monitoring wells, M3 and M4, are estimated with more uncertainty, but the calibrated value of the transmissivity lies within the confidence intervals of the transmissivities of monitoring wells M3 and M4 presented in Table 2-5.

The parameters found for the phreatic monitoring wells, with the exception of monitoring well M10, have larger confidence intervals. These monitoring wells are not in the pumped aquifer so the conceptual model of Hantush does not apply. In addition, pumping influences are damped as shown in Figure 2-5 for monitoring well M11. These shapes can be approximated by many pumping response functions and many combinations of well function parameters, resulting in high parameter uncertainty.

Table 2-5: Hantush parameters obtained from response functions with corresponding 95% confidence interval

Piezometer name	T (m^2/day)	c (day)	S (-)
M1	2480 [67.7, 89500]	52.9 [15.3, 183]	8.80e-3 [7.46e-4, 1.11e-1]
M2	3130 [595, 15000]	105 [93.1, 119]	2.25e-3 [8.93e-4, 5.90e-3]
M3	1400 [820, 2420]	202 [186, 220]	1.33e-3 [9.24e-4, 1.89e-3]
M4	2800 [1560, 5020]	148 [101, 218]	1.94e-3 [1.54e-3, 2.48e-3]
M5	742 [7.10e-4, 9.27e8]	262 [3.96e-2, 2.32e6]	7.73e-4 [8.54e-9, 5.37e1]
M6	2000 [1790,2250]	144 [116, 180]	1.10e-3 [8.15e-4, 1.47e-3]
M7	2190 [1960, 2450]	99.3 [85.3, 116]	1.35e-3 [1.03e-3, 1.78e-3]
M8	4050 [2370, 6840]	13.5 [11.0, 16.7]	3.10e-2 [2.01e-2, 4.88e-2]
M9	4750 [104, 2.24e5]	12.4 [5.66, 27.2]	3.46e-2 [3.36e-3, 3.63e-1]
M10	2650 [1680, 4190]	54.8 [50.6, 59.4]	8.90e-3 [6.63e-3, 1.20e-2]
M11	2520 [274, 24500]	87.3 [57.1, 135]	4.91e-3 [1.30e-3, 1.92e-2]

It is noted that the distinction between semi-confined and phreatic monitoring wells is made by fitting the steady well function of de Glee to the steady drawdowns estimated from time series analysis. Estimation of aquifer parameters directly from the well function of Hantush is only possible for semi-confined monitoring wells, which are not known a priori. Aquifer parameters for filter M10 also have acceptable confidence intervals but are definitely not screened in the semi-confined layer. The parameters of the Hantush pumping response function cannot be used to distinguish semi-confined from phreatic monitoring wells.

More generally, deriving groundwater model parameters directly from physically based pumping response functions requires that the hydrogeological setting can be satisfactorily described by the aquifer schematization implicit in the pumping response function. As pointed out by Harp and Vesselinov (2011), aquifer parameters derived directly from a well function provide at best indicative values for the aquifer parameters. The advantage of the method presented in this study is that it does not assume a priori a certain hydrogeological setting. On the contrary, it can increase hydrogeological insight and may be used to develop a conceptual model of the aquifer system.

2.6.5 Estimation of long term stationary drawdowns

A well known issue with pumping tests lasting no more than a few days is the underestimation of drawdowns as a result of the delayed response of the water table [*Neuman*, 1975]. Although first described for unconfined aquifers, the delayed response of the water table can also be observed for semi-confined aquifers [*Hemker*, 1999; *Narasimhan*, 1999]. As the response to pumping in the presented case study was determined over a few hours with a maximum of half a day, delayed water table response can result in a possible bias in the estimated drawdowns, whether in the semi-confined or in the phreatic layer. How this relates to longer pumping tests is a subject for future investigations.

2.7 Conclusion

In this study, a method was presented to use time series analysis to develop a conceptual model of the aquifer system and to generate calibration targets for a steady groundwater model. Time series analysis of heads measured in the vicinity of a well field were used to estimate the response to pumping, which was used to classify the monitoring wells as semi-confined or phreatic. A two-layer groundwater model was calibrated, satisfactorily reproducing the drawdowns derived from time series analysis.

The presented method is a way to derive aquifer parameters indirectly by estimating steady pumping drawdowns from time series analysis and use those as calibration targets in a groundwater model. Alternatively, direct derivation of aquifer parameters from the Hantush well function, when used as a response function for time series analysis, was successful for only two monitoring wells out of eleven. A necessary condition for deriving aquifer parameters directly from an analytical expression is that the conceptual groundwater model implicit in the analytical well function is an adequate description of the real hydrogeological situation. Further research is needed to develop a method that incorporates the delayed response of the water table in time series analysis.

In this study, it is shown that time series analysis can lead to qualitative and quantitative insights regarding the local hydrogeological system, possibly offering complementary information to the available bore logs. In the case of groundwater head fluctuations influenced by pumping wells, the method presented here allows for the systematic use of data collected around a well field to estimate drawdowns that can be used to calibrate a steady groundwater model. It constitutes, in essence, a virtual steady pumping test. Model parameters are obtained from the calibration of a groundwater model on drawdowns estimated by time series analysis. The use of steady drawdowns as calibration targets drastically simplifies the necessary input data and boundary conditions of the groundwater model. Pumping is the only stress that needs to be entered. Although precipitation and evaporation time series are needed for time series analysis, no recharge needs to be entered in the groundwater model, which eliminates an important source of uncertainty. Head values of head dependent boundaries are set to zero thereby eliminating another source of uncertainty.

2.8 Appendix: derivation of the well step response

The well function of Hantush is defined as:

$$W(\frac{r^2 S}{4Tt}, \frac{r}{\sqrt{Tc}}) = \frac{1}{4\pi T} \int_{\frac{r^2 S}{4Tt}}^{\infty} \frac{1}{u} \exp(-u - \frac{r^2}{4Tcu}) du \qquad (2.21)$$

where T, c and S represent respectively aquifer transmissivity [L^2/T], hydraulic resistance of the aquitard [T] and aquifer storativity [-].

Defining $\alpha = \frac{1}{4\pi T}$, $\beta = \frac{1}{\sqrt{Tc}}$ and $\gamma = \frac{1}{cS}$ as new parameters, equation (2.21) can be written

$$S_w(\frac{r^2 \beta^2}{4\gamma t}, r\beta) = \alpha \int_{\frac{r^2 \beta^2}{4\gamma t}}^{\infty} \frac{1}{u} \exp(-u - \frac{r^2 \beta^2}{4u}) du \qquad (2.22)$$

the derivative of which is

$$\theta_w(t) = -\frac{\alpha}{t} \exp(-\frac{\beta^2 r^2}{4\gamma t} - \gamma t) \qquad (2.23)$$

Chapter 3 A time series analysis framework for the flood wave method to estimate groundwater model parameters

Abstract

The flood wave method is implemented within the framework of time series analysis to estimate aquifer parameters for use in a groundwater model. The resulting extended flood wave method is applicable to situations where groundwater fluctuations are affected significantly by time varying precipitation and evaporation. Response functions for time series analysis are generated with an analytic groundwater model describing stream-aquifer interaction. Analytical response functions play the same role as the well function in a pumping test, which is to translate observed head variations into groundwater model parameters by means of a parsimonious model equation. An important difference as compared to the traditional flood wave method and pumping tests is that aquifer parameters are inferred from the combined effects of precipitation, evaporation, and stream stage fluctuations. Naturally occurring fluctuations are separated in contributions from different stresses. The proposed method is illustrated with data collected near a low-land river in the Netherlands. Special emphasis is put on the interpretation of the stream bed resistance. The resistance of the stream bed is the result of stream line contraction instead of a semi-pervious stream bed, which is concluded through comparison with the head loss calculated with an analytical two-dimensional cross-section model.

Adapted from C. Obergfell, M. Bakker, and K. Maas, A time-series analysis framework for the flood-wave method to estimate groundwater model parameters, Hydrogeology Journal, (2016) 24:1807–1819 doi: 10.1007/s10040-016-1436-5, 2016

3.1 Introduction

The development of methods to estimate aquifer parameters from stream-aquifer interaction dates back to the 1960s and the early application of computers in hydrology [*Cooper and Rorabaugh*, 1963; *Pinder et al.*, 1969; *Venetis*, 1970]. The approach proposed at that time, referred to as the flood wave method, is similar to a pumping test, as the groundwater head in an aquifer is perturbed by a single stress, in this case a flood wave in a stream adjacent to the aquifer. The aquifer diffusivity is obtained by fitting a simple equation for stream-aquifer interaction to the observed heads. This equation fulfills the same function as the well functions of pumping tests. *Hall and Moench* [1972] refined the method by using convolution integrals to relate stream stage fluctuations and head fluctuations. Later, *Moench and Barlow* [2000] extended the method by adding equations for a set of different stream-aquifer configurations. Alternatively, groundwater head response to a time series of stream stage fluctuations can be obtained analytically by replacing the time series of observed stream stage by a series of basis splines [*Knight and Rassam*, 2007; *Rassam et al.*, 2008].

A limitation of the flood wave method is that it is applicable only to situations where head fluctuations can be clearly related to river stage fluctuations [*Ha et al.*, 2007]. In many cases, however, this is not possible as fluctuations due to other stresses, like recharge and evaporation, interfere with fluctuations due to stream stages variations. To solve this issue, the influence of each stress needs to be identified separately. This is where time series analysis can improve the flood wave method.

The objective of this study is to embed the flood wave method into a time series analysis framework in order to derive aquifer parameters for use in distributed groundwater models. The framework is the method of predefined response functions [*Von Asmuth et al.*, 2008], in which a specific response function (also referred to as a transfer function) is chosen for each stress. Each function is able to simulate the head response due to an impulse of a specific stress. Convolution of each response function with the corresponding stress time series results in the separate fluctuations caused by each stress, where it is assumed that the system's response is linear. The method of pre-defined response functions has recently been extended to simulate non-linear reactions of the phreatic water table in Australia [*Peterson and Western*, 2014; *Shapoori et al.*, 2015a]. An evaluation of the method using synthetic data was presented by *Shapoori et al.* [2015c]. Another extension of the method concerns the estimation of aquifer parameters from time series analysis in the vicinity of well fields [*Obergfell et al.*, 2013; *Shapoori et al.*, 2015b].

Typically, the selected response functions do not depend on physical parameters. For example, a scaled gamma distribution function is commonly used as the impulse response function for groundwater recharge. The novelty in this study is two-fold. First, an analytical groundwater model is used as the predefined response function similar to the functions used in the flood wave method. Second, the flood wave method is placed in the framework of time series analysis.

The resulting approach is an extension of the flood-wave method in the sense that it is applicable to situations in which other time-varying stresses than stream stage variations have a significant effect on head fluctuations.

This study is organized as follows. First, the method of time series analysis by predefined response functions is reviewed and it is explained how the flood wave method can be placed in a time series framework. Next, a description of the hydrogeological situation of the field site is given for which response functions are developed. The time series model is fitted to data collected near the Dutch lowland river 'Aa', and aquifer parameters are estimated. These parameters are then entered into a numerical distributed groundwater model to evaluate their adequacy as parameters estimates. The physical significance of the parameter values is discussed, with a special emphasis on the interpretation of the resistance of the stream bed.

3.2 Review of time series analysis with pre-defined response functions

3.2.1 Response functions

In this study, the flood wave method is placed in a time series analysis framework. Time series analysis is performed with the method of predefined response functions [*Von Asmuth et al.*, 2002]. Transfer functions, a term widely used in system theory and time series analysis, can be considered as synonymous to response functions. Similar to linear systems theory [*Hespanha*, 2009], output signals are obtained by convolution of response functions with input signals. Response functions are mathematical expressions relating input and output signals [*Box and Jenkins*, 1969]. In this study, groundwater systems are approximated as linear in the sense that output signals are proportional to input signals. Hydraulic stresses like precipitation, evaporation, river stage variations, and pumping are the input signals and head fluctuations form the output signal. Conditions for when the approximation of linearity is reasonable are reviewed in *Barlow et al.* [2000].

A time series of head fluctuations $\varphi(t)$ at a specific point in space can be obtained by convolving a stress time series $p(t)$ with the corresponding impulse response function $\theta(t)$:

$$\varphi(t) = \int_0^t p(\tau)\theta(t-\tau)d\tau \qquad (3.1)$$

where t is time. In this study, $\varphi(t)$ is used for head fluctuations caused by one specific stress while $h(t)$ is used to refer to the head fluctuations caused by the superposition of all stresses. The dimension of $\theta(t)$ is determined by the dimension of the stress so that the product $p(\tau)\theta(\mathrm{t}-\tau)d\tau$ has the dimension

length, like heads (in contrast to linear system theory, where transfer functions are dimensionless [*Hespanha*, 2009]). Note that the dependence of the response function on spatial coordinates is omitted in this notation. The response function can also be interpreted as the weighting function in a moving average process [*Olsthoorn*, 2008]. As a comparison, in runoff hydrology, the familiar unit hydrograph is the response function relating precipitation (the input signal) to stream discharge (the output signal).

The response function of precipitation represents the passage through the unsaturated zone, followed by a recession curve describing the subsurface drainage of the infiltrated water [e.g.,*Besbes and de Marsily*, 1984]. A first approximation for the response function of evaporation is the response function of precipitation multiplied by a negative scale factor. Alternatively, evaporation can be attributed its own response function describing, for example, how the root zone reacts to a drought period [*Peterson and Western*, 2014]. The response functions for river stage variations and pumping represent the propagation of the head change from the river or the pumping well to a point in the aquifer.

3.2.2 Discrete inputs and continuous transfer functions

In this section, it is described how time series of groundwater heads are modeled given discrete time series of stresses and continuous transfer functions. The unit step function $s(t)$ is obtained from the impulse response function $\theta(t)$ as

$$s(t) = \int_0^t \theta(t-\tau)d\tau \tag{3.2}$$

The step function has the dimension of length per dimension of stress.
The function

$$\psi(t,\Delta t) = s(t) - s(t-\Delta t) \tag{3.3}$$

is called the block response and represents the response to a unit stress applied from $t = 0$ to $t = \Delta t$. In this study, the block function is used as the response function of a given stress. Time is discretized in stress periods, where Δt_i is the length of stress period i . Stress p_i is constant over stress period i from $t = t_i$ to $t = t_i + \Delta t_i$. Since the system is approximated as linear, the head at time t_j can be obtained by summing the effects at time t_j of all past stress periods:

$$\varphi(t_j) = \sum_{i=1}^{j} p_i \psi\left(t_j - t_{i-1}, \Delta t_i\right) \tag{3.4}$$

where

$$t_j = \sum_{i=1}^{j} \Delta t_i \tag{3.5}$$

The heads $h(t)$ in the aquifer are obtained as the following sum:

$$h(t_j) = d + \varphi_p(t) + \varphi_e(t) + \varphi_s(t) + n(t) \tag{3.6}$$

where $h(t)$ is the head, d is the drainage base which is defined as the head that is reached when all stresses are zero, and $\varphi_p(t)$, $\varphi_e(t)$, and $\varphi_s(t)$ represent the contributions of precipitation, evaporation, and stream stage respectively. $n(t)$ represents the residual time series defined as the difference between observed and simulated heads. If the characteristics of the residual time series substantially depart from white noise, modeling the residual is recommended [*Von Asmuth and Bierkens*, 2005]. In this study, an exponentially decreasing noise model is adopted.

3.3 Field site

The field site is located in the area managed by the Dutch Water Board Aa and Maas in the southeastern part of the Netherlands (Figure 3-1). Piezometers were placed by the Water Board, perpendicular to the river Aa, as part of a larger monitoring program of groundwater levels. The Aa is a small, 67 km long low-land river, with an average flow of 11 m^3/s at its mouth.

The field site is situated near the eastern edge of the Dutch Central Graben. The edge of the graben is a fault zone of low permeability, referred to as the Peel border fault zone. The graben is subsiding since the beginning of the Oligocene (ca 25 millions years ago) and is filled with sediments over a thickness of approximately 2000 m. Regional bore logs from the Dutch Geological Survey in the vicinity of the field site suggest that a clay layer is present at a depth of approximately 30 m bgl. This clay layer belongs to the fluvial formation of Waalre, deposited by the Rhine about 2 millions years ago. The clay layer is approximately 1 m thick and can be considered as the impermeable base of the hydrogeological system. The system above the clay layer consists of a main aquifer separated from a thin phreatic top layer by an ensemble of fine silty layers. The stratigraphy of the site is given in Table 3-1. It is noted that the course of the river Aa has been modified in the twentieth century, which explains the absence of alluvial strata corresponding to the river Aa itself.

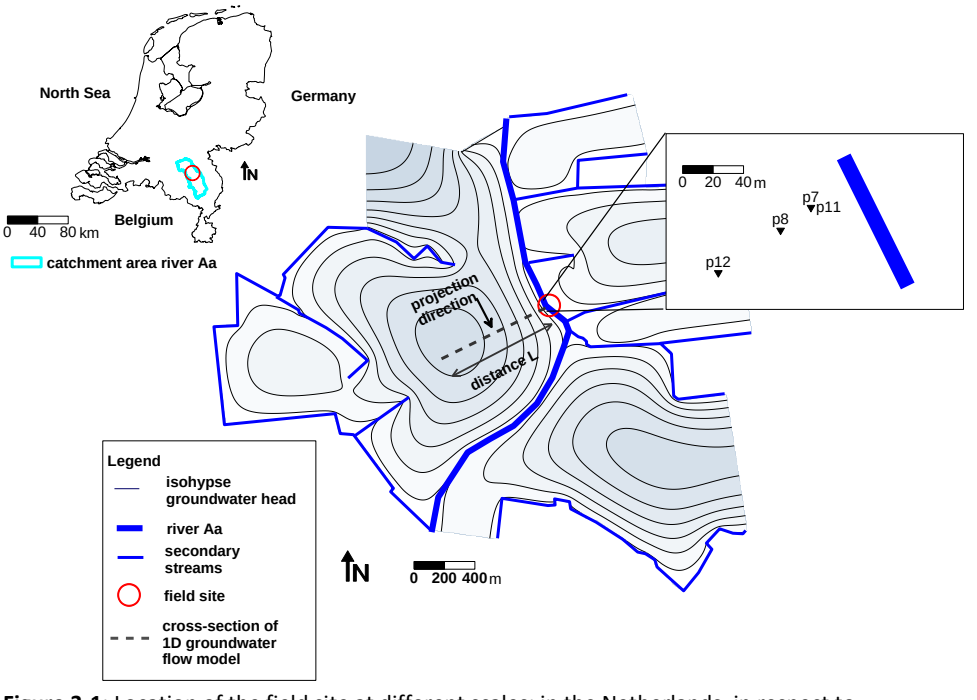

Figure 3-1: Location of the field site at different scales: in the Netherlands, in respect to local streams, in respect to the river Aa

Table 3-1: site stratigraphy

Formation name	Indicative age	Indicative top-bottom depth (m bgl)*	Lithology
Boxtel	Middle Pleistocene-Lower Holocene (0.1-0.01 Ma)	0-5	Fine sand with interspersed silt sub-layers
Beegden	Middle Pleistocene (0.6-0.1 Ma)	5-15	Fluvial (Meuse) medium coarse sand
Sterksel	Lower-Middle Pleistocene (0.8-0.6 Ma)	15-20	Fluvial (Rhine) coarse sand
Stramproy	Lower Pleistocene (2.2-0.8 Ma)	20-30	Eolian and fluvial (Rhine) sands with interspersed peat /silt sublayers
Waalre**	Upper Pliocene-lower Pleistocene (3.6-2.2 Ma)	30-32	Fluvial (Rhine) clay

* bgl = below ground level, with ground level at ≃ 2.5 m NAP (NAP is the Dutch datum, approximately corresponding to mean sea level)

** Base of groundwater model

Based on head data of the Dutch Geological Survey within 5 kilometers of the field site, the groundwater system is a recharge area, drained by the river Aa and its tributary streams. It is a rural area, mainly covered by crop fields and meadows, with occasional patches of woods.

A map of the river Aa and the piezometers is shown in Figure 3-1. Heads and stream levels were measured with pressure transducers. Piezometers P7 and P8 were screened at 4 m bgl and are located at a distance of 25 and 50m from the river bank, respectively. Piezometers P11 and P12 were screened at 1.5 m bgl and are located at a distance of 25 and 70 m from the river bank, respectively. The head regularly dropped below the bottom of piezometer P11.

The river stage was recorded 300 m upstream of the piezometers. The precipitation time series was obtained by interpolating the measurements at three weather stations within 15 km from the investigation site. The evaporation time series was obtained from a weather station 11 km from the field site. The evaporation values correspond to the Makkink reference evaporation, which is representative for Dutch meadow land cover under average meteorological conditions [*Bartholomeus et al.*, 2014]. The measurements in the piezometers, the measured rainfall, evaporation and river stage are used to estimate aquifer parameters to be used in a numerical model of the area.

3.4 Method

3.4.1 Response function from a one-dimensional model schematization

For application of the flood wave method in a time series framework, a vertical cross-section is considered along the dashed line in Figure 3-1. The cross-section is shown in Figure 3-2.

The conceptual model consists of a thin, phreatic top layer consisting of relatively low permeable material underlain by a semi-pervious layer (aquitard), and a semi-confined layer. The following approximations are adopted.

- The stream fully penetrates the aquifer. Head loss due to stream line contraction or due to a semi-pervious stream bed are lumped in the specific resistance of the stream bed (resistance per unit length of stream bed) w [TL^{-1}] defined as:

$$Q_s = \frac{h(x=0) - h_s}{w} \tag{3.7}$$

where Q_s [L^2T^{-1}] is the flux from the aquifer to the stream per unit length of stream, $h(x=0)$ [L] is the head at the interface between the semi-pervious stream bank and the aquifer, and h_s [L] is the stream stage.

- The boundary opposite to the river is approximated by a zero constant head boundary, at a distance $2L$ from the stream. For the case of precipitation and evaporation, this is equivalent to a water divide at a distance L from the stream.
- The piezometers are approximately positioned along a flow line.
- Precipitation surplus reaches the groundwater table instantaneously (the depth to the water table is about 1m).
- The base of the system is impermeable.
- The storage of the semi-confined layer is negligible with respect to the phreatic storage of the phreatic layer.
- The semi-confined layer has a uniform transmissivity.
- Flow in the top layer is vertical.
- The resistance to vertical flow is neglected in the semi-confined layer (Dupuit approximation).
- The river stage variations result in negligible changes in the distance between the river bank and the piezometers.

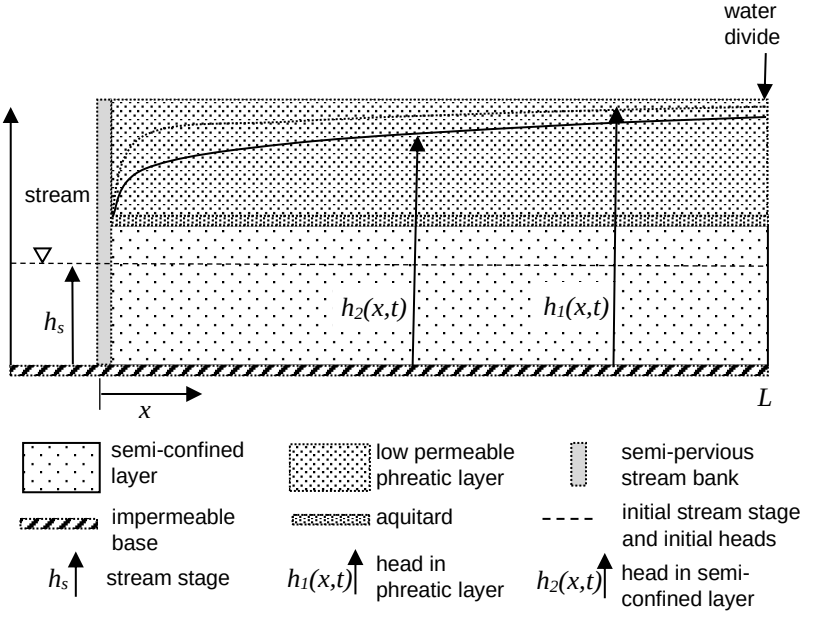

Figure 3-2: Conceptual model of the vertical cross-section for response to recharge.

The heads in the two layers satisfy the following set of two linked differential equations:

$$\begin{cases} \dfrac{h_2 - h_1}{c} = S\dfrac{\partial h_1}{\partial t} - R \\ T\dfrac{\partial^2 h_2}{\partial x^2} + \dfrac{h_1 - h_2}{c} = 0 \end{cases} \tag{3.8}$$

where $h_1(t)$ and $h_2(t)$ are the heads in the phreatic and semi-confined layers, respectively, x is the distance from the stream bank, R [LT^{-1}] is the areal recharge, T [L^{2}T^{-1}] is the transmissivity of the semi-confined layer, S [-] is the storage coefficient of the phreatic layer, c [T] is the resistance to vertical flow of the aquitard. For the step response to recharge, the boundary conditions are:

$$\begin{aligned} &\frac{\partial h_2}{\partial x} = 0,\ x = L \\ &T\frac{\partial h_2}{\partial x} = \frac{h_2 - h_s}{w},\ x = 0 \end{aligned} \tag{3.9}$$

where the stream stage h_s [L] is 0 m. For the step response to stream stage fluctuations, the boundary conditions are:

$$\begin{aligned} &h_2 = 0,\ x = 2L \\ &T\frac{\partial h_2}{\partial x} = \frac{h_2 - h_s}{w},\ x = 0 \end{aligned} \tag{3.10}$$

with $h_s = 1$ for $t > 0$. For both step responses, the initial conditions are:

$$h_1(x, t = 0) = h_2(x, t = 0) = 0 \tag{3.11}$$

Solutions for the two step responses are obtained with a Laplace Transformation. The Laplace Transformation of the differential equation and associated boundary conditions are given in appendix 1. The solution in the Laplace domain for the step response to precipitation is

$$\bar{h}_1 = \frac{p\bar{h}_2 + c}{p(cSp+1)} \tag{3.12}$$

and

$$\bar{h}_2 = \frac{1}{Sp}\left(\frac{-\cosh\left(\gamma(L-x)\right)}{p\left(Tw\gamma\sinh(\gamma L)+\cosh(\gamma L)\right)}+\frac{1}{p}\right) \tag{3.13}$$

where $\bar{h}_1$ and $\bar{h}_2$ are the Laplace transformed step responses in layers 1 and 2, p is the Laplace parameter, and γ is

$$\gamma = \sqrt{\frac{Sp}{T(cSp+1)}} \tag{3.14}$$

The responses to precipitation and evaporation are assumed to be equal in magnitude but opposite in sign.

For the step response to the river stage,

$$\bar{h}_1 = \frac{\bar{h}_2}{cSp+1} \tag{3.15}$$

and

$$\bar{h}_2 = -\frac{\sinh\left(\gamma(2L-x)\right)}{p\left(Tw\gamma\cosh(2\gamma L)+\left(\sinh(2\gamma L)\right)\right)} \tag{3.16}$$

These solutions can be verified by substituting them in the corresponding differential equations and boundary conditions. Back transformation of the step functions from the Laplace domain to the time domain is performed numerically by the method of Stehfest [*Stehfest*, 1970].

3.4.2 Time series modeling

The extended flood wave method, now in a time series framework, is run by calculating the groundwater heads at each time step and at each piezometer using equation (3.6). The parameters of the time series model are estimated by a modified Gauss-Newton algorithm [*Hill*, 1998] by maximizing the Nash-Sutcliff coefficient E [*Nash and Sutcliffe*, 1970] defined as:

$$E = 1 - \frac{\sum_{i=1}^{N}\left(h_{o,i} - h_{m,i}\right)^2}{\sum_{i=1}^{N}\left(h_{o,i} - \mu_o\right)^2} \tag{3.17}$$

where $h_{o,i}$ is the observed head at time i, $h_{m,i}$ is the modeled head at time i, and μ_o is the average observed head.

It is recalled that the parameters of the extended flood wave method are the transmissivity of the semi-confined layer T [L^2T^{-1}], the storage coefficient of the phreatic layer S [-], the resistance to vertical flow of the aquitard c [T], the specific resistance of the stream bed w [TL^{-1}], the distance between the river bank and the constant head boundary $2L$ [L] and the drainage base *d* [L], and parameter α of the exponentially decreasing noise model. These parameters are estimated by maximizing the Nash Sutcliffe coefficient (3.17). The drainage base is fixed to the average stream stage over the simulation period. The river stage time series was consequently modified by taking the stage relative to the average stage instead of taking the absolute stage value.

3.5 Analysis and interpretation

The observed heads and the heads explained by the deterministic part of the time series model are presented in Figure3-3. The separate contributions of the three stresses are presented in Figure 3-4. The observed heads indicate that the average head and the amplitude of the fluctuation increases with the distance from the draining stream and is the largest for the phreatic piezometer P12 located 70 m from the stream bank (Figure 3-1). This is satisfactorily reproduced by the time series model. The peaks observed for P12 caused by precipitation cannot be simulated by the time series model. For the semi-confined piezometers P7 and P8, the influence of the stream stage dominates the fast fluctuations while precipitation and evaporation cause slower fluctuations. Within the modeled time period (October 2011 - February 2012), evaporation decreases which is reflected by the decreasing contribution (in absolute value) of the evaporation component for all 3 piezometers. Note also that the contribution of the stream stage to the head fluctuations in piezometer P8 is damped compared to piezometer P7 and is almost absent in the case of the phreatic piezometer P12.

The Nash-Sutcliffe coefficients are given for each piezometer in Table 3-2. The second column gives the coefficients including the noise model. The third column gives the coefficients for the deterministic part only.

Table 3-2 Nash-Sutcliffe coefficient of the modeled fluctuations using the extended flood wave method

Piezometer	Nash-Sutcliffe with noise model	Nash-Sutcliffe deterministic
P7	0.96	0.89
P8	0.95	0.82
P12	0.90	0.76

The optimal parameters are given below. The estimates of the 95% confidence intervals are given in brackets. The estimated correlation coefficients are given in Table 3-3.

- Transmissivity semi-confined layer T : 108 m^2d^{-1} [80-147]
- Resistance to vertical flow of the aquitard c : 79 d [48-127]
- Phreatic storage coefficient S : 0.14 [0.11-0.17]
- Stream bed specific resistance w : 0.044 dm^{-1} [0.031-0.065]
- Distance L : 640m [420-986]
- Exponent of noise model α : 0.15 [0.11,0.19]

The confidence intervals vary from +/- 21% to +/- 50%, which is similar to confidence intervals obtained with pumping tests. The distance is strongly correlated with the noise decay parameter. Note, however, that the two parameters are not estimated for use in a distributed numerical groundwater model, like the other estimated parameters.

Table 3-3: Correlation coefficients for the parameters of the extended flood wave method

	T	c	S	w	L	α
T	1	-0.20	-0.38	0.22	-0.53	0.80
c		1	-0.72	-0.52	-0.17	0.10
S			1	0.35	0.29	-0.43
w				1	-0.64	0.48
L					1	-0.92
α						1

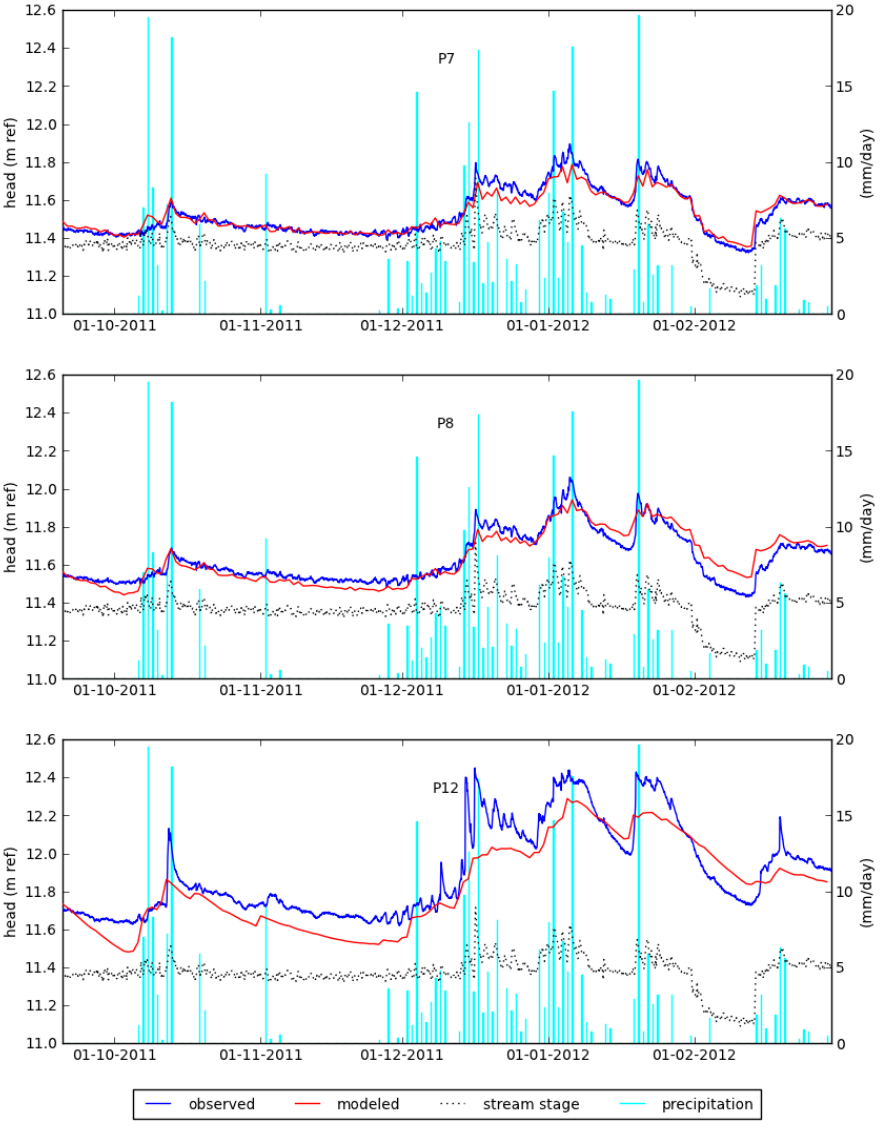

Figure 3-3: Time series model of the head at piezometers P7, P8, and P12 with observed head, observed river stage, and observed precipitation

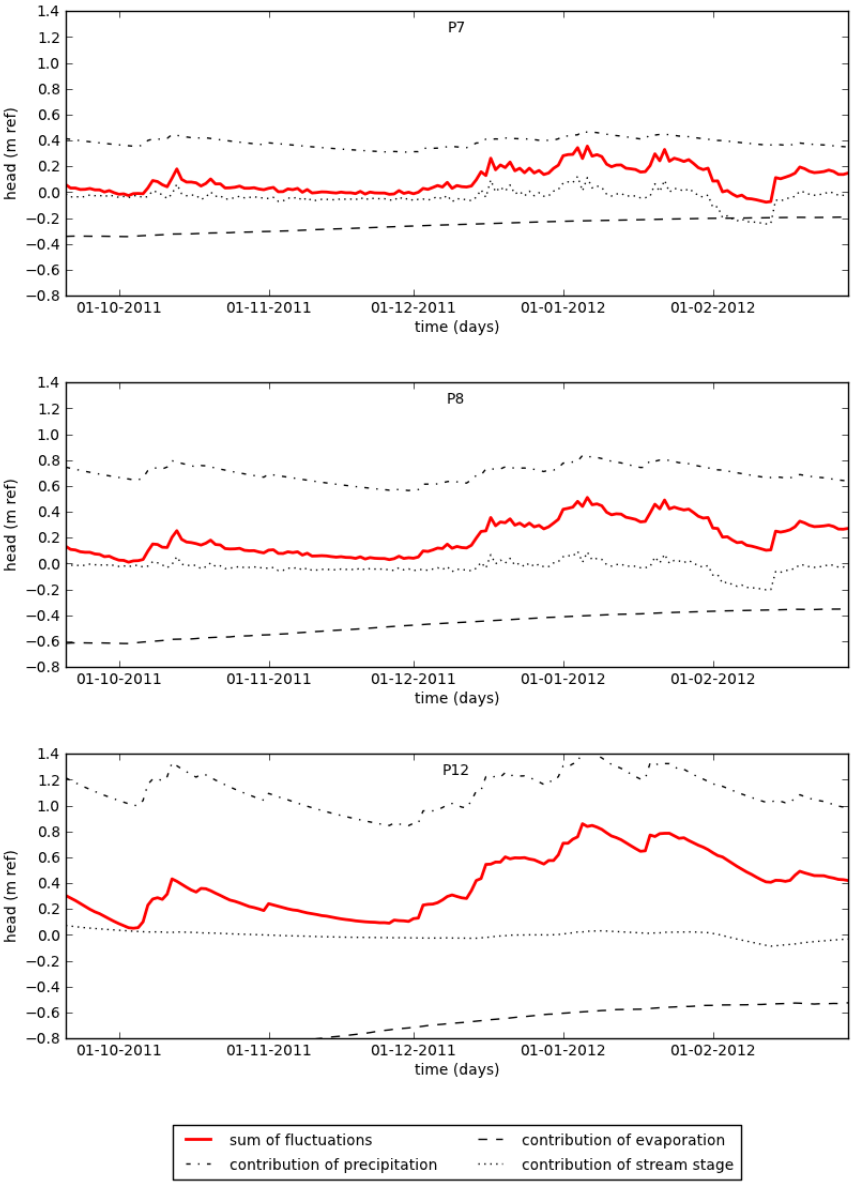

Figure 3-4: Modeled contributions of the different stresses to the fluctuations of the groundwater head at piezometers P7, P8, and P12, as inferred from the time series model

Transmissivity

The value of the transmissivity of the semi-confined layer is lower than *a priori* expected. The layer thickness as described in Table 3-1 is estimated as 25 m, and from the bore log descriptions, a hydraulic conductivity of a least 10 m/d is expected. An estimated transmissivity of 108 m^2/d suggests an aquifer thickness

less than 15 m. An explanation for an apparently thinner aquifer is the presence of silt and peat layers in the formation of Stramproy, constituting the lower 10 m of the semi-confined layer. These semi-pervious layers were assumed to be discontinuous with no confining effect, but the results suggest that the formation of Stramproy acts as a semi-pervious layer reducing the thickness of the investigated semi-confined layer.

Storage coefficient

The value of the storage coefficient obtained for the phreatic layer is 0.14, which is a reasonable value for phreatic layers. It is interesting to mention that *Barlow et al.* [2000] applied the flood wave method to find a specific storage coefficient of 9.8×10^{-5} m^{-1} for a shallow water table aquifer with a thickness of about 20m. The explanation given for this apparent elastic storage was that the thick capillary fringe confines the aquifer. This does not seem to be the case in the present study. An important difference is that the monitoring well in *Barlow et al.* [2000] is much deeper than the monitoring well used in this study.

Specific stream bed resistance

The response functions lump the head loss due to a semi-pervious stream bed and head loss due to the significant vertical flow component in the vicinity of the stream; the latter is referred to a stream line contraction. The estimated value of the specific stream bed resistance is 0.044 dm^{-1}. This low value suggests that the head loss is exclusively the result of stream line contraction. This is supported by field observation of the stream bed which did not reveal the presence of a semi-pervious river bed. This hypothesis is tested by evaluating the magnitude of the head loss due to stream line contraction using an analytical, two-dimensional cross-sectional model of an aquifer discharging into a stream.

The two-dimensional cross-section shown in Figure 3-5 represents an aquifer fed with areal recharge R, discharging into a shallow stream. The aquifer is a finite strip of thickness D [L], with horizontal and vertical hydraulic conductivities k_x and k_y, respectively. The bottom and top boundaries are impermeable, except along the stream bed. The width of the stream is $2B$ [L]. The origin of the coordinate system is at the stream-aquifer boundary.

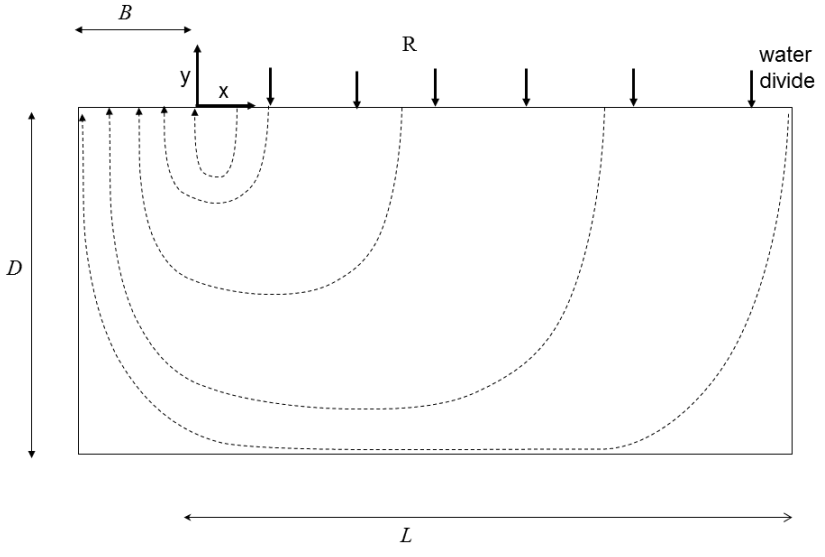

Figure 3-5: Two-dimensional groundwater flow of precipitation discharging into a stream

The stream is in direct contact with the aquifer, with no semi-pervious stream bed. Aquifer discharge into the stream is assumed to be equally distributed over the stream bed.

The solution is:

$$\varphi(x,y)=\sum_{n=1}^{\infty}\frac{\frac{d\bar{\varphi}_n}{dy}(y=0)}{\alpha_n\sinh(\alpha_n D)}\left(\cosh(\alpha_n(D+y))\cos\left(\frac{\alpha_n(L-B-x)}{\sqrt{a}}\right)-c\,\mathrm{os}\left(\frac{\alpha_n}{\sqrt{a}}(1-B/L)\right)\cosh(\alpha_n D)\right) \tag{3.18}$$

with $a=\frac{k_x}{k_y}$, $\alpha_n=\frac{n\pi}{L}\sqrt{a}$ and $\frac{\mathrm{d}\bar{\varphi}_n}{\mathrm{d}y}(\mathrm{y}=0)=-2(-1)^n\frac{R}{k_y}\frac{\sqrt{a}}{\alpha_n B}\sin\left(\frac{\alpha_n B}{\sqrt{a}}\right)$. (3.19)

The derivation of this solution is given in appendix 2.

The two-dimensional head distribution is plotted in Figure 3-6 for an isotropic situation with a recharge rate of $R=$ 0.001 md^{-1}, $L=$ 640m, thickness $D=$ 15m, and $k_x=k_y=$ 6.7md^{-1}.

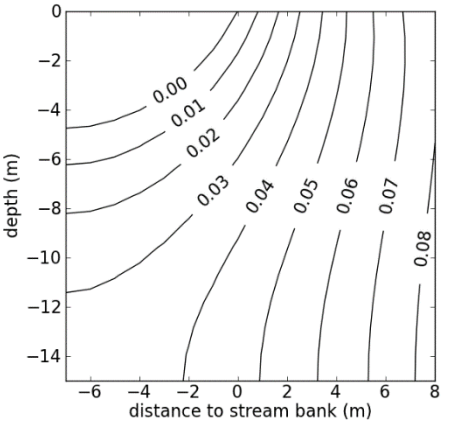

Figure 3-6: Groundwater head (in meter) in a two dimensional cross-section of an aquifer discharging into a stream, obtained from equation (18) with a recharge rate of $R =$ 0.001 md^{-1}, $L =$ 640m, thickness $D =$ 15m, and $k_x = k_y =$ 6.7md^{-1}; the contour line h=0 is the approximate bottom of the stream.

The two-dimensional cross-sectional model is used to estimate the magnitude of the head loss due to stream line contraction. The one-dimensional (Dupuit) solution to the stated problem with boundary condition (3.9) and $h_s = 0$, is well known and equals

$$\varphi(x) = R\left(-\frac{x^2}{2k_x D} + \frac{Lx}{k_x D} + Lw\right) \tag{3.20}$$

Head loss by stream line contraction is accounted for by the specific stream bed resistance w. Different values of w correspond to different values of the vertical anisotropy factor. For example, consider an aquifer of thickness $D =$ 15m and horizontal permeability $k_x = 6.7$ m.d^{-1} (transmissivity $T = 108$ m^2.d^{-1}). The head calculated by the one-dimensional and two-dimensional models are compared in Figure 3-7. Blue corresponds to the head of the one-dimensional model, red corresponds to the head of the isotropic two-dimensional model at a depth of half of the layer thickness. The value of w in the one-dimensional model is adjusted so that the one-dimensional and two-dimensional models coincide for large values of x, which gives $w = 0.04$ d.m^{-1}. This value is approximately equal to the value obtained by parameter estimation of the time series model so that it may be concluded that the specific stream bed resistance estimated with the extended flood wave method can be used to represent head losses due to stream line contraction.

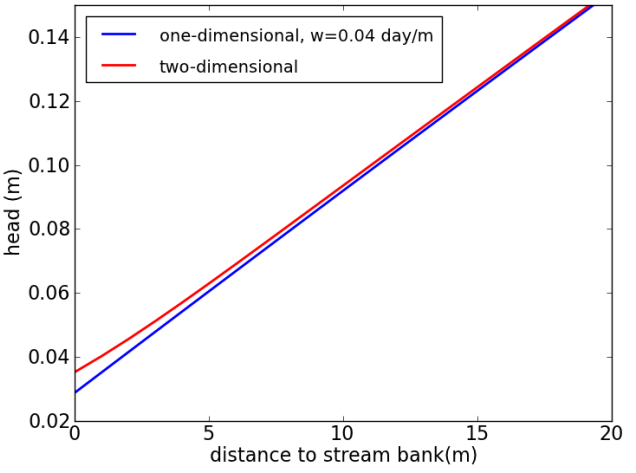

Figure 3-7: Heads for one-dimensional model with $w = 0.04$ d.m^{-1} and recharge $R = 0.001$ m.d^{-1} (blue) and two-dimensional model (red) at depth of half of layer thickness.

3.6 Use of the derived parameters in a numerical groundwater model

In this section, the aquifer parameters estimated with the extended flood wave method are used in a distributed numerical groundwater flow model to evaluate their adequacy as first estimates. This is to be compared with using parameters obtained from a pumping test or from the original flood wave method into a numerical groundwater model.

A distributed numerical groundwater model of the field site was built using the same schematization and approximations. The numerical model was implemented with the finite element code Microfem [*Hemker and de Boer*, 1997], which allows for the refinement of the mesh along the streams which were imported from a GIS-shape file. The numerical model consists of a phreatic, low permeable top layer overlying a semi-confined layer where the Dupuit approximation is adopted. Horizontal flow in the phreatic layer is made negligible by fixing the transmissivity to a small value. Model boundaries are either head-dependent when corresponding to a stream, or no-flow boundaries when approximately corresponding to a water divide. Head-dependent boundaries are attributed a head value of zero assuming that stream fluctuations do not influence each other. The modeled area is shown in Figure 3-1.

The stream bed resistance w' [T] in the numerical model is obtained through multiplication of the specific resistance w [TL^{-1}] obtained with the extended flood wave method through multiplication with the half width B of the stream with $B = 7$ m.

Parameters of the numerical model that were not estimated with the extended flood wave method are:

- stream bed resistance for streams other than the river Aa: 0.5 d;
- width of streams other than the river Aa: 2 m;
- transmissivity of the phreatic layer: 0.1 m^2d^{-1};
- specific storage coefficient of the semi-confined layer: 10^{-4} m^{-1}.

Trying other realistic values for these parameters had only a minor impact on the calculated heads.

Groundwater heads are calculated with Microfem as suggested by *Olsthoorn* [2008] by first evaluating the step responses at the place of the piezometers, after which head fluctuations are obtained by convolution of the block response functions with their corresponding stress time series. Finally, the simulated groundwater heads are obtained by adding the drainage base (which is the mean river stage here) as given in (3.6). The fit obtained from the numerical groundwater model is satisfying for the semi-confined piezometers, with Nash-Sutcliff coefficients of 0.87 and 0.80 for P7, P8 respectively. The fit for the phreatic piezometer P12 is less good, with a Nash-Sutcliffe coefficient of 0.73, similar to the value of 0.76 obtained with the extended flood wave method (Table 3-2). As with the extended flood wave method, the model failed to reproduce the fluctuation peaks in piezometer 12 (Figure 3-8).

3.7 Discussion and conclusion

The objective of this study is to derive aquifer parameters for use in groundwater models from naturally fluctuating heads observed in the vicinity of a stream. The original flood wave method cannot be applied when the effects of stream stage variations cannot be distinguished from those of precipitation and evaporation by simple inspection of the groundwater head hydrograph. To deal with this problem, the flood wave method is implemented in the framework of time series analysis to identify the fluctuations associated with each of the stresses (in this study precipitation, evaporation, and stream stage variations). The method is called the extended flood wave method. Convolution of a stress with its corresponding response function provides the effect of that stress on the head. From a time series modeling perspective, the method proposed is a variation of the method of predefined response functions (Von Asmuth, et al.,2002). The response functions of the extended flood wave method are to be compared with the well function of a pumping test: they translate observed heads into aquifer parameters with a minimum of parameters. An important difference with the original flood wave method and pumping tests is that aquifer parameters are estimated from the superimposed effects of precipitation, evaporation, and stream stage fluctuations.

The method is illustrated with a case study for an aquifer drained by a low-land river in the Netherlands. The response functions of the time series model represent a cross-section of an aquifer underlying a low permeable phreatic layer, discharging into a stream. The model describes the essential features of the

hydrogeological situation, while keeping it as simple as possible to restrict the number of parameters to optimize. The time series model results in a good fit for the semi-confined piezometers, reproduces the slow fluctuations of the phreatic top layer, but fails to reproduce the quick reactions in the top layer, probably due to non-linear processes which are not taken into account by the model.

The order of magnitude of the estimated parameters gives qualitative insight into the groundwater system considered. The value of the transmissivity, for example, suggests a new interpretation of the bore logs. The intercalated silt and peat sub layers, revealed by the bore logs at a depth of about 15 m below ground level, might practically form the aquifer bottom instead of a deeper clay layer as initially assumed. The low value found for the resistance of the stream bed suggests the absence of a semi-pervious river bed. Head loss is the result of stream line contraction in the vicinity of the river, as confirmed by comparing head losses evaluated with an analytical solution for two-dimensional flow in a vertical cross section of an aquifer discharging into a stream.

As for pumping tests, aquifer parameters that are estimated with the extended flood wave method can be used in a numerical distributed groundwater flow model as prior estimates. It is essential that the numerical model shares the same schematization and assumptions as used in the extended flood wave method, similar to what is done with pumping tests. A numerical groundwater model, parametrized in this way, results in a pretty good fit, except again for the quick reactions in the top layer.

Some evaluative remarks are made about the methodology proposed in this study. First, the time series model was fitted over a relatively short time period which did not allow the observations time series to be split into a calibration and a validation period. Note that this is similar to pumping tests that are usually conducted over a short period of time. A validation period is particularly recommended when a time series model is used for predictions.

Second, the conceptual model needs to be kept as simple as possible while incorporating sufficient complexity to match the hydrogeological situation. In an early phase of this study, a simpler groundwater model without the phreatic layer was used, but no reasonable fit with the observed head was possible. The minimum complexity that needs to be incorporated is the additional layer with phreatic storage. Third, the extended flood wave method relies on a simplification of the reality like any model. The validity of the approximations needs to be considered by the practitioner for each new situation. For example in this study, the fluctuations of the river had negligible impact on the distance between the observation wells and the river bank. This might not be the case for other rivers. The parallel should be drawn again with pumping tests requiring the choice of an adequate well function. Different contexts require different solutions. Barlow et al., 2000 offer a number of solutions that could be used as an alternative.

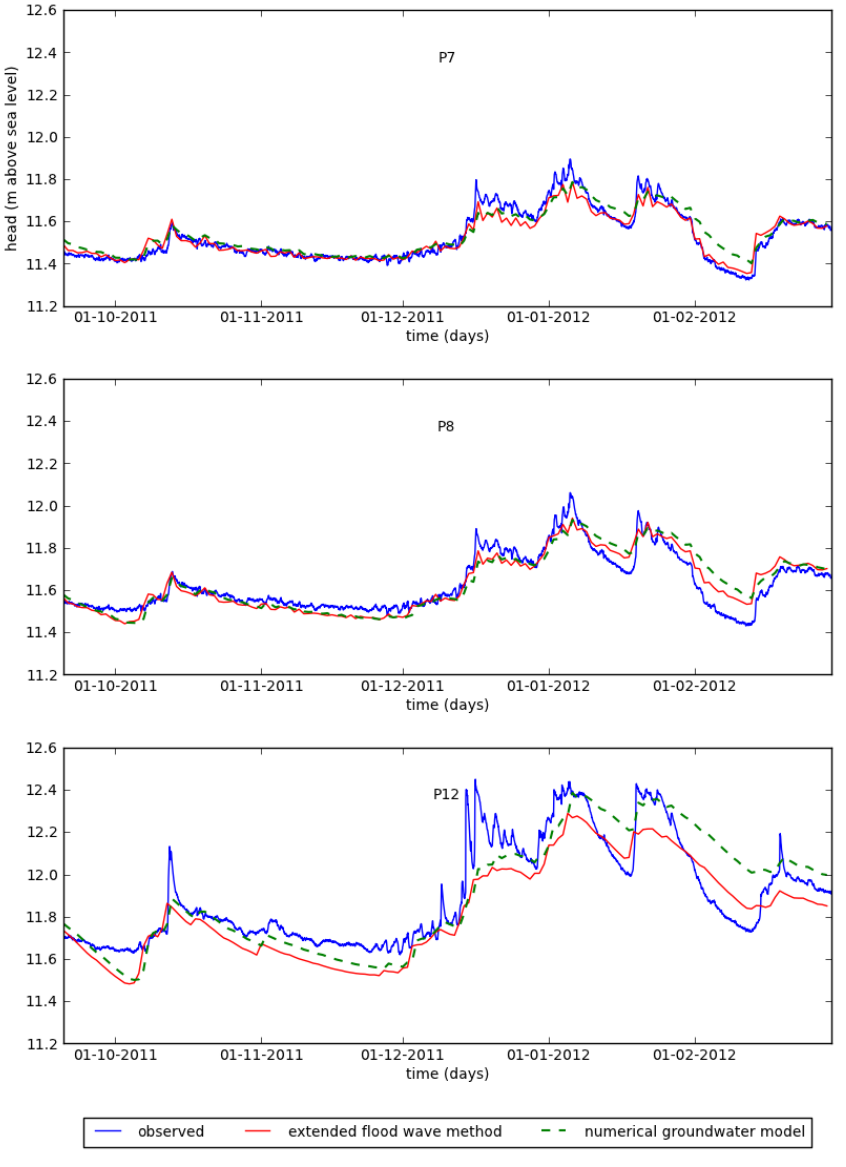

Figure 3-8: Comparison of heads simulated with the time series model and heads calculated with the numerical groundwater flow model with the same parameters as the time series model

3.8 Appendix 1: Laplace transform of the boundary value problem leading to the step functions

Laplace transformation of the set of equations (3.8) with boundary conditions (3.9) and (3.10) initial conditions (3.11) yields the following relations:

$$\begin{aligned} \bar{h}_1 &= \frac{p\bar{h}_2 + cR}{p(cSp+1)} \\ \frac{\mathrm{d}^2\bar{h}_2}{\mathrm{d}x^2} &- \gamma^2\bar{h}_2 + \frac{\gamma^2 R}{Sp^2} = 0 \end{aligned} \tag{3.21}$$

Boundary conditions for recharge:

$$\begin{aligned} &\frac{\mathrm{d}\bar{h}_2}{\mathrm{d}x} = 0,\ x = L \\ &T\frac{\mathrm{d}\bar{h}_2}{\mathrm{d}x} = \frac{\bar{s}_2}{w},\ x = 0 \end{aligned} \tag{3.22}$$

Boundary conditions for stream stage variation:

$$\begin{aligned} &\bar{h}_2 = 0,\ x = 2L \\ &T\frac{\mathrm{d}\bar{h}_2}{\mathrm{d}x} = \frac{\bar{h}_2 - \frac{1}{p}}{w},\ x = 0 \end{aligned} \tag{3.23}$$

where $\bar{h}_1$ and $\bar{h}_2$ are respectively the Laplace transforms of the head in the phreatic and semi-confined aquifer, and p denotes the Laplace domain variable [T^{-1}].

3.9 Appendix 2: Derivation of the equation for the two-dimensional cross-sectional flow

In this appendix, the equation for the two-dimensional flow system presented in section 3.5 is derived. The corresponding conceptual model was shown in Figure 3-5. It features a two-dimensional groundwater flow, fed by precipitation and discharging into a stream. The origin of the coordinate system in Figure 3-5 is the top of the stream bank on top of the flow system. In the derivation of the solution, by means of a cosine transformation, the origin of the coordinate system needs to be located on the water divide on top of the aquifer, as shown in Figure 3-9.

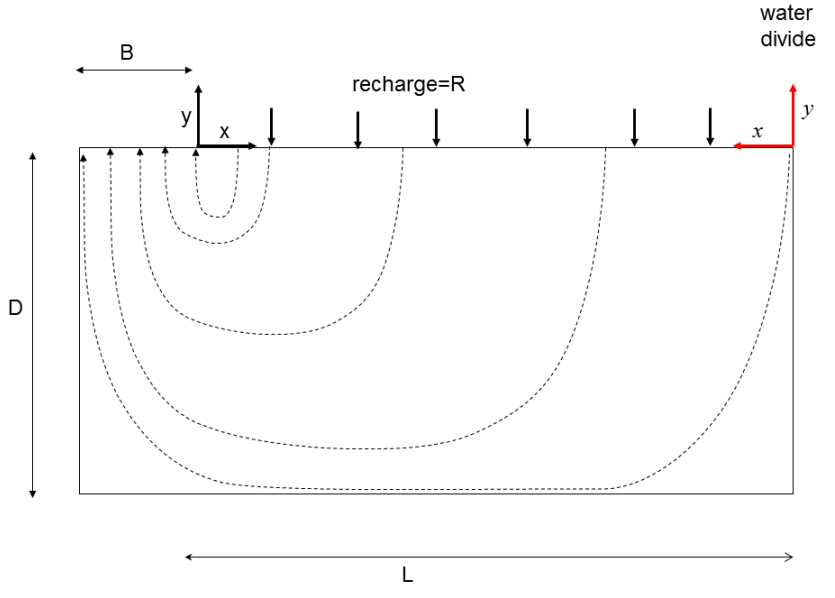

Figure 3-9: Two-dimensional groundwater flow of precipitation discharging into a stream with water divide as origin of coordinates system (red)

As shown in Figure 3-9, the coordinate X used in Figure 3-5 is transformed into the coordinate $x = L - X$.

The head $\varphi(x, y)$ satisfies Laplace's equation:

$$k_x \frac{\partial^2 \varphi}{\partial x^2} + k_y \frac{\partial^2 \varphi}{\partial y^2} = 0 \qquad (3.24)$$

with boundary conditions

$$\begin{cases} \varphi(x=L, y=0)=0 \\ \dfrac{\partial \varphi}{\partial x}(0, y)=0 \\ \dfrac{\partial \varphi}{\partial x}(L+B, y)=0 \\ \dfrac{\partial \varphi}{\partial y}(x,-D)=0 \\ \dfrac{\partial \varphi}{\partial y}(x,0)=\dfrac{R}{k_y} \quad 0 \le x \le L \\ \dfrac{\partial \varphi}{\partial y}(x,0)=-\dfrac{(L-B)}{B}\dfrac{R}{k_y} \quad L < x < L+\mathrm{B} \end{cases} \tag{3.25}$$

Defining the vertical anisotropy factor as:

$$a=\frac{k_x}{k_y} \tag{3.26}$$

a new parameter α_n is defined to condense the notation in the Fourier transformation:

$$\alpha_n=\frac{n\pi}{L}\sqrt{a} \tag{3.27}$$

The Fourier cosine transformation, with period $2L$, of the head $\varphi(x, y)$ is:

$$\begin{cases} \bar{\varphi}_0(y)=\dfrac{1}{L}\displaystyle\int_0^L \varphi(x, y)dx \\ \bar{\varphi}_n(y)=\dfrac{2}{L}\displaystyle\int_0^L \varphi(x, y)\cos\left(\dfrac{n\pi x}{L}\right)dx \\ \varphi(x, y)=\bar{\varphi}_0(y)+\displaystyle\sum_{n=1}^{n=+\infty}\bar{\varphi}_n(y)\cos\left(\dfrac{n\pi x}{L}\right) \end{cases} \tag{3.28}$$

The transformation of the differential equation is:

$$\frac{\mathrm{d}^2\bar{\varphi}_\mathrm{n}}{\mathrm{dy}^2}-\alpha_\mathrm{n}{}^2\bar{\varphi}_\mathrm{n}=0 \tag{3.29}$$

Transformation of the boundary conditions for $n>0$ gives

$$\begin{cases} \dfrac{d\bar{\varphi}_n}{dy}(y=-D)=0 \\ \dfrac{d\bar{\varphi}_n}{dy}(y=0)=-2(-1)^n\dfrac{R}{k_y}\dfrac{\sqrt{a}}{\alpha_n B}\sin\left(\dfrac{\alpha_n B}{\sqrt{a}}\right) \end{cases} \tag{3.30}$$

For n>0, the solution of the cosine transformed function is

$$\bar{\varphi}_n(y)=\frac{\dfrac{d\bar{\varphi}_n}{dy}(y=0)}{\alpha_n\sinh(\alpha_n D)}\cosh(\alpha_n(D+y)) \tag{3.31}$$

which allows to determine all terms of the cosine except for n=0:

$$\varphi(x,y)=\bar{\varphi}_0(y)+\sum_{n=1}^{\infty}\frac{\dfrac{d\bar{\varphi}_n}{dy}(y=0)}{\alpha_n\sinh(\alpha_n D)}\cosh(\alpha_n(D+y))\cos(\alpha_n x) \tag{3.32}$$

For n=0, the differential equation (3.29) implies that $\dfrac{d\bar{\varphi}_0}{dy}$ is a constant, which in turns, from the 4th condition in (3.25), results in the following implications:

$\dfrac{d\varphi}{dy}(y=-D)=0 \Rightarrow \dfrac{d\bar{\varphi}_0}{dy}(y=-D) \Rightarrow \dfrac{d\bar{\varphi}_0}{dy}(y)=0$. So $\bar{\varphi}_0$ is a constant.

This constant can be determined from the 1st condition in (3.25):
$\varphi(x=L,y=0)=0$. Filling this condition in (3.32) with $x=L$ and $y=0$ gives:

$$\bar{\varphi}_0(y)=\sum_{n=1}^{\infty}(-1)^n\frac{\dfrac{d\bar{\varphi}_n}{dy}(y=0)}{\alpha_n\sinh(\alpha_n D)}\cosh(\alpha_n D) \tag{3.33}$$

The Fourier series is now completely defined resulting in the solution:

$$\varphi(x,y)=\sum_{n=1}^{\infty}\frac{\dfrac{d\bar{\varphi}_n}{dy}(y=0)}{\alpha_n\sinh(\alpha_n D)}\left(\cosh(\alpha_n(D+y))\cos\left(\frac{\alpha_n x}{\sqrt{a}}\right)-c\cos\left(\frac{\alpha_n(L-B)}{\sqrt{a}}\right)\cosh(\alpha_n D)\right) \tag{3.34}$$

with $\frac{d\bar{\varphi}_n}{dy}(y=0) = -2(-1)^n \frac{R}{k_y} \frac{\sqrt{a}}{\alpha_n B} \sin\left(\frac{\alpha_n B}{\sqrt{a}}\right)$.

Chapter 4 Estimation of average diffuse aquifer recharge using time series modeling of groundwater heads

Abstract
A new method is presented to estimate average diffuse aquifer recharge of water table aquifers in temperate climates using time series analysis of water table level fluctuations. An accurate estimate of the recharge caused by rainfall requires an accurate estimate of the influence of evaporation. In temperate climates, evaporation imprints a seasonal component in the water table fluctuations. As such, recharge is estimated from time series models fitted to observed heads under the additional constraint that the seasonal harmonic of the observed head is reproduced as the sum of the transformed seasonal harmonics present in precipitation, evaporation, and pumping. An explicit equation is presented, in terms of the model parameters, for the damping and phase shift of the response to the seasonal harmonic of the stresses. Taking into account the seasonal harmonic of the observed heads results in more reliable recharge estimates compared to standard time series analysis. The method is limited to systems that are sufficiently linear and that remain unaltered over the analysis period. Head fluctuations and stresses should contain a seasonal harmonic that can be estimated with accurately. Runoff must be negligible or quantifiable. The method is applied to measured heads obtained from piezometers situated on and around the ice-pushed sand ridge of Salland in the Netherlands and compares well with recharge estimates based on the saturated zone chloride mass balance.

Adapted from C. Obergfell, M. Bakker, and K. Maas, Estimation of Average Diffuse Aquifer Recharge Using Time Series Modeling of Groundwater Heads, Water Resources Research, 55(3), 2194-2210, doi: 10.1029/2018WR024235, 2019

4.1 Introduction

Natural groundwater recharge, the replenishment of aquifers from precipitation, is one of the major subjects of investigation in hydrology, but still remains a difficult component to estimate in the water balance of an area [e.g., *Healy*, 2012; *Bakker et al.*, 2013]. A large number of techniques exist to try to quantify groundwater recharge for various time and space scales [*Healy and Cook*, 2002]; each technique requires different input data, from simple head measurements to detailed hydrochemistry. *Scanlon et al.* [2002] review the various techniques and propose an iterative approach to recharge estimation, refining the estimates as additional data are gathered. A wide variety of approaches is recommended in order to increase the confidence in recharge estimates. The topic of this study is to add a new approach to estimate average diffuse aquifer recharge over large time periods (years to tens of years). It is based on time series analysis of measured head variations combined with measured stresses on the aquifer, including rainfall, reference evaporation and pumping.

One approach to estimate recharge from measured head variations and rainfall is the water table fluctuation method. In its original form, it is applicable to short-term water level rises that occur in response to individual storm events [*Meinzer*, 1923; *Healy and Cook*, 2002; *Healy*, 2012], neglecting the slow but continuous water table recession that may take place in response to previous recharge events. Recent developments aimed at applying the water-table fluctuation method over longer time periods, while systematically taking into account the effect of aquifer drainage and cumulating the effect of successive rain events. This can be achieved using the master recession curve (MRC) method [*Heppner and Nimmo*, 2005; *Nimmo et al.*, 2015], either by quantifying the drainage intensity [*Crosbie et al.*, 2005], or by using an analytical groundwater model [*Cuthbert*, 2010]. In all these methods, identification of the drainage parameters and the specific yield remain a challenge.

In groundwater hydrology, time series analysis has been used primarily to model and predict groundwater heads. Different methods are employed: transfer function noise models of the Box and Jenkin's type [e.g., *Baggelaar*, 1988; *Gehrels et al.*, 1994; *van Geer and Zuur*, 1997], models based on the convolution of response functions [e.g., *Von Asmuth et al.*, 2002; *Manzione et al.*, 2012; *Peterson and Western*, 2014], or physically based models [e.g., *Berendrecht et al.*, 2006]. A common issue in many of these methods is the correlation between model parameters that determine the influence of evaporation and pumping [e.g. *Shapoori et al.*, 2015c]. Equally good fits of the observed heads can be obtained when, for example, the effects of groundwater pumping are compensated by the effects of evaporation, or vice versa [*Shapoori et al.*, 2015c]. This problem of equifinality is undesirable, especially when the model parameters are intended to be used to quantify physical quantities like groundwater recharge [e.g., *Beven*, 1993].

The objective of this study is to estimate time-averaged groundwater recharge using time series analysis of groundwater heads. A reliable estimate of

the recharge requires an accurate identification of the influence of evaporation on groundwater head fluctuations. In temperate climates, evaporation, more than any other stress, dictates the seasonal behaviour of the water table fluctuation. It stands to reason that if two parameter sets of a time series model give a similar fit, the evaporation is better estimated by the parameter set that matches the seasonal behaviour better. The seasonal behaviour of the water table can be characterized by the sinusoidal component with a period of one year, referred to here as the seasonal harmonic. The approach presented in this study uses the seasonal harmonic as an additional signature that is implemented in the form of a model optimization constraint. The inclusion of multiple signatures of the hydrological response when calibrating a model is also applied in other parts of hydrology [e.g., *Koutsoyiannis*, 2010; *Euser et al.*, 2013; *Hrachowitz et al.*, 2014].

This study is organized as follows. First, time series analysis by the method of predefined response functions is reviewed briefly. Second, equations are derived for the seasonal harmonic response caused by rainfall, evaporation, and pumping; these equations are used as a constraint when estimating the time series model parameters. Third, a case study is presented to illustrate the efficacy of the presented approach. In the discussion, recharge estimates obtained with the proposed approach are compared to results from standard time series analysis where the seasonal harmonic is not used as a constraint, recharge estimates for time periods with different mean heads are compared, and the possible effects of the uncertainty in the seasonal harmonic are discussed. Finally, the estimated long-term recharge is compared with an estimate obtained from the saturated zone chloride mass balance method.

4.2 Methods

4.2.1 Time series analysis with pre-defined response functions

The method of time series analysis with predefined response functions is described in several papers [e.g., *Von Asmuth et al.*, 2002; *Peterson and Western*, 2014; *Obergfell et al.*, 2016]. It is briefly reviewed here. The head fluctuations $\varphi(t)$ due to stress time series $q(t)$ at a point in space is obtained by convolution of $q(t)$ with the corresponding impulse response function $\theta(t)$:

$$\varphi(t) = \int_0^t q(\tau)\theta(t-\tau)d\tau \tag{4.1}$$

where t is time. In this study, $\varphi(t)$ is used for the head fluctuation caused by one specific stress, while $h(t)$ is used for the head fluctuation caused by the superposition of all stresses. The dependence of the response function on spatial

coordinates is omitted in this notation. $\theta(t)$ has the shape of the response of the groundwater head to an instantaneous stress event of unit strength (for example an instantaneous shower of unit height). The dimension of $\theta(t-\tau)$ is determined by the dimension of the stress so that the product $q(\tau)\theta(t-\tau)$ has the dimension length, like heads.

Stress time series are commonly piecewise continuous (daily rainfall, for example) while response functions are continuous, so that relation (4.1) needs to be modified as follows. The unit step response function $s(t)$ is obtained from the impulse response function $\theta(t)$ as

$$s(t) = \int_0^t \theta(t-\tau)d\tau \tag{4.2}$$

The step response function has the dimension of length per dimension of stress. From the step response function, the block response function is derived as

$$\psi(t,\Delta t) = s(t) - s(t-\Delta t) \tag{4.3}$$

and represents the response to a unit stress distributed uniformly from $t=0$ to $t=\Delta t$. Time is discretized in stress periods, where Δt_i is the length of stress period i. Stress q_i is approximated as uniform over stress period i from $t=t_i-\Delta t_i$ to $t=t_i$. The head at time t_i is obtained by summing the effects at time t_j of all past stress periods

$$\varphi(t_j) = \sum_{i=1}^{j} q_i \psi\left(t_j - t_{i-1}, \Delta t_i\right) \tag{4.4}$$

where

$$t_j = \sum_{i=1}^{j} \Delta t_i \tag{4.5}$$

This is a discrete form of convolution. Alternatively, the series $\varphi(t_i)$ can be seen as a weighted moving average of the series q, ψ being the weighting function. The modeled heads $h(t)$ are obtained by adding the contributions of all stresses $\varphi_i(t)$ plus a reference level

$$h(t) = \sum_i \varphi_i(t) + d \tag{4.6}$$

where d is called the drainage base here.

The observed heads $h_o(t)$ are equal to the modeled heads plus a residual $r(t)$:

$$h_o(t) = \sum_i \varphi_i(t) + d + r(t) \tag{4.7}$$

Autocorrelation in the residuals is removed by modeling them with an exponential decay process [*Von Asmuth and Bierkens*, 2005]. The residual at time t_i is related to the residual at time t_{i-1} as:

$$r(t_i) = r(t_{i-1}) \exp\left(-\alpha\left(t_i - t_{i-1}\right)\right) + n(t_i) \tag{4.8}$$

where α is the residual decay factor and $n(t_i)$ represents approximate white noise.

Three types of stresses are considered here to simulate head fluctuations: precipitation, evaporation, and pumping. The impulse response function considered for these stresses is a scaled gamma distribution:

$$\theta(t) = M \frac{a^n t^{n-1}}{\Gamma(n)} \mathrm{e}^{-at} \tag{4.9}$$

where M is a scaling factor, a and n define the shape of the function, and $\Gamma(n)$ is the gamma function of n . This response function is commonly applied for precipitation and evaporation [e.g. *von Asmuth et al.*, 2012]. It is also appropriate to simulate the slow response to pumping in a phreatic aquifer when piezometers are not in the direct vicinity of the pumping wells. The corresponding step response function $s(t)$ is a scaled incomplete gamma function of the form:

$$s(t) = \frac{M}{\Gamma(n)} \int_0^t a^n \tau^{n-1} e^{-a\tau} d\tau = M\Gamma(n, at) \tag{4.10}$$

where $\Gamma(n, at)$ is the lower incomplete gamma function of n and at [e.g., *Abramowitz and Stegun*, 1964]. The parameters M , a and n are referred to here as the first, second and third parameter of the incomplete gamma function.

The observed heads and stresses are written with respect to their means, so that (4.7) becomes

$$h_o(t) - \bar{h}_o = \sum_i \left(\varphi_i(t) - \bar{\varphi}_i\right) + d - \bar{h}_o + \sum_i \bar{\varphi}_i + r(t) \tag{4.11}$$

The drainage base is set equal to the mean observed head $\bar{h}_o$ minus the sum of the mean contributions of the stresses (similar to *Von Asmuth et al.* [2002])

$$d = \bar{h}_o - \sum_i \bar{\varphi}_i \tag{4.12}$$

so that

$$h_o(t) - \bar{h}_o = \sum_i \left(\varphi_i(t) - \bar{\varphi}_i\right) + r(t) \tag{4.13}$$

The mean response $\bar{\varphi}_i$ to stress i is computed, using (4.9) as the response function, as

$$\bar{\varphi}_i = \bar{q}_i \int_0^\infty \theta_i(t-\tau)d\tau = \bar{q}_i M_i \tag{4.14}$$

The scaling parameter M_i corresponds to the final response of the groundwater head when stress i is applied continuously with unit intensity.

4.2.2 Estimation of the mean recharge

In this study, the responses to precipitation and to reference evaporation are assumed to have the same shape, sharing the same parameters a and n defined in (4.9), and differ only by their final response magnitudes M_p and M_e, respectively. The ratio of the magnitudes is called f

$$f = \frac{M_e}{M_p} \tag{4.15}$$

further referred to as the evaporation factor.

In the absence of run-off, R represents the diffuse, time averaged groundwater recharge, approximated as precipitation minus all forms of evaporation, which is the sum of interception, transpiration, and soil evaporation, expressed by the relation:

$$R = P - fE \tag{4.16}$$

where P and E are measured precipitation and measured reference evaporation [LT^{-1}], respectively. Possible seasonal dependence of the evaporation factor is not taken into account. The passage through the unsaturated zone is

taken into account by the response to recharge, which mimics a dispersion process [Besbes and de Marsily, 1984; Gehrels et al., 1994].

4.2.3 Seasonal harmonic

Accurate identification of the influence of evaporation on head fluctuations is a crucial requirement for a reliable estimation of the recharge. In the proposed method, this is achieved by taking the best estimate of the seasonal harmonic of the observed heads into account as an additional signature. The seasonal behaviour is represented by the seasonal harmonic component $y(t)$ defined as:

$$y = A\sin(\omega(t-T)) \tag{4.17}$$

where A is the amplitude, T is the phase shift (in days), and ω is $2\pi / 365.25$ (d^{-1}). Since ω is already known, the parameters A and T of a measured time series can be determined with a least squares procedure. A discrete Fourier transformation of the signals using for example a Fast Fourier Transform scheme is an equivalent alternative if all time series are available at equidistant points in time.

Convolution of the seasonal harmonic of a stress time series with amplitude A_s and phase shift T_s with an impulse response function $\theta(t)$ results in a seasonal harmonic with a transformed amplitude $\tilde{A}_s$ and a phase shift $\tilde{T}_s$, as demonstrated in Appendix 1:

$$\tilde{y}(t) = \int_0^\infty A_s \sin\left(\omega\left(t-\tau-T_s\right)\right)\theta(\tau)d\tau = \tilde{A}_s \sin\left(\omega\left(t-\tilde{T}_s\right)\right) \tag{4.18}$$

When the scaled gamma function (4.9) is used for the impulse response function $\theta(t)$, the amplitude ratio $\tilde{A}_s / A_s$ and phase shift Δt_s are (Appendix 1):

$$\frac{\tilde{A}_s}{A_s} = \frac{M_s}{\left(1+\frac{\omega}{a_s}^2\right)^{\frac{n_s}{2}}} \tag{4.19}$$

$$\Delta t_s = \tilde{T}_s - T_s = \frac{n_s}{\omega}\arctan\frac{\omega}{a_s} \tag{4.20}$$

Addition of the seasonal harmonics of the responses to precipitation (amplitude $\tilde{A}_p$ and phase shift $\tilde{T}_p$) and evaporation (amplitude $\tilde{A}_e$ and phase shift $\tilde{T}_e$) results in a new seasonal harmonic given by

$$\tilde{A}_p \sin(\omega(t-\tilde{T}_p)) + \tilde{A}_e \sin(\omega(t-\tilde{T}_e)) = \tilde{A}_2 \sin(\omega(t-\tilde{T}_2)) \qquad (4.21)$$

where amplitude $\tilde{A}_2$ and phase shift $\tilde{T}_2$ are given by:

$$\tilde{A}_2 = \sqrt{\tilde{A}_p^2 + \tilde{A}_e^2 + 2\tilde{A}_p\tilde{A}_e \cos\left(\omega\left(\mathrm{T}_e - \mathrm{T}_p\right)\right)} \qquad (4.22)$$

$$\tilde{T}_2 = \frac{1}{\omega}\arctan\left(\frac{\tilde{A}_e \sin\left(\omega(\mathrm{T}_e - \mathrm{T}_p)\right)}{\tilde{A}_p + \tilde{A}_e \cos\left(\omega(\mathrm{T}_e - \mathrm{T}_p)\right)}\right) + \tilde{\mathrm{T}}_p \qquad (4.23)$$

where Δt_p is the time delay between the seasonal harmonic of the measured time series of precipitation and the seasonal harmonic of the response to precipitation, calculated by relation (4.20). In the derivation of (4.22) and (4.23) it is used that $\tilde{T}_e - \tilde{T}_p = T_e - T_p$, which holds because $\Delta t_e = \Delta t_p$ and the response of precipitation and evaporation have the same parameters a and n (see Eq. (4.20)).

Addition of the seasonal harmonics of the combined response to precipitation and evaporation (amplitude $\tilde{A}_2$ and phase shift $\tilde{T}_2$) to the seasonal harmonic of the response to pumping (amplitude $\tilde{A}_w$ and phase shift $\tilde{T}_w$) results in a new seasonal harmonic with amplitude $\tilde{A}_3$ and phase shift $\tilde{T}_3$ given by:

$$\tilde{A}_3 = \sqrt{\tilde{A}_2^2 + \tilde{A}_w^2 + 2\tilde{A}_w\tilde{A}_2 \cos\left(\omega\left(\tilde{T}_w - \tilde{T}_2\right)\right)} \qquad (4.24)$$

$$\tilde{T}_3 = \frac{1}{\omega}\arctan\left(\frac{\tilde{A}_w \sin\left(\omega\left(\tilde{T}_w - \tilde{T}_2\right)\right)}{\tilde{A}_w + \tilde{A}_2 \cos\left(\omega\left(\tilde{T}_w - \tilde{T}_2\right)\right)}\right) + \tilde{T}_2 \qquad (4.25)$$

where Δt_w is the time delay between the seasonal harmonic of the measured pumping time series and the seasonal harmonic of the response to pumping.

The amplitude A_h and phase shift T_h of the seasonal harmonic of the measured heads is set equal to the sum of the seasonal harmonics of the

responses of all stresses in the time series model. When precipitation and evaporation are the only stresses, this gives the constraint

$$\begin{cases} A_h = \tilde{A}_2 \\ T_h = \tilde{T}_2 \end{cases} \tag{4.26}$$

When pumping is also included, this gives the constraint

$$\begin{cases} A_h = \tilde{A}_3 \\ T_h = \tilde{T}_3 \end{cases} \tag{4.27}$$

4.2.4 Parameter estimation

The time series model is fitted to the available observed heads as given in (4.13), under the constraints (4.26) or (4.27). Parameter optimization is performed by minimizing the objective function $S(\mathbf{p})$ defined as half of the sum of the squared noise terms n_i defined in (4.8):

$$S(\mathbf{p}) = \frac{1}{2}\sum_{i=1}^{N_o} n_i^2 \tag{4.28}$$

where N_o is the number of observations, $\mathbf{p}$ is the vector of N_p model parameters, corresponding to the parameters of the scaled incomplete gamma function of each response function as defined in (4.10) plus the noise decay parameter as defined in (4.8). The search for the minimum of the objective function is performed using a modified Gauss-Newton algorithm [e.g., *Hill*, 1998] starting from initial values selected by applying a preliminary Latin Hypercube sampling of the parameters space [*Iman et al.*, 1981]. Note that starting the optimization from different initial parameter values does not affect the estimation outcome, suggesting the identification of a global optimum.

The constraints (4.26) or (4.27) constitute a system of non-linear equations solved at each iteration of the optimization process for parameters n_p and f applying the modified Powell method, implemented in the MINPACK routines package [*Moré et al.*, 1980], and called from the open-source Python package Scipy [*Jones et al.*, 2001]. The constraints imposed on the model parameters limit the search for the optimal parameters to a sub-region that is unlikely to contain the optimum of the unconstrained models but it corresponds to parameters sets that lead to models that are physically more realistic.
The covariance matrix $\mathbf{C}$ of the logarithm of the optimized parameters is approximated as [e.g., *Yuen*, 2010]:

$$\mathbf{C} = \sigma^2 \mathbf{H}^{-1} \tag{4.29}$$

where $\mathbf{H}$ is the Hessian of the objective function, and σ^2 is the variance of the noise. The Hessian is approximated as $\mathbf{H} \simeq \mathbf{J}^T \mathbf{J}$ where $\mathbf{J}$ is the Jacobian matrix. Confidence intervals of optimized parameters are estimated assuming a Normal distribution around the optimum, scaled by the variance of the parameter as given by the covariance matrix. For an optimal value $\ln(p_i)$ of log-transformed parameter p_i, the lower and upper limits of the 95% confidence interval are:

$$\ln(p_i) \pm 1.96\sigma_{\ln(p_i)} \tag{4.30}$$

The confidence intervals of the back-transformed parameters are obtained by taking the exponential of the lower and upper bounds of the log-transformed parameters. The confidence interval of the estimated recharge is computed using Monte-Carlo simulations of parameters M_p and a_p based on the covariance matrix of the optimized time series models. For each realization, parameters n_p and f are obtained by the constraints described in 4.2.3, using the approach described above. Recharge is inferred from parameter f by applying relation (4.16). The confidence intervals are therefore consistent with constraints (4.26) and (4.27).

4.3 Site description

4.3.1 Hydrogeology

The proposed method is applied to a field site in the ice-pushed ridge of Salland, in the Dutch province of Overijssel, in the vicinity of a drinking water supply well field (Figure 4-1).

Figure 4-1. Field site location

Ice-pushed ridges, also referred to as push moraines, build up at the margin of glaciers. The ice-pushed ridge of Salland was formed during the second to last ice age called the Saalian ice age, from about 200,000 to 130,000 years ago. This period corresponds to the southernmost advance of the ice sheet in Northern Europe during the Pleistocene time. The highest elevation point of the ridge is about 60 m above NAP (the datum used in the Netherlands).

Ice-pushed ridges consist of thrust sheets, the strikes of which generally dip 30-40^{o} towards a glacial basin. In the Netherlands, the thrust sheets consist mainly of sandy formations with possible intercalations of less permeable formations. This internal structure can result in an anisotropic permeability field which is difficult to simulate in a groundwater model due to its heterogeneous character. In Salland, the strike direction is North-South with thrusts dipping to the west.

Both sides of the sand ridge are drained areas corresponding to former water-logged bogs. These zones have been drained in the Middle Ages and are now flat meadows drained by a network of small canals and ditches (Figure 4-2). The vegetation on the ridge consists of heather, grassland, deciduous trees and rather sparse coniferous woods.

4.3.2 Data

Measurements at five piezometers are analyzed. The location of the piezometers is shown in Figure 4-2. Their characteristics are listed in Table 4-1. Heads were recorded twice a month. In the second half of the 1990's, the head fluctuation regime changes as a result of massive dredging works in the main river draining the aquifer investigated. Time series analysis is therefore performed up to that

moment, over the period 1982-1995, which is a period for which measurements are available for all piezometers except piezometer 4 for which data were only available after 1984.

Table 4-1. Piezometers analyzed to estimate groundwater recharge

PN	ID	X	Y	Z	SELEV	MH	Dist
1	28AP0093	224550	488100	2.10	11.60	9.24	2750
2	28AL0019	224668	488474	8.07	10.32	9.15	2900
3	28CP0197	227398	485958	4.70	15.26	8.52	825
4	28CP0204	226894	485364	2.83	21.26	9.59	1025
5	28AP0134	226181	488081	-2.50	22.40	8.46	1800

PN: piezometer number
ID: piezometer identification code of the Dutch Geological Survey Institute.
X (resp. Y): Easting (resp. Northing) in meters, EPSG:28992 Amersfoort/New geographical coordinates system.
Z: depth of the middle of the screen (m NAP)
SELEC: Surface elevation (meter NAP)
MH: Median observed heads (meter NAP)
DIST: Distance to middle of well field (meter)

Daily precipitation and reference evaporation are obtained from the Royal Netherlands Meteorological Institute (KNMI). The reference evaporation is Makkink reference evaporation, defined as the evaporation of well-watered short grass on a regional scale [*De Bruin*, 1987]. Precipitation was measured at the meteorological station of Hellendoorn (Figure 4-2). Daily reference evaporation, which varies much less in space than precipitation, was measured at the meteorological station of de Bilt, about 85 km to the south-west of the field site. A drinking water production well field is in operation on the ridge of Salland since 1954, with pumping records available from 1974 onwards. The average groundwater extraction is 5.10^6 m^3/year. The location of the well field is shown in Figure 4-2.

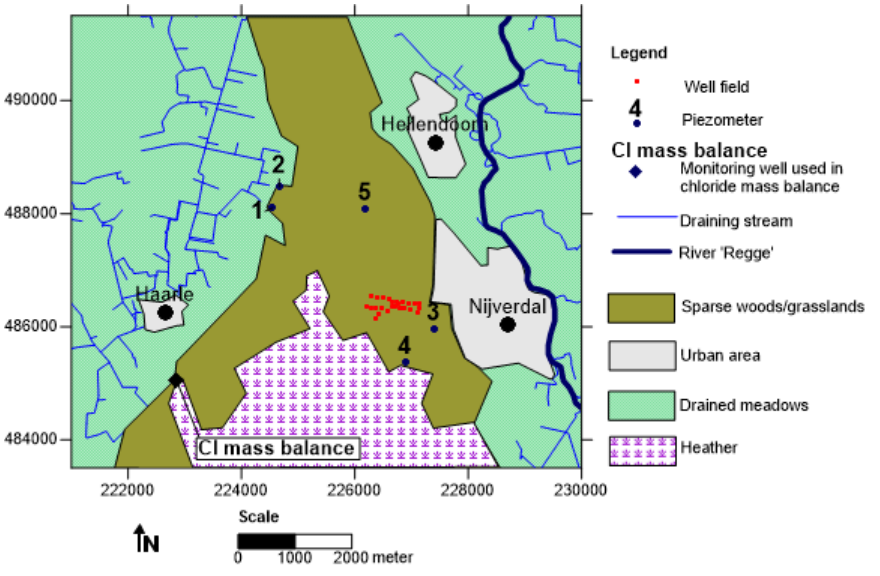

Figure 4-2. Field site

The stress time series and the corresponding seasonal harmonics are plotted in Figure 4-3, together with the hydrographs of piezometers 1 and 3. As the parameters of the response to separate wells could not be identified, the combined discharge of all wells was added in one stress time series, which is a common approximation. The combined pumping time series shows a significant trend, but no significant difference was found between the seasonal harmonics of the pumping time series estimated before and after detrending so detrending was omitted here. Piezometer 1 is a relatively shallow well with a faster reaction to recharge while piezometer 3 is a deeper well with a slower reaction to recharge.

4.4 Results

4.4.1 Model parameters and recharge

The proposed time series modeling approach is applied to the five piezometers given in Table 4-1. For each piezometer, the 9 model parameters are fitted, of which 2 parameters are obtained from the constraint on the seasonal harmonic and the drainage base is computed with (4.12). The effect of pumping was negligible for piezometers 1 and 2, so that only 6 parameters were fitted. The observed and modeled head fluctuations are shown in figure 4-4. The optimal parameters, together with their 95% confidence intervals, are presented in Table 4-2. The corresponding recharge estimates are given in Table 4-3.

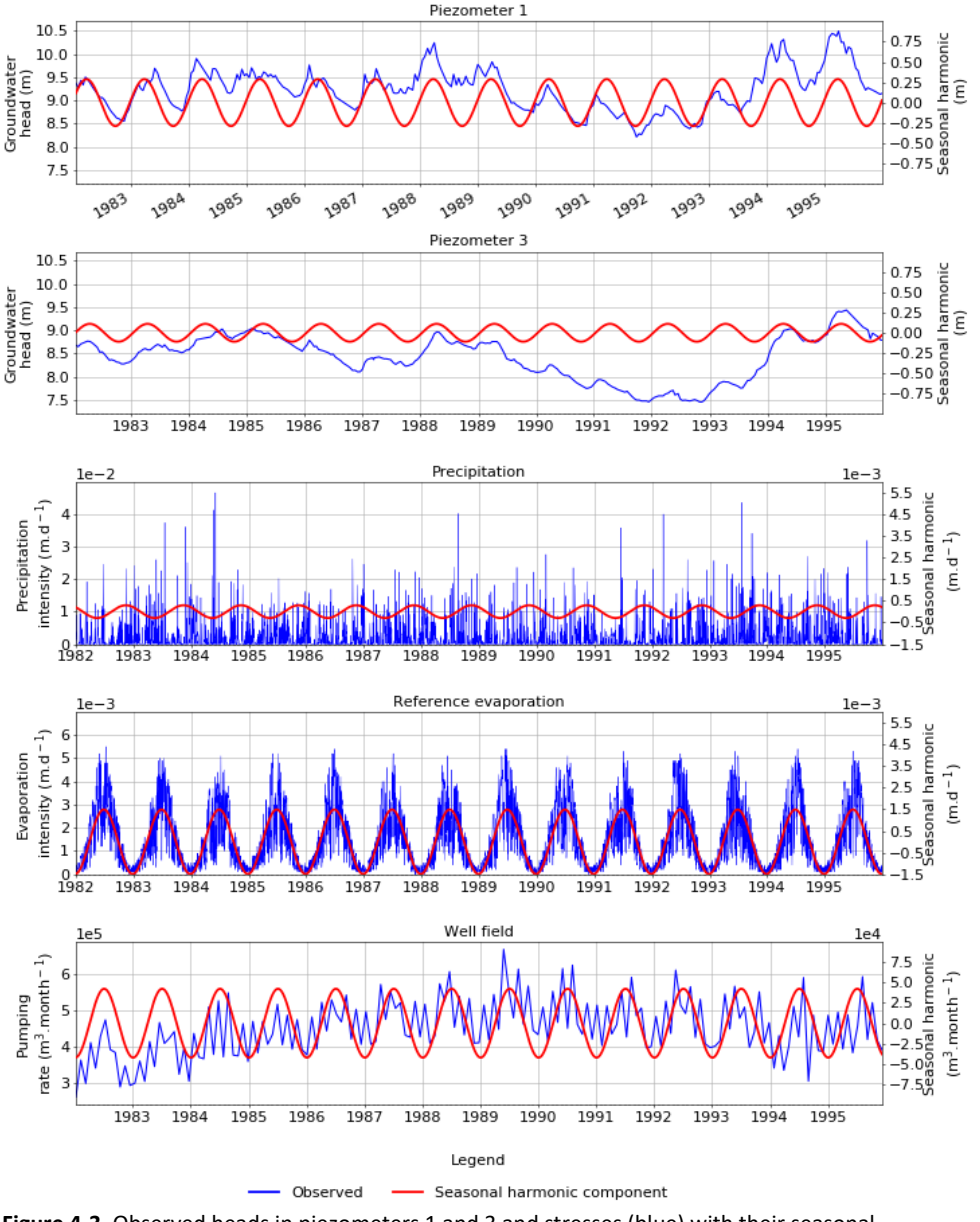

Figure 4-3. Observed heads in piezometers 1 and 3 and stresses (blue) with their seasonal harmonic component (red lines and right axis)

The goodness of fit of the time series models is expressed as the Nash-Sutcliffe coefficient [*Nash and Sutcliffe*, 1970] defined as

$$NS = 1 - \frac{\sum_{i=1}^{N_o} \left(h_{m,i} - h_{o,i} \right)^2}{\sum_{i=1}^{N_o} \left(h_{o,i} - \bar{h}_o \right)^2} \tag{4.31}$$

where N_o is the number of observed heads, $h_{m,i}$ is the modeled head at time i, $h_{o,i}$ is the observed head at time i, and $\bar{h}_o$ is the mean observed head. The Nash-Sutcliffe coefficient exceeds 90% for all piezometers, which indicates good fits of the observed heads. Besides the Nash-Sutcliffe coefficient, the standard diagnostics checks on model errors were applied. The resulting noise $n(t)$, defined in (4.8), is uncorrelated with a distribution close to Normal.

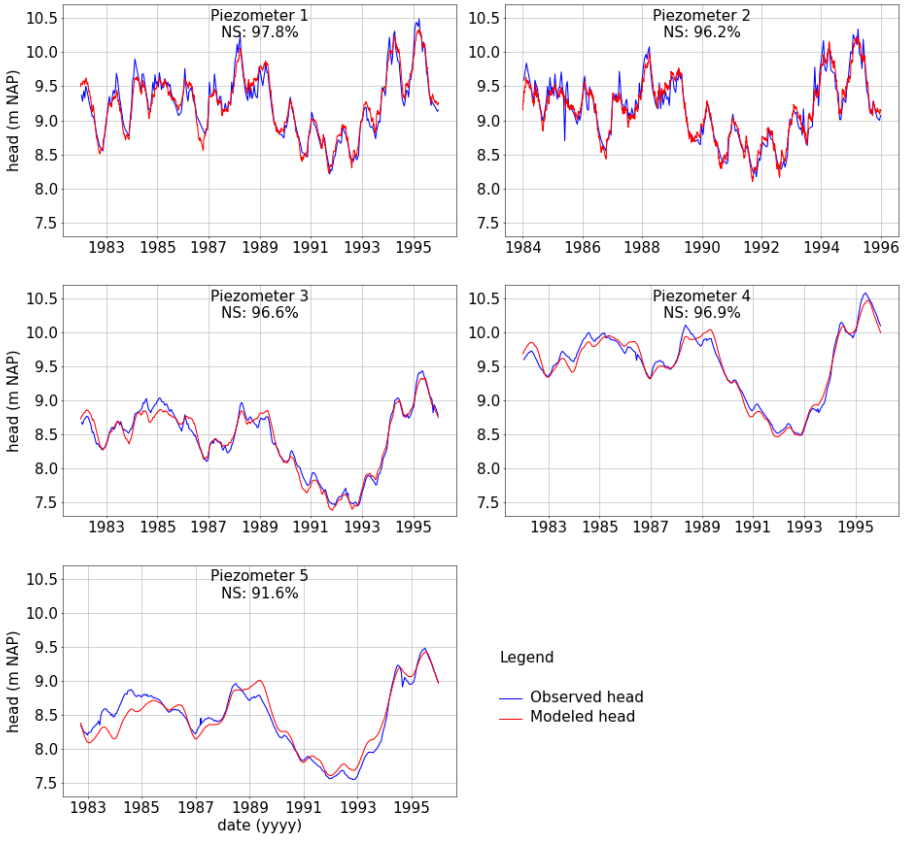

Figure 4-4. Observed heads (blue) and modeled heads (red) of the 5 piezometers, with corresponding Nash-Sutcliffe coefficients

Table 4-2. Estimated parameters with 95% confidence intervals for models optimized under constraints (4.26) or (4.27); M_p, a_p, n_p are the first, second and third parameter of the response function to precipitation; M_w, a_w, n_w are the first, second and third parameter of the response function to pumping, f is the evaporation factor, α is the exponential decay factor of the noise model, and d is the drainage base.

		Estimated parameters values per piezometer				
Symbol	Unit	1	2	3	4	5
M_p .10e^3	m	1.56 [1.51,1.60]	1.53 [1.48,1.59]	2.09 [2.05,2.12]	2.17 [2.12,2.22]	1.80 [1.75,1.82]
a_p x 10e^{-3}	d^{-1}	2.37 [2.30,2.44]	1.93 [1.84,2.02]	2.43 [2.40,2.47]	3.29 [3.24,3.35]	4.42 [4.34,4.50]
n_p *	-	1.11 [1.11,1.12]	0.97 [0.96,0.98]	1.55 [1.54,1.56]	2.02 [2.01,2.03]	2.41 [2.40.2.42]
f *	-	1.03 [1.01,1.05]	0.97 [0.95,0.99]	0.67 [0.65,0.68]	0.73 [0.71,0.74]	0.88 [0.87,0.88]
M_w x 10e^{-4}	m	-	-	1.34 [1.30,1.38]	1.12 [0.90,1.14]	-
a_w x 10e^{-4}	d^{-1}	-	-	1.37 [1.21,1.56]	0.96 [0.64,1.42]	-
n_w	-	-	-	1.06 [0.97,1.16]	1.13 [1.11, 1.58]	-
α x 10e^{-2}	d^{-1}	4.31 [3.65,5.14]	5.78 [4.65,7.21]	0.73 [0.54,0.98]	0.26 [0.22,0.95]	1.80 [1.59,2.03]
d **	m above datum	8.05	7.87	7.62	8.47	6.57***

*: inferred from constraints (4.19) and (4.20)
**: relation (4.12)
***: sum of pumping effects and drainage base

Table 4-3. Estimated mean yearly recharge for period 1982-1995 based on the optimized seasonal harmonic under constraints (4.26) or (4.27)

Piezometer	1	2	3	4	5
R (m/year)	0.250 [0.243,0.256]	0.296* [0.286,0.306]	0.447 [0.440,0.454]	0.416 [0.406,0.421]	0.333 [0.329,0.337]

(*): for period 1984 to 1995

4.5 Discussion

4.5.1 Estimated groundwater recharge

The estimated recharge values for piezometers 1 and 2 represent shallow water table conditions (resp. 0.250 m/year and 0.296 m/year), and are lower than the recharge estimated for piezometers 3 and 4 (resp. 0.447 m/year and 0.416 m/year), representing deep water table conditions. Shallow water tables are favorable for evaporation and transpiration [*Doble and Crosbie*, 2017] which can explain this difference. Different vegetation covers constitute a second explanation. In particular, the extended heather field near piezometers 3 and 4 favor water table replenishment.

Piezometer 5 lies on the sand ridge and characterizes deep water table conditions, like piezometers 3 and 4. Identification of the pumping influence is difficult in this piezometer due to the relatively large distance (1800 m) from the center of the well field. The heads measured in this piezometer have consequently been simulated without pumping influence; The effect of pumping at this piezometer is relatively constant and included in the drainage base.

4.5.2 Comparison with standard time series analysis

In this study, groundwater recharge is estimated with time series models where parameters are fitted with the constraint that the observed seasonal harmonic matches the sum of the seasonal harmonics of the stresses after transformation by the convolution relations of the time series model. This constraint distinguishes the proposed approach from standard time series. The model parameters obtained by the proposed method are expected to provide more reliable estimates of the mean groundwater recharge. The proposed approach is compared to the standard approach for piezometers 1 and 3. The results are given in Table 4-4. In both cases, the fits in terms of Nash Sutcliffe coefficients are similar. In contrast, the model parameters estimated with the proposed method lead to lower recharge estimates for piezometer 1 and 3. The difference between both approaches regarding the modeling of the seasonal harmonic is illustrated in Figure for piezometers 1 and 3. The two graphs at the top show the seasonal harmonic of the observed heads and the seasonal harmonic calculated with the proposed method and the standard method. The seasonal harmonic modeled with the proposed method matches the seasonal harmonic of the observed heads exactly while the seasonal harmonic modeled with the standard method shows a clear discrepancy. The other graphs in Figure show the stress-specific seasonal harmonics calculated with the proposed and standard methods. The largest difference is caused by the amplitude of the seasonal harmonic of the response to evaporation, as expected.

Table 4-4: Comparison of proposed approach with standard time series analysis

	Piezo. 1 Standard method	Piezo. 1 Proposed method	Piezo. 3 Standard method	Piezo. 3 Proposed method
Nash Sutcliffe %	94.7	97.8	96.9	96.5
M_p .10e^3	1.62 [1.56,1.68]	1.56 [1.51,1.60]	2.19 [2.08,2.31]	2.09 [2.05,2.12]
a_p x 10e^{-3}	2.18 [2.05,2.32]	2.37 [2.30,2.44]	2.26 [2.13,2.41]	2.43 [2.40,2.47]
n_p	1.07 [1.05,1.09]	1.11 [1.11,1.12]	1.51 [1.49,1.54]	1.55 [1.54,1.56]
f	0.92 [0.88,0.97]	1.03 [1.01,1.05]	0.54 [0.65,0.68]	0.67 [0.65,0.68]
M_w .10e^{-4}	-	-	1.39 [1.34,1.44]	1.34 [1.30,1.38]
a_w x 10e^{-4}	-	-	1.17 [0.98,1.44]	1.37 [1.21,1.56]
n_w	-	-	1.17 [0.98,1.44]	1.06 [0.97,1.16]
α (d^{-1}) x 10e^{-2}	7.06 [5.94,8.52]	4.31 [3.65,5.14]	2.71 [2.34,3.17]	0.73 [0.54,0.98]
d (m NAP)	7.76	8.05	7.14	7.62
R (m/y)	0.306 [0.282,0.332]	0.250 [0.243,0.256]	0.515 [0.501,0.531]	0.447 [0.440,0.454]

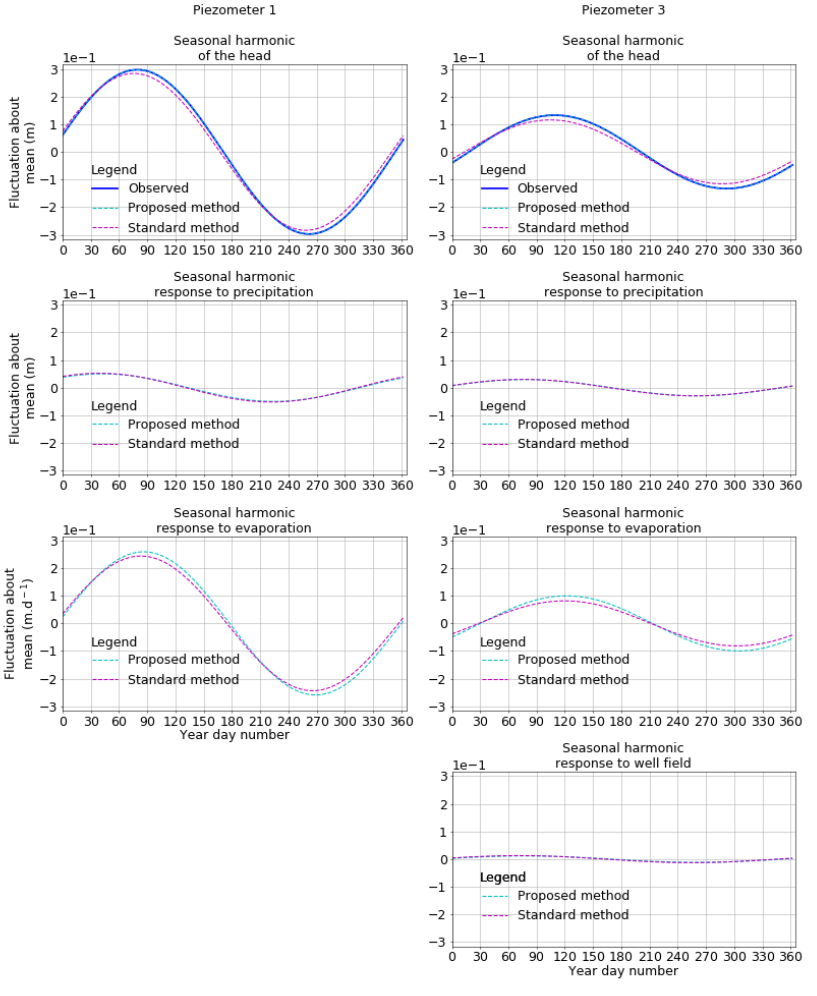

Figure 4-5. Comparison of the seasonal harmonics obtained with the proposed and standard methods

4.5.3 Mean recharge for different time periods

The mean recharge for a period of multiple years depends on the specific time period unless the period is very long. It is expected that the estimated recharge is lower for a multi-year period with a relatively low mean head while the estimated recharge is expected to be higher for a multi-year period with a relatively high mean head. In fact, if the draining resistance of the aquifer remains constant, a linear relation is expected between the estimated mean recharge for a period and the mean groundwater head for that same period. To test this hypothesis, the

mean recharge is estimated for several multi-year periods. Each investigated period is a multiple of whole years in order to equally represent all seasons. Furthermore, the heads at the beginning and end of the period do not deviate more than 0.2 m so that the mean head is a reasonable representation of the head in the period, and the period contains a balanced number of head rises and head declines. Each selected time period is at least 3 years long for the fast head fluctuations (piezometers 1 and 2) and 5 years for the slow head fluctuations (piezometers 3, 4 and 5).

Time periods conforming to the above stated conditions were generated with a computer script. When two intervals share the same mean head (+/- 0.05m), the longest interval is used. In this fashion, 8 time periods were identified for piezometer 1, and 7 time periods for piezometer 3. The mean recharge is estimated for each period with the proposed method and is plotted versus the mean head in the corresponding period in Figure. Linear regression lines can be fitted through the estimates obtained with the proposed method with an r^2 of 0.94 for piezometer 1 and 0.96 for piezometer 3. Note that for piezometer 5, no significant regression line could be found (not shown).

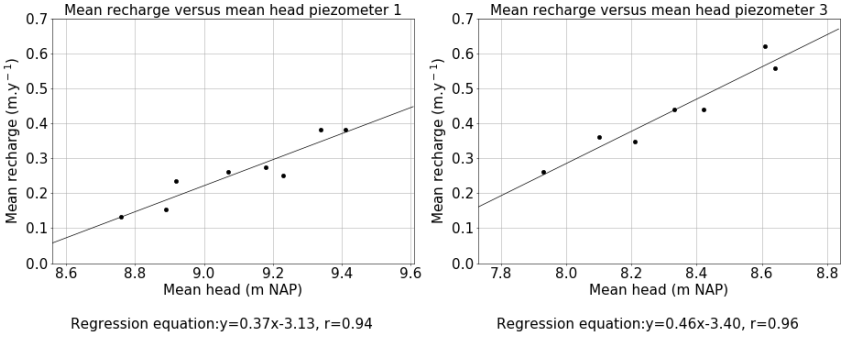

Figure 4-6: Estimated recharge with the proposed method over different time periods for piezometers 1 and 3 and best fit straight line.

4.5.4 Uncertainty of constraints

The main idea of the proposed method is that a better estimate of the recharge is obtained with time series analysis when the best estimate of the seasonal component of the measured heads is equal to the sum of the responses of the best estimates of the seasonal components of the stresses. It is shown, for the case study, that the proposed approach leads to more reasonable estimates of the recharge with narrower confidence intervals than the standard approach without the constraint.

The question arises whether the proposed method can be further improved. In the proposed method, the best estimates of the seasonal harmonics

of the measured heads and measured stresses are used. The uncertainty of these estimates is presented in Tab. The relative uncertainty of the seasonal harmonics of the heads is smaller for piezometers 1 and 2 than for the other piezometers. For the stresses, the relative uncertainty of the seasonal harmonic of the evaporation is the smallest while it is the largest for the precipitation. This is encouraging, as the evaporation has the largest influence on the seasonal variation of the head. A better estimate of the recharge may be obtained when the uncertainty in the seasonal harmonics is taken into account during the parameter estimation process. One way to do this is to perform parameter estimation with a multi-objective function where both the objective function (4.28) and the constraint (4.26) or (4.27) are minimized simultaneously [e.g., Efstratiadis and Koutsoyiannis, 2010]. Another approach is to estimate parameters with a soft constraint (e.g., a range) by penalizing the objective function based on the extent that the condition is not met. In both approaches, the uncertainty of the seasonal harmonic may be taken into account in either assigning weights in the multi-objective optimization or in penalizing the objective function when applying a soft constraint, but this is the topic of further research.

Table 4-5: Uncertainty in the seasonal harmonic of the different time series; the uncertainty of the amplitude is given as the ratio of the estimated amplitude and the associated standard deviation; the uncertainty of the time-lag is expressed in days.

Time series	Amplitude with relative standard deviation	Time-lag with standard deviation (days)
Piezometer 1	0.30 m [rel. stdev=2.3%]	340 [stdev=1.5]
Piezometer 2	0.30 m [rel. stdev=2.7%]	325 [stdev=1.5]
Piezometer 3	0.13 m [rel. stdev=6.0%]	3 [stdev=4.0]
Piezometer 4	1.00 m [rel. stdev=10.0%]	41 [stdev=5.0]
Piezometer 5	0.10 m [rel. stdev=8.0%]	66 [stdev=5.0]
Precipitation	3.8E-4 m/d [rel. stdev=26.0%]	211 [stdev=14.0]
Evaporation	1.5E-3 m/d [rel. stdev=1.0%]	255 [stdev=0.5]
Pumping	1.3E+3 m3/d [rel. stdev=3.0%]	246 [stdev=1.7]

4.6 Recharge estimation by the chloride mass balance method

The recharge estimates obtained from time series analysis are compared with recharge estimates obtained with the saturated zone chloride mass balance method, assuming that the chloride in the groundwater is exclusively of atmospheric origin (rainwater and dry deposition) [e.g. *Eriksson and Khunakasem*, 1969; *Allison and Hughes*, 1978; *Simmers*, 1988]. In the present case study, this condition is reasonable because infiltration from surface water, chloride dissolution of minerals in the soil matrix, and chloride from anthropogenic

sources can all be neglected. Furthermore, chloride originating from vegetation decomposition can be assumed to be entirely recycled during the growing season.

Under steady state conditions, the atmospheric chloride deposition flux equals the vertical chloride flux arriving at the groundwater table at the bottom of the root zone:

$$\bar{P}[\mathrm{Cl}]_a = \bar{R}[\mathrm{Cl}]_{gw} \tag{4.32}$$

where $\bar{P}$ and $\bar{R}$ are the mean precipitation and recharge rates [LT^{-1}], respectively , $[\mathrm{Cl}]_a$ is the mean concentration of atmospheric chloride (including dry deposition) [ML^{-1}], and $[\mathrm{Cl}]_{gw}$ is the mean chloride concentration in the groundwater at the groundwater table [ML^{-1}].

The atmospheric chloride concentration in the Netherlands may be computed from the chloride concentration of the precipitation $[\mathrm{Cl}]_p$ as [*Ridder et al.*, 1984]:

$$[\mathrm{Cl}]_a = \frac{[\mathrm{Cl}]_p}{f_{dp}} \tag{4.33}$$

where f_{dp} equals 0.83 with standard deviation of 0.10, which is applicable for open field deposition rates [*Ridder et al.*, 1984]. The chloride concentration of the precipitation is taken as the average of the three closest stations of the Dutch National Precipitation Chemistry Monitoring Network [van der Swaluw et al., 2010] which equals 1.9 mg/l with a standard deviation of 0.3 mg/l. The mean recharge can now be computed as:

$$\bar{R} = \frac{\bar{P}[\mathrm{Cl}]_p}{f_{dp}[\mathrm{Cl}]_{gw}} \tag{4.34}$$

Chloride concentrations where measured in a monitoring well (code B28C0263) situated in a heather field at the western side of the ridge of Salland (Figure). The well is screened approximately 2 m below the highest measured water table and measurements were taken at four times between 1982 and 1995. Measured chloride concentrations are assumed to represent a mixture of the rainfall of the two years prior to the sampling date (based on a recharge of approximately 300 mm/year and a porosity of 0.3), so that the value of $\bar{P}$ in (4.34) is the mean precipitation of the two years prior to the sampling date.

The recharge is estimated for four two-year periods based on four chloride measurements (Table 4-6). A confidence interval for the estimated recharge is generated by a Monte Carlo simulation where all variables were

assumed to follow a Normal distribution centered on their measured values. Note that generating confidence intervals for recharge estimates obtained with the chloride mass balance is not common but has recently been advocated [e.g. *Alcalá and Custodio*, 2014; 2015; *Crosbie et al.*, 2018]. A standard deviation of 5% of the mean was used for the mean precipitation and for the measured groundwater chloride concentration in addition to the standard deviations of $[Cl]_p$ and f_{dp} mentioned above.

The mean recharge over the period 1989-1995, estimated with the chloride mass balance, equals 0.345 m/year, with an estimated confidence interval of [0.240,0.500]. The piezometer used for the chloride mass balance is located in an area with soil and vegetation cover similar to piezometers 3 and 4 but with a shallower groundwater table.

Considering the uncertainties associated with the chloride mass balance method and the difference in water table depth at the location of the piezometer considered, it is concluded that the results obtained using time series analysis are in reasonable agreement with the results obtained with the chloride mass balance.

Table 4-6: Estimated mean yearly recharge for two-year periods prior to sampling date and 95% confidence intervals

Sampling Date	[Cl] groundwater mg/l	Mean P (mm/year)	Estimated recharge (m/year)
2-10-1989	5.7	820	0.325 [0.230,0.460]
4-11-1993	6.7	920	0.310 [0.220,0.480]
15-9-1994	6.4	960	0.340 [0.240,0.480]
31-8-1995	5.5	995	0.410 [0.285,0.580]
Average			**0.345 [0.240,0.500]**

4.7 Conclusion

Time series analysis of measured heads was applied to estimate the long-term mean recharge of water table aquifers in temperate climates where the seasonal trend of the evaporation results in a significant seasonal trend in the head. The proposed approach can be used to estimate the diffuse recharge with time series models that fit the observed heads as well as possible while requiring that the sum of the transformed seasonal harmonics present in the time series of the stresses equals the seasonal harmonic of the observed heads. In standard time series analysis, model parameters often exhibit a high degree of correlation, leading to problems of equifinality which may result in poor and unreliable

recharge estimates. Taking into account the seasonal harmonic of the observed heads as additional constraint results in more reliable and physically meaningful recharge estimates.

The proposed method is applied to head observations obtained from piezometers situated on and around the ice-pushed sand ridge of Salland in the Netherlands, using the best estimate of the seasonal harmonics of the observed time series. Recharge estimates over different time periods yield consistent results; the estimated mean recharge is linearly related to the mean head in the time period. A comparison with the saturated zone chloride mass balance yields recharge estimates of comparable magnitude.

There are four major requirements for application of the proposed method. First, the seasonal harmonic of the observed series can be estimated accurately. Second, the response of the system to recharge does not change over time, which precludes areas with significant land use changes or areas where the draining conditions of the aquifer are altered. Third, the aquifer system must be sufficiently linear. This condition can be considered as fulfilled when good model fits are obtained. And fourth, runoff is negligible or quantifiable.

The proposed method of time series analysis allows for the estimation of time averaged diffuse recharge that can be used in groundwater modeling or catchment water balances. Where the density of piezometers is large, like in the Netherlands, the method opens the possibility to estimate the recharge at many points which can be interpolated to generate a recharge map; such a map was generated by *Alcalá and Custodio* [2014] for Spain or *Crosbie et al.* [2018] for parts of Australia, using the chloride mass balance method.

4.8 Appendix

In this appendix, a derivation of equations (4.19) and (4.20) is given. The seasonal harmonic (4.17) is written as the real part of a complex function:

$$y(t) = A\mathrm{e}^{i\omega(t-T)} \tag{4.35}$$

The response of the seasonal harmonic is obtained from the convolution as

$$\tilde{y}(t) = \int_0^\infty y(t-\tau)\theta(\tau)d\tau \tag{4.36}$$

Substitution of (4.35) for $y(t)$ and (4.9) for θ gives

$$\tilde{y}(t) = AM\int_0^\infty \mathrm{e}^{-i\omega(t-T-\tau)}\frac{a^n\tau^{n-1}}{\Gamma(n)}\mathrm{e}^{-a\tau}d\tau \tag{4.37}$$

Defining a new variable

$$\beta = a - i\omega \tag{4.38}$$

and rearrangement of terms gives

$$\tilde{y}(t) = AM\,\frac{a^n\,\mathrm{e}^{-i\omega(t-T)}}{\Gamma(n)}\int_0^\infty \mathrm{e}^{-\beta\tau}\,\tau^{n-1}d\tau \tag{4.39}$$

which may be rewritten as

$$\tilde{y}(t) = AM\,\frac{a^n\,\mathrm{e}^{i\omega(t-T)}}{\Gamma(n)}\,\frac{1}{\beta^n}\int_0^\infty (\beta\tau)^{n-1}\,\mathrm{e}^{-\beta\tau}d\left(\beta\tau\right) \tag{4.40}$$

The integral equals the gamma function of n [e.g., *Abramowitz and Stegun*, 1964] so that

$$\tilde{y}(t) = AM\,\frac{a^n\,\mathrm{e}^{-i\omega(t-T)}}{\beta^n} \tag{4.41}$$

Replacing β again by $a - i\omega$ and division of the numerator and denominator by a^n give

$$\tilde{y}(t) = \frac{AM}{\left(1 - i\dfrac{\omega}{a}\right)^n}\,\mathrm{e}^{-i\omega(t-T)} \tag{4.42}$$

Rewriting the denominator as

$$\left(1 - i\frac{\omega}{a}\right)^n = \left(1 + \frac{\omega^2}{a^2}\right)^{\frac{n}{2}}\,e^{-in\arctan\left(\frac{\omega}{a}\right)} \tag{4.43}$$

And combining terms gives:

$$\tilde{y}(t) = \frac{AM}{\left(1+\frac{\omega^2}{a^2}\right)^{\frac{n}{2}}} \mathrm{e}^{-i\omega\left((t-T-\frac{n}{\omega}\arctan\frac{\omega}{a}\right)} \tag{4.44}$$

Comparison of (4.44) with (4.18) gives equations (4.19) and (4.20).

Chapter 5 Identification and explanation of a change in the groundwater regime using time series analysis

Abstract
Time series analysis is applied to identify and analyze a transition in the groundwater regime in the aquifer below the sand ridge of Salland in the Netherlands, where groundwater regime refers to the range of head variations throughout the seasons. Standard time series analysis revealed a discrepancy between modeled and observed heads in several piezometers indicating a possible change in the groundwater regime. A new time series modeling approach is developed to simulate the transition from the initial regime to the altered regime. The transition is modeled as a weighted sum of two responses, one representing the initial state of the system, the other representing the altered state. The inferred timing and magnitude of the change provided strong evidence that the transition was the result of significant dredging works that increased the river bed conductance of the main river draining the aquifer. The plausibility of this explanation is corroborated by an analytical model. This case study and the developed approach to identify a change in the groundwater regime, are meant to stimulate a more systematic application of time series analysis to detect and understand changes in groundwater systems which may easily go unnoticed in groundwater flow modeling.

Adapted from C. Obergfell, M. Bakker, and K. Maas Identification and explanation of a change in the groundwater regime using time series analysis, Groundwater, doi: 10.1111/gwat.12891, 2019

5.1 Introduction

The worldwide increase in groundwater demand requires increased care in assessing groundwater reserves, especially in the context of a changing climate [e.g.*Wada et al.*, 2017]. The awareness of the vulnerability of groundwater systems has motivated recent studies to better understand groundwater table dynamics and detect signs of over-exploitation by searching for correlations between hydrological variables and climate forcings or land use changes [*Stoll et al.*, 2011; *Witte et al.*, 2015; *Luo et al.*, 2016].

In groundwater hydrology, time series analysis has been applied to quantify decreasing trends in groundwater head [*Weider and Boutt*, 2010], the effect of groundwater pumping [e.g. *Baggelaar*, 1988; *Van Geer et al.*, 1988; *Von Asmuth et al.*, 2008; *Harp and Vesselinov*, 2011; *Obergfell et al.*, 2013; *Shapoori et al.*, 2015b] or to quantify the effects of river stage fluctuations [*Barlow et al.*, 2000; *Obergfell et al.*, 2016]. The use of time series analysis to identify the effect of land use changes [e.g. *Gehrels et al.*, 1994] or civil engineering interventions remains marginal, in spite of the sophistication of groundwater monitoring networks and the development of new analysis softwares [e.g., *von Asmuth et al.*, 2012; *Peterson and Western*, 2014; *Collenteur et al.*, 2019].

The objective of this study is to present a case study to illustrate how time series analysis can be applied to identify and analyze a transition in the groundwater regime and help detect its cause. In this study, the term groundwater regime refers to the range of head variations of a time series throughout the seasons.

The field site is a phreatic aquifer under a Pleistocene sand ridge in the Netherlands, where measured heads were indicative of a change in the regime. This study is organized as follows. After a presentation of the field site, a standard time series analysis is presented, which clearly indicate a discrepancy between modeled and observed heads as the result of a regime change. A new modeling approach is then presented in which the response to recharge changes over time. The insights of the magnitude and timing of the change in the regime were the start of a search for a physical explanation. At the end of the study, an explanation is found and an analysis is presented to corroborate the proposed explanation.

5.2 Study area

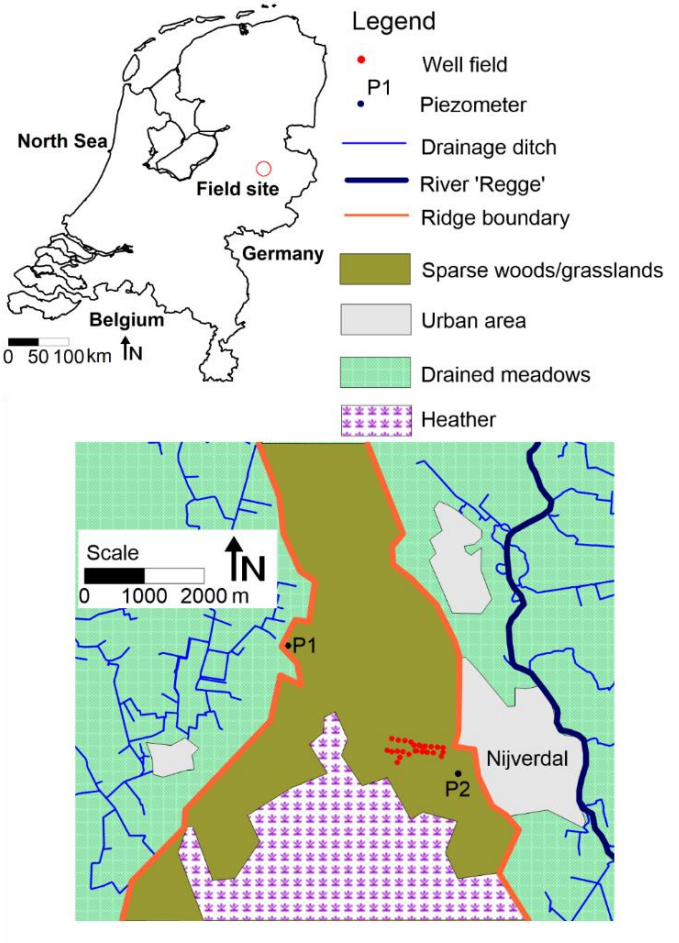

Figure 5-1: Field site at the ice-pushed ridge of Salland

The study area is located in the Eastern part of the Netherlands (Figure 5-1). The middle of the study area is formed by the ice-pushed ridge of Salland which is approximately 12 km long and 2-5 km wide, with a maximum elevation of about 60 m NAP (Dutch datum, approximately equal to mean sea level). The ridge built up at the margin of a glacier during the southernmost advance of the ice sheet in Northern Europe in the Pleistocene time (Saalian ice-age, from about 200,000 to 130,000 years ago). The ridge consists of sand and the vegetation on the ridge consists of heather, grassland, deciduous trees, and coniferous woods.

Measurements at two representative piezometers in the area are used in this study. Their characteristics are listed in Table 5-1. Piezometer 1 represents head fluctuations at a relatively short distance from draining ditches, with a fast reaction to recharge. Piezometer 2 represents head fluctuations on the sand ridge, with a much slower reaction to recharge (Figure 5-2). Heads were recorded twice a month.

Table 5-1. Description of piezometers

Piezometer	Geological Survey id	Screen level (m NAP)	Surface elevation (m NAP)	Median observed head (m NAP)
1	28AP0093	2.10	11.60	8.86
2	28CP0197	4.70	15.26	8.59

Daily precipitation and reference evaporation are obtained from the Royal Netherlands Meteorological Institute [*KNMI*, 2018]. The reference evaporation is Makkink reference evaporation, defined as the evaporation of well-watered short grass on a regional scale [*De Bruin*, 1987]. Precipitation was measured at the meteorological station of Hellendoorn (Figure 5-1). Daily reference evaporation, which varies much less in space than precipitation, was measured at the meteorological station of de Bilt, about 85 km to the south-west of the field site. A drinking water production well field is in operation on the ridge of Salland since 1954 (Figure 5-1). The average groundwater extraction is $5 \cdot 10^6$ m^3/year. The time series of the stresses are shown in Figure 5-2 and the location of the well field is shown in Figure 5-1.

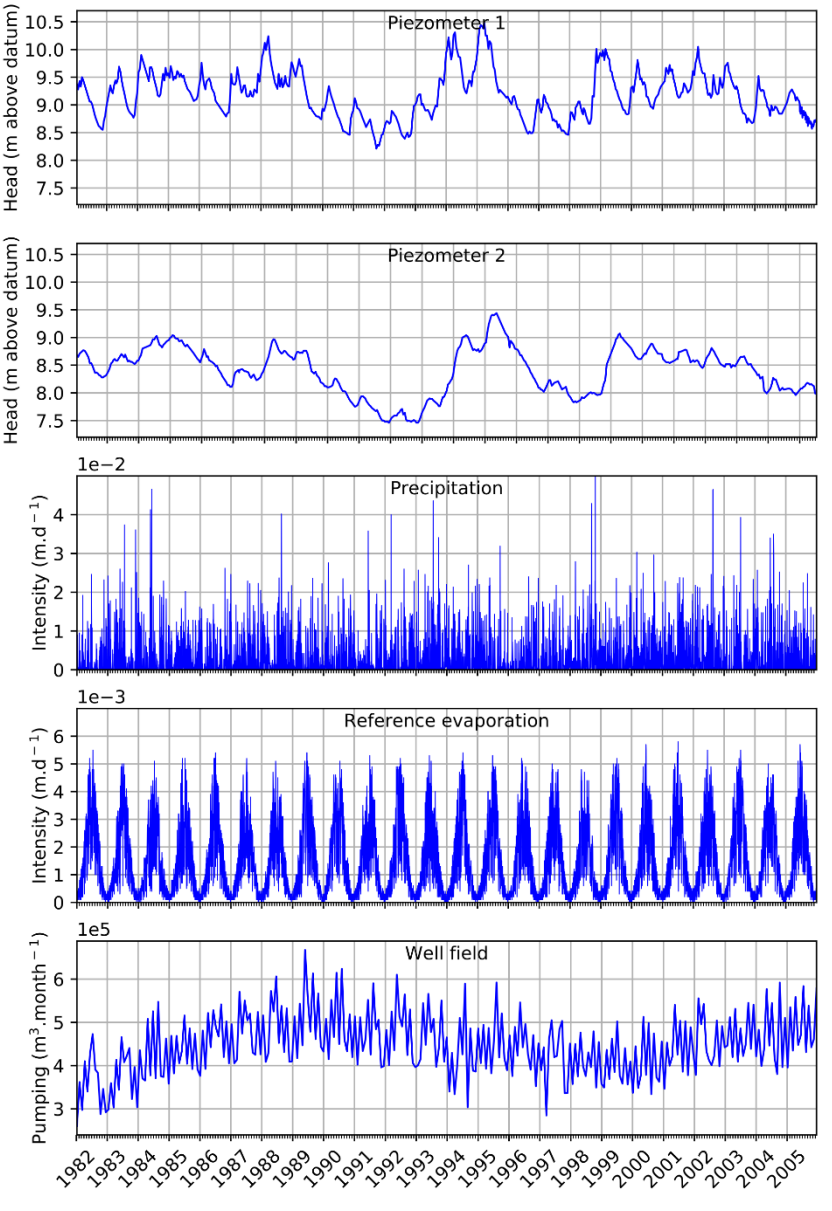

Figure 5-2: Time series of heads and stresses

5.3 Time series modeling

5.3.1 Standard approach

As a first step, a standard time series model is fitted to the observed heads, using the method of predefined response functions [*Von Asmuth et al.*, 2002]. In this method, the head fluctuation $\varphi(t)$ at an observation well, resulting from a stress applied on a groundwater system (precipitation, evaporation or pumping) is obtained by convolution of the time series $q(t)$ of the stress with a corresponding impulse response function $\theta(t)$:

$$\varphi(t) = \int_0^t q(\tau)\theta(t-\tau)d\tau \tag{5.1}$$

where t is time. The dependence of the response function on spatial coordinates is omitted in this notation. The response function $\theta(t)$ describes the reaction of the groundwater head to an instantaneous stress event of unit magnitude. In this study, the scaled Gamma distribution is used as the impulse response function

$$\theta(t) = M\frac{a^n t^{n-1}}{\Gamma(n)}\mathrm{e}^{-at} \tag{5.2}$$

where M is a scaling factor, a and n define the shape of the function, and $\Gamma(n)$ is the Gamma function of n . The Gamma distribution is used frequently to simulate the response to recharge in time series models [e.g., *Von Asmuth et al.*, 2002; *Manzione et al.*, 2012; *Obergfell et al.*, 2013; *Peterson and Western*, 2014]. The use of a Gamma distribution for the impulse response to recharge, including passage through the unsaturated zone, was pioneered by *Besbes and de Marsily* [1984], and theoretically represents a succession of identical linear reservoirs [*Nash*, 1957]. The Gamma distribution is also applied here to simulate the slow response to pumping in a phreatic aquifer when piezometers are not in the direct vicinity of the pumping wells. Closer to the wells or in semi-confined aquifers, well functions such as Hantush may be more appropriate as pumping response functions [e.g., *Von Asmuth et al.*, 2008; *Obergfell et al.*, 2013].

The mean μ and standard deviation σ of the response function are related to parameters a and n as [*Weisstein*, 2018b]:

$$\mu = \frac{n}{a} \tag{5.3}$$

$$\sigma = \frac{\sqrt{n}}{a} \tag{5.4}$$

The observed heads are modeled as the sum of the response to recharge, the response to pumping and a reference level d :

$$h_o = \varphi_r + \varphi_w + d + r \tag{5.5}$$

where $r(t)$ is the remaining residual, and φ_r is the response to recharge R :

$$\varphi_r(t) = \int_0^t R(\tau)\theta_r(t-\tau)d\tau \tag{5.6}$$

where θ_r is the impulse response function of recharge. The recharge in (5.6) is approximated as [e.g. *Von Asmuth et al.*, 2002]

$$R(\tau) = P(\tau) - fE(\tau) \tag{5.7}$$

where $P(\tau)$ is the measured precipitation, $E(\tau)$ is the measured reference evaporation, and f is a scaling factor. Run off is neglected given the absence of streams on the ridge, the high permeability of the soil, the flat to gently sloping relief of the sand ridge and its surroundings, and the moderate climate [*Meinardi et al.*, 1998]. The term φ_w in (5.5) is the response to pumping discharge $Q(\tau)$:

$$\varphi_w = \int_0^t Q(\tau)\theta_w(t-\tau)d\tau \tag{5.8}$$

where θ_w is the impulse response function of pumping. Modeling the residuals with an exponential decay process transforms the time series of residuals into a noise time series $n(t)$ that is approximately white [*Von Asmuth and Bierkens*, 2005]. The residual at time t_i is related to the residual at time t_{i-1} as

$$r(t_i) = r(t_{i-1})\exp\left(-\alpha\left(t_i - t_{i-1}\right)\right) + n(t_i) \tag{5.9}$$

where α is the residual decay factor and $n(t_i)$ is the remaining noise at time t_i. The observed heads and stresses are written with respect to their arithmetic means over the considered time period, so that (5.5) becomes

$$h_o - \bar{h}_o = \left(\varphi_r - \bar{\varphi}_r\right) + \left(\varphi_w - \bar{\varphi}_w\right) + \left(\bar{\varphi}_r + \bar{\varphi}_w\right) - \bar{h}_o + d + r \tag{5.10}$$

where the overbar indicates the arithmetic mean. The drainage base is set equal to the mean observed head $\bar{h}_o$ minus the sum of the mean contributions of the stresses (similar to *Von Asmuth et al.* [2002])

$$d = \bar{h}_o - \left(\bar{\varphi}_r + \bar{\varphi}_w\right) \tag{5.11}$$

so that

$$h_o - \bar{h}_o = \left(\varphi_r - \bar{\varphi}_r\right) + \left(\varphi_w - \bar{\varphi}_w\right) + r \tag{5.12}$$

The mean response $\bar{\varphi}_r$ is computed, using (4.9) as the response function, as

$$\bar{\varphi}_r = \bar{R}\int_0^\infty \theta_r(t-\tau)d\tau = \bar{R}M_r \tag{5.13}$$

M_r is the final response of the groundwater head when the recharge is applied continuously with unit intensity. Similarly, $\bar{\varphi}_w = \bar{Q}M_w$.

Parameter optimization is performed by minimizing the objective function $S(\mathbf{p})$ defined as half of the sum of the squared noise terms n_i defined in (4.8):

$$S(\mathbf{p}) = \frac{1}{2}\sum_{i=1}^{N_o} n_i^2 \tag{5.14}$$

where $\mathbf{p}$ is the vector of N_p log-transformed model parameters and N_o is the number of observations. The search for the minimum of the objective function was performed using a modified Gauss-Newton algorithm [e.g., *Hill*, 1998]. The covariance matrix $\mathbf{C}$ of the optimized parameters is approximated as [e.g., *Carrera and Neuman*, 1986; *Yuen*, 2010]:

$$\mathbf{C} \simeq \sigma^2\mathbf{H}^{-1} \simeq \sigma^2\left(\mathbf{J}^T\mathbf{J}\right)^{-1} \tag{5.15}$$

where $\mathbf{H}$ is the Hessian of the objective function, $\mathbf{J}$ is the Jacobian matrix, and σ^2 is the sample variance of the noise

$$\sigma^2 = \frac{1}{N_o}\sum_{i=1}^{N_o}\left(n_i - \bar{n}\right)^2 \tag{5.16}$$

where $\bar{n}$ is the arithmetic mean of the noise.

In the parameter optimization process, all parameters are log-scaled except for the drainage base to prevent parameters going negative during the estimation process. The optimum is used as the starting point for a second optimization without log-scaled parameters to compute a covariance matrix.

5.3.2 Results of standard time series analysis

Standard time series analysis is applied to the entire observation period from 1982 to 2005. The model parameters for the standard model consist of five parameters M_r, a_r and n_r of the response function to recharge, the factor f and the exponential noise decay factor α. For piezometer 2, three additional parameters are optimized: the parameters M_w, a_w and n_w of the response function to pumping. For piezometer 1, the effect of pumping could not be identified. The goodness of fit of the time series models is expressed as the Nash-Sutcliffe coefficient [*Nash and Sutcliffe*, 1970] defined as

$$NS = 1 - \frac{\sum_{i=1}^{N_o}\left(h_{m,i} - h_{o,i}\right)^2}{\sum_{i=1}^{N_o}\left(h_{o,i} - \bar{h}_o\right)^2} \tag{5.17}$$

where $h_{m,i}$ is the modeled head at time i and $h_{o,i}$ is the observed head at time i.

The observed and modeled heads for piezometers 1 and 2 are shown in Figure 5-3. The blue line corresponds to the observed head and the red line corresponds to the best fit obtained over the whole period 1982-2005. The Nash-Sutcliffe coefficient is 77.3% for piezometer 1 and 77.2% for piezometer 2.

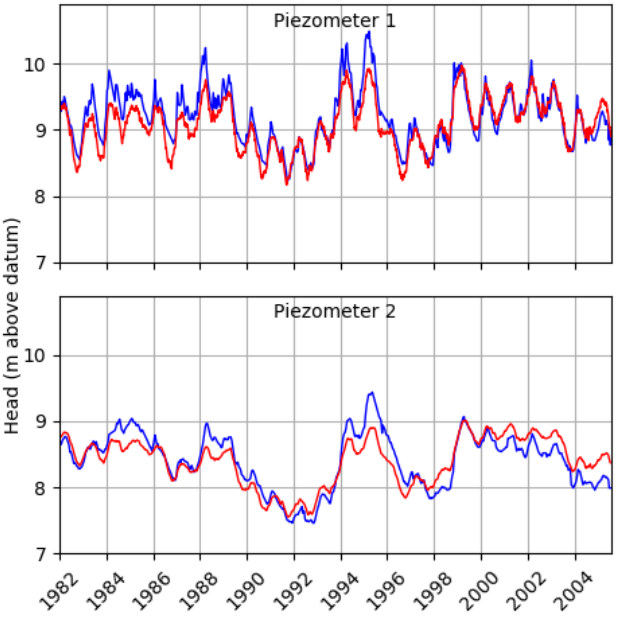

Figure 5-3: Observed heads (blue) and modelled heads (red) over the period 1982-2005, standard time series analysis

The models that are fitted over the entire period 1982-2005 structurally underestimate the observed heads before 1997 and overestimate the observed heads after 1997. One of the reasons for the poor fit could be a linear decreasing trend resulting from the intensification of groundwater use and land use changes in the Netherlands [*Witte et al.*, 2015]. Fitting a trend to the observed time series only results in a slight improvement of the fit for piezometer 1 but not for both piezometers, so this hypothesis is rejected.

As a next step in the investigation, the model is fitted separately over the period 1982-1997 and over the period 1997-2005 (Figure 5-4). In both cases, excellent fits are obtained over the calibration period but the model structurally departs from the observed heads outside the calibration period. The model calibrated over the period 1982-1997 clearly overestimates the observed heads after 1997 and the model calibrated over the period 1997-2005 clearly underestimates the observed heads before 1997.

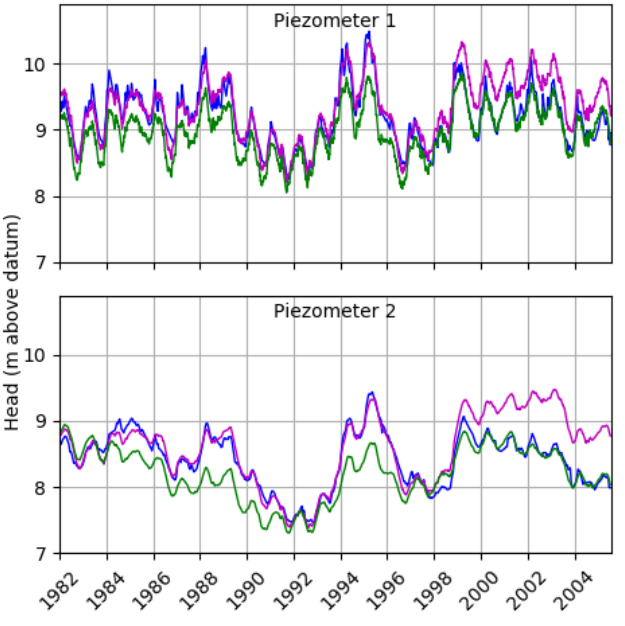

Figure 5-4: Observed heads in piezometers 1 and 2 (blue), models calibrated over the period 1982-1997 (magenta) and models calibrated over the period 1997-2005 (green)

Further analysis showed that no trend in the precipitation or evaporation time series can be detected that may contribute to the observed head decline. The only significant reported land-use change that affects the recharge rate is an ecohydrological project involving the yearly conversion of 100 ha of woods into heather. This project aimed at restoring wetter conditions as heather reportedly results in lower evaporation than woods. However, this project started after 2001 and cannot explain a change in the regime in the mid 1990's. Furthermore, this intervention is expected to result in a rising trend of the heads while the opposite is observed. Regarding other factors, no increase of pumping or decline of stream stages were reported in the mid 1990's. At this point, it is concluded that the groundwater regime over the period 1982-1997 underwent a substantial change in the middle of the 1990s.

5.4 Modeling of the transition period

A new method is proposed to simulate the transition from one system response to another system response (possible physical reasons for such a transition are discussed in the next sections). The main idea is to replace the response to recharge by a weighted sum of two responses, one representing the initial state and the other representing the altered state.

The transition from one response to another response is implemented as follows. Suppose that the response function changes from $\theta_1(t)$ to $\theta_2(t)$. Convolution of these response functions with the recharge time series results in two different responses, $\varphi_1(t)$ and $\varphi_2(t)$. The transition from the first to the second state can be described by a weighted sum of the two responses:

$$\varphi(t) = \omega(t)\varphi_1(t) + (1-\omega(t))\varphi_2(t) \tag{5.18}$$

where $\varphi(t)$ is the weighted sum of the two responses and $\omega(t)$ is the weighting function. The weighing function $\omega(t)$ is chosen to be an S-shaped curve that varies from 1 to 0:

$$\omega(t_i) = \frac{1}{e^{\beta(t-\sigma)}+1} \tag{5.19}$$

where β is a shape factor that determines the smoothness of the transition and σ is the middle of the transition time, when the function takes a value of 0.5. A new time series model is fitted to the entire observation period. Nine parameters are fitted for piezometer 1: M_r, a_r and n_r of the response function to recharge before the transition, M_r, a_r and n_r of the response function to recharge after the transition, the factor f, the exponential noise decay factor α, and the parameter σ of the transition function (5.19). The solution is not sensitive to the sharpness of the transition for piezometer 1 so that the shape factor β was fixed to 50 which corresponds to a sharp transition. For piezometer 2, parameters M_w, a_w and n_w of the response function to pumping are also included for a total of 13 parameters.

The new model gives a good fit for the entire measurement period for both piezometers (Figure 5-5). The Nash-Sutcliffe has increased from 75.3% to 93.5% for piezometer 1 and from 66.4% to 95.5% for piezometer 2. The sum of squared residuals has decreased by 73 % for piezometer 1 and by 87% for piezometer 2. An improvement of the fit was expected, of course, as the complexity of the model, and hence the number of parameters, was increased. The question arises whether the improvement of the fit is significant enough to justify the increase in complexity. One way to answer this question is to compare the values of the Akaike Information Criterium (AIC) for the model residuals [e.g., *Banks and Joyner*, 2017, Eq 6]:

$$AIC = (2k+1) + N\log(S/N) \tag{5.20}$$

where k is the number of parameters, N is number of data points, and S is the sum of squared residuals. The AIC drops from -1889 to -2690 for piezometer 1 and

from -1629 to -2775 for piezometer 2, indicating that the additional complexity of including the transition in regime is justified. It is noted, however, that the residuals are correlated, while the AIC theory is developed assuming uncorrelated residuals. A second evaluation of the AIC was performed with a time interval between residuals which is sufficiently long to consider the resulting residuals uncorrelated (based on the noise decay factor). For piezometer 1, a time interval of 4 months leads to approximately uncorrelated residuals while for piezometer 2, a time interval of 23 months must be used. With approximately uncorrelated residuals, the AIC drops from -229 to -306 for piezometer 1 and from -25 to -55 for piezometer 2, which confirms that using the model with the regime transition is justified.

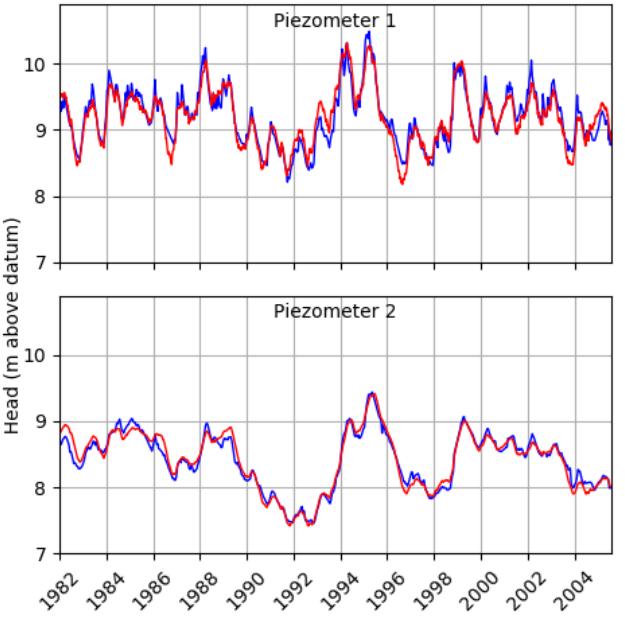

Figure 5-5: Fit obtained with a weighted sum of responses to recharge. Observed head (blue) and modeled head (red)

The transition time was identified with reasonable confidence intervals for both piezometers. The sharpness of the transition was determined with statistical significance for piezometer 2 and was fixed for piezometer 1, as stated. The resulting weighting function for piezometer 2, including the 95% limits, is shown in Figure 5-6.

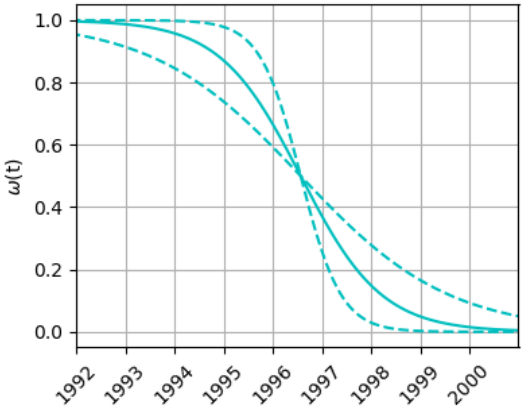

Figure 5-6: Weighting function $\omega(t)$ for piezometers 2 with 95% confidence limits (dotted lines); the transition time corresponds to the time at which the weighing function $\omega(t)$ takes the value 0.5.

The response functions that prevails before and after the transition are shown in Figure 5-7. The corresponding parameters are shown in Table 5-2 in terms of M_r, μ_r and σ_r .

Table 5-2: Comparison of the parameters of the response function to recharge that prevails before and after the system transition time; numbers in brackets are lower and upper limits of the 95% confidence intervals.

	Piezometer 1 before transition	Piezometer 1 after transition	Piezometer 2 before transition	Piezometer 2 after transition
M_r x10e³	1.59 [1.54,1.64]	1.18 [1.15,1.21]	2.06 [2.03,2.09]	1.60 [1.58,1.62]
μ x 10e²	4.89 [4.7,5.08]	3.69 [3.53,3.87]	6.50 [6.43,6.56]	5.16 [5.10,5.21]
σ x 10e²	4.71 [4.50,4.92]	3.57 [3.37,3.78]	5.15 [5.08,5.21]	4.06 [3.99,4.11]

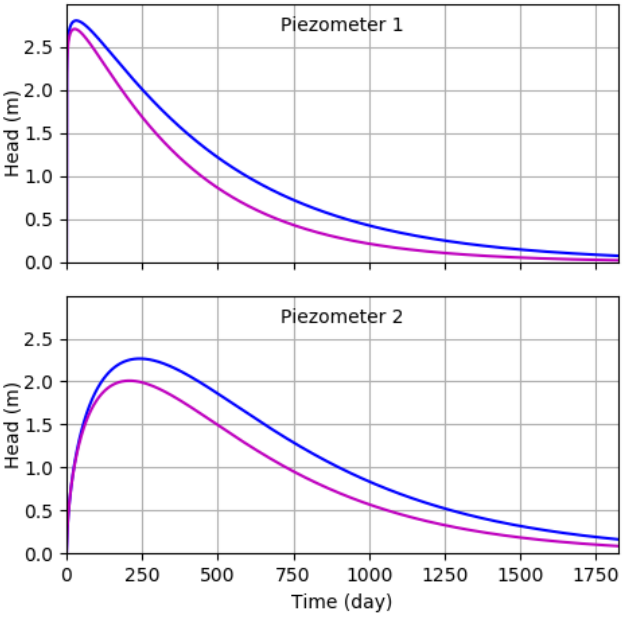

Figure 5-7: Comparison of the impulse response functions before (blue) and after the transition (red) for piezometers 1 and piezometer 2; Time zero corresponds to the time of a short recharge event of unit magnitude.

The quicker recession of the response to recharge after the transition indicates that groundwater is drained faster. The next step is to search for an underlying physical reason.

5.5 Physical explanation

The local waterboard reported that significant dredging works had been carried out in the river the 'Regge' (Figure) between 1992 and 1994 as part of an environmental cleanup project. Archived documents indicated that 250,000 m^3 of sediments (contaminated with heavy metals) were removed from the river bed over a distance of 8 kilometers. A probably unintentional consequence was an increase of the river bed conductance and thus of the draining capacity of the river. This explanation is consistent with the reduction of the response to recharge shown in Figure 5-7.

As a final step in the investigation, a short theoretical analysis is presented to determine whether a change in the river bed conductance can indeed result in the change in the response function presented in Table 5-1. A simplified East-West

cross section over the sand ridge is shown in Figure 5-8. The hydraulic conductivity is k, approximate saturated thickness is D, storage coefficient is S and length of the cross section is L. The aquifer is bounded on the left by a fixed head representing the drained meadows to the west of the study area. The aquifer is bounded to the right by a river representing the river 'Regge'.

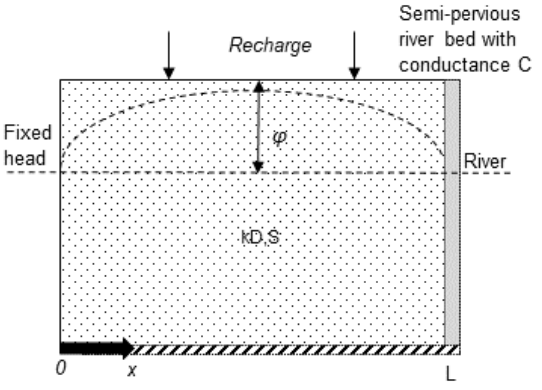

Figure 5-8: Simplified cross-section of study area

Flow into the stream is computed as:

$$Q_s = C\varphi(x = L) \tag{5.21}$$

where Q_s [L^2T^{-1}] is the flux from the aquifer to the river per unit length of river, $\varphi(x = L)$ is the head in the aquifer relative to the stream stage at the semi-pervious stream bank , and C is the river bed conductance [LT^{-1}]. The base of the aquifer is impermeable and aquifer parameters are uniform and constant. Heads are measured with respect to the heads on the left and right sides of the cross-section (which are equal). Initially, the head is zero everywhere. The analytical solution for the response function due to a constant recharge starting at time $t = 0$ is given by *Bruggeman* [1999, eq 137-48]. The response function $\theta(t)$ is characterized by its moments of order k defined as:

$$M_k = \int_0^\infty t^k \theta(t)dt \tag{5.22}$$

The three first moments are considered here and evaluated by numerical integration of the solution of Bruggeman. Alternatively, the moments can be

obtained by solving the differential equation for the moments of the response function [e.g., *Bakker et al.*, 2007; *Carr and Simpson*, 2018].
The moments are recombined and expressed as the mean response time μ and the standard deviation σ of the response function [*Weisstein*, 2018a]:

$$\mu = \frac{M_1}{M_0} \tag{5.23}$$

$$\sigma^2 = \frac{M_2}{M_0} - \mu^2 \tag{5.24}$$

In the simplified model, precipitation reaches the groundwater table instantaneously, which implies that the time it takes for infiltrated water to percolate through the unsaturated zone is neglected. This approximation does not affect the estimation of parameter M_r which determines the final response to recharge. Values obtained for this parameter with the analytical solution should therefore correspond approximately to the values obtained with the time series model. In contrast, neglecting the passage through the unsaturated zone results in a smaller mean response time μ_r and standard deviation σ_r. However, the change of these two parameters as a result of variations of the river bed conductance remains comparable to the time series model.

Values that approximate the situation of piezometer 2 are chosen with k =40 m/day, D =30 m, S =0.3, and L =4000 m. The values corresponding to the magnitude of the final response to precipitation M_r, the mean time μ_r and standard deviation σ_r are evaluated for river bed conductance values C ranging from 10 to 80 m/d, at a distance $x = L/2$. The results are plotted in Figure 5-9.

An increase of the river bed conductance from C = 10 m/d to C = 50 m/d leads to a theoretical reduction of approximately 5 to 10% of the parameters M_r, μ_r and σ_r of the response function to recharge. These reductions support the conjecture that the observed transition in groundwater regime is the result of dredging works that increased the conductance of the river bed.

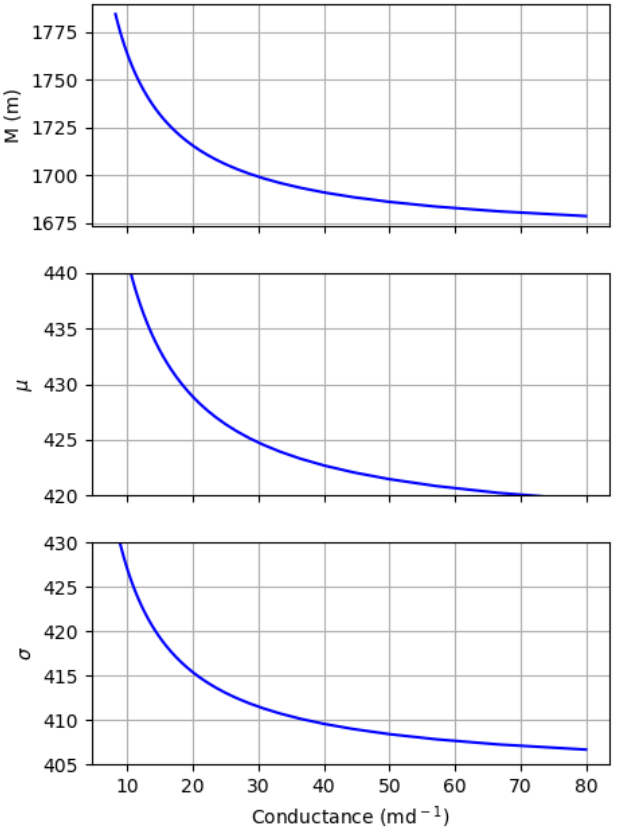

Figure 5-9: Influence of the river bed conductance C on the characteristics of the impulse response function to recharge

5.6 Conclusion

In this study, it is shown how time series analysis can be used as an investigative tool to identify and analyze changes in the groundwater regime that are otherwise unnoticed. Standard time series analysis revealed a systematic discrepancy between modeled and observed heads in the phreatic aquifer under the sand ridge of Salland in the Netherlands. The investigated piezometers exhibit two different fluctuation regimes that can be modeled accurately when considered separately. A new time series modeling approach is developed that incorporates a weighted sum of two modeled responses to recharge, one representing the initial state and the other representing the altered state. The new approach results in excellent fits of the heads over the entire observation

period. The results of the new approach initiated a search for the physical causes of the regime change, leading to the conclusion that dredging works in the river draining the aquifer are most likely the cause of the groundwater regime change. The local water board was not aware of this change to the groundwater regime and the change had not been incorporated in any of the groundwater models used for water management purposes.

Finally, it is pointed out that changes in climate, land use, or groundwater pumping, which are the usual suspects when changes in head variations are observed, do not appear to be involved here. Time series analysis of observed heads is an instrumental tool to understand the history of the dynamics of an aquifer and deserves a more systematic application in the analysis of groundwater systems.

.

Chapter 6 Synthesis

6.1 Introduction

The objective of this thesis was to develop time series analysis methods for the estimation of aquifer parameters and recharge to be used in groundwater models and to develop time series analysis methods for the identification and quantification of a regime change. The methods developed to meet this objective have been presented in the four preceding chapters. This concluding chapter reflects on two themes related to all methods presented: the complementarity of groundwater flow modeling and time series modeling and the issue of parameter uncertainty.

6.2 The complementarity of groundwater flow modeling and time series modeling

The complementarity of groundwater flow modeling and time series analysis was explored in this thesis in different case studies. In Chapters 2, the virtual steady cone of depression of a well field obtained from time series analysis was used to calibrate a steady state groundwater flow model. In Chapter 3, groundwater model parameters were obtained directly from the response functions of the time series model, which were an analytical solution to a groundwater flow model describing stream-aquifer interaction. In Chapter 4, average groundwater recharge was estimated from time series analysis, using the same data as is available for a groundwater hydrologist when setting up a groundwater flow model. Note that recharge rates are obtained independently from a groundwater flow model, as such circumventing the correlation between recharge and aquifer transmissivity [e.g., *Strack*, 1989]. Finally, in Chapter 5, an analytical groundwater flow model was used to corroborate that dredging works had probably resulted in a regional drop of the water table, as identified in first instance by means of time series analysis.

In addition to estimates of model parameters, the interpretation of time series models provides physical insight regarding the functioning of the groundwater system. This was especially apparent in Chapter 5, where time series analysis was used as a detective tool to determine the timing and magnitude of a change in the groundwater regime and explain its origin. In Chapter 2, the position of a semi-confining layer relative to the screen depth of the monitoring wells was inferred from the time series models. In Chapter 3, the resistance to flow at the stream/aquifer interface was identified as resulting from stream line contraction.

The complementarity between time series modeling and groundwater flow modeling encourages a systematic application of both modeling approaches. Groundwater modeling can be used to simulate groundwater flow based on a

conceptualization of the groundwater system. Time series analysis can be used for example to estimate groundwater model parameters, derive calibration targets to be used in groundwater models, or identify changes in regimes that need to be incorporated in a groundwater model.

6.3 Parameters uncertainty

Unambiguous estimation of the parameters of the response functions is crucial for a reliable physical interpretation of time series models. In this research, parameter estimation was performed using a modified-Gauss-Newton algorithm to minimize the sum of the squares of the differences between modeled and observed heads. The modified Gauss-Newton optimization algorithm is a local search in the sense that the minimum is sought within a single valley of the objective function landscape.

A first limitation of this method is that if the objective function landscape contains multiple valleys, the global minimum may be missed when the initial vector of parameters is chosen too far from the global optimum. Although preliminary Latin Hypercube sampling can be performed to investigate the possible presence of multiple optima (as was the case in Chapters 3), the possibility to miss the global optimum cannot be excluded.

A second limitation of the Gauss Newton optimization approach is that the confidence intervals of the parameters are derived assuming that the time series model can be reasonably described near the optimum by a first order approximation of the model [Vrugt and Bouten, 2002]. There is no clear-cut criterium to assess the applicability of this first order approximation. One approach is to compare the confidence intervals obtained with the Gauss-Newton approach with the confidence intervals obtained with an algorithm involving massive parameters sampling, such as Monte Carlo Markov Chain (MCMC) methods [e.g. , Vrugt and Bouten, 2002]. However, the application of massive parameter sampling is not straightforward either.

First, they require sufficient computational capacity [Keating et al., 2010] as the model must be run thousands of times to approach the posterior probability distribution of the parameters. Second, the lack of consensus about how to start and end the parameter chain is in itself a source of uncertainty. It is indeed not clear in practical applications how long the 'burn-in' part of the chain should be. This corresponds to initial parameters values that are too far from the most probable parameter values (and as such, should be rejected). Regarding the ending of the chain, it is often not clear how long the chain should be so that an even longer chain would result in negligible changes of the statistical properties of the chain.

Hence, there is a tension between on one side an efficient parameter estimation method such as a modified Gauss-Newton algorithm assuming that the first order approximation of the time series model is reasonable, and, on the other side, a computationally demanding sampling of the posterior probability distribution of the parameter vector, which is not immune to uncertainty either.

Schweder and Hjort [2016] argue that the confidence (of estimated parameters) derives from the transparency of the method of constructing the confidence intervals. As long as the procedures to apply massive parameter sampling, such as MCMC, remain so diverse, this argument for transparency plead in favor of a relatively simple modified Gauss Newton algorithm. Improvement of the uncertainty estimates of time series analysis is recommendable for future research.

6.4 Future prospects

Linearity of the groundwater system is an essential assumption in the modeling approach in this thesis, so that groundwater levels can be computed as the convolution of a time series of a stress with the impulse response function for this stress. This approach is inadequate when non-linear reactions of the unsaturated zone are no-longer negligible. An alternative approach is needed for those situations, for example the application of a vertical soil moisture module [e.g., *Berendrecht et al.*, 2006; *Peterson and Western*, 2014]. Such an approach was investigated during this thesis research but did not lead to satisfying results as a consequence of model over-parametrization. The difficulty is to find a tradeoff between model complexity and parameter parsimony.

Regarding the estimation of groundwater recharge as proposed in Chapter 4, additional work is needed for situations in which the seasonal signals are weak and relatively uncertain. In these situations, the propagation of the uncertainty in the estimated recharge must be considered, for example using multi-objective optimization. Furthermore, when runoff is not negligible, recharge can possibly be estimated with a bucket model, as proposed by *Peterson and Western* [2014].

6.5 Epilogue

Science is about trying to understand how nature works and technology is about applying science to cope with nature. Purposeless curiosity drives the scientific mind while the need to control nature (which to some extent is a condition to survive), drives technology. Groundwater hydrology, in that sense, can be considered as mainly a technological discipline, applied initially to ensure satisfying primary needs such as drinking water, and is now also applied to save water and energy, for example using aquifer storage and recovery or aquifer thermal energy storage.

The question arises whether time series analysis offers the opportunity to widen the perspective of groundwater hydrologists and provide the opportunity to gain insight in how nature works. There were a few moments during the investigations conducted as part of this thesis that had the flavor of curiosity driven research. This was the case in Chapter 4 with the introduction of the seasonal components of time series. Taking into account seasonal components of time series relates groundwater hydrology to the influence of seasons and their damped and delayed imprints on water table fluctuations. In

Chapter 5, the elucidation of a change in the groundwater regime involved the consultation of forest and agriculture scientists, as well as civil engineers, which is reminiscent of the connection of groundwater hydrology to a wide range of earth science and engineering topics.

The application of time series analysis to better understand how nature works is an exciting perspective that may lead to insights that are worth discussing beyond the groundwater hydrology community.

Literature

Abramowitz, M., and I. A. E. Stegun (1964), *Handbook of Mathematical Functions*, Dover Publications, New-York, N.Y., 1046pp.

Alcalá, F. J., and E. Custodio (2014), Spatial average aquifer recharge through atmospheric chloride mass balance and its uncertainty in continental Spain, *Hydrological Processes*, *28*(2), 218-236.

Alcalá, F. J., and E. Custodio (2015), Natural uncertainty of spatial average aquifer recharge through atmospheric chloride mass balance in continental Spain, *Journal of Hydrology*, *524*, 642-661.

Allison, G., and M. Hughes (1978), The use of environmental chloride and tritium to estimate total recharge to an unconfined aquifer, *Soil Research*, *16*(2), 181-195.

Baggelaar, P. K. (1988), Time series analysis in groundwater level decline studies: principle and example (in Dutch), *H2O*, *21*, 443-450.

Bakker, M., K. Maas, and J. R. Von Asmuth (2008), Calibration of transient groundwater models using time series analysis and moment matching, *Water Resour. Res.*, *44*(4), W04420.

Bakker, M., R. P. Bartholomeus, and T. P. A. Ferré (2013), Preface "Groundwater recharge: processes and quantification", *Hydrol. Earth Syst. Sci.*, *17*(7), 2653-2655.

Bakker, M., K. Maas, F. Schaars, and J. R. von Asmuth (2007), Analytic modeling of groundwater dynamics with an approximate impulse response function for areal recharge, *Advances in Water Resources*, *30*(3), 493-504.

Banks, H. T., and M. L. Joyner (2017), AIC under the framework of least squares estimation, *Applied Mathematics Letters*, *74*, 33-45.

Barlow, P. M., L. A. DeSimone, and A. F. Moench (2000), Aquifer response to stream-stage and recharge variations. II. Convolution method and applications, *Journal of Hydrology*, *230*(3–4), 211-229.

Bartholomeus, R., B. Voortman, and J.-P. M. Witte (2014), Measurements and knowledge of hydrological processes are required for accurate estimations of evaporation with groundwater models (in Dutch), *Stromingen*, *19*(2).

Berendrecht, W. L., A. W. Heemink, F. C. van Geer, and J. C. Gehrels (2006), A non-linear state space approach to model groundwater fluctuations, *Advances in Water Resources*, *29*(7), 959-973.

Besbes, M., and G. de Marsily (1984), From infiltration to recharge: use of a parametric transfer function, *Journal of Hydrology*, *74*, 271-293.

Beven, K. (1993), Prophecy, reality and uncertainty in distributed hydrological modelling, *Advances in Water Resources*, *16*(1), 41-51.

Bierkens, M. F. P. (1998), Modeling water table fluctuations by means of a stochastic differential equation, *Water Resour. Res.*, *34*(10), 2485-2499.

Box, G. E. P., and G. M. Jenkins (1969), *Time series analysis: forecasting and control*, Prentice Hall, Englewood Cliffs, New Jersey.

Bruggeman, G. A. (1999), *Analytical solutions of geohydrological problems*, 959 pp., Elsevier, Amsterdam.

Carr, E. J., and M. J. Simpson (2018), Accurate and efficient calculation of response times for groundwater flow, *Journal of Hydrology*, *558*, 470-481.

Carrera, J., and S. P. Neuman (1986), Estimation of Aquifer Parameters Under Transient and Steady State Conditions: 3. Application to Synthetic and Field Data, *Water Resources Research*, *22*(2), 228-242.

Collenteur, R. A., M. Bakker, R. Calje, S.Klop, and F. Schaars (2019), Untangling groundwater head series using time series analysis and Pastas, Under review, *Groundwater*.

Cooper, H. H., and M. I. Rorabaugh (1963), Ground-water movements and bank storage due to flood stages in surface streams, *Report Rep. 1536J*.

Crosbie, R. S., P. Binning, and J. D. Kalma (2005), A time series approach to inferring groundwater recharge using the water table fluctuation method, *Water Resources Research*, *41*(1).

Crosbie, R. S., L. J. M. Peeters, N. Herron, T. R. McVicar, and A. Herr (2018), Estimating groundwater recharge and its associated uncertainty: Use of regression kriging and the chloride mass balance method, *Journal of Hydrology*, *561*, 1063-1080.

Cuthbert, M. O. (2010), An improved time series approach for estimating groundwater recharge from groundwater level fluctuations, *Water Resources Research*, *46*(9).

De Bruin, H. A. R. (1987), From Penman to Makkink, paper presented at Evaporation and weather, TNO Comitee on Hydrological Research.

de Glee, G. J. (1930), On groundwater flow by water abstraction by means of deep wells, PhD thesis (in Dutch).

de Vries, J. J. (2000), Groundwater level fluctuations - the pulse of the aquifer, paper presented at Evaluation and Protection of Groundwater Resources, IAH/UNESCO, Wageningen.

Doble, R. C., and R. S. Crosbie (2017), Review: Current and emerging methods for catchment-scale modelling of recharge and evapotranspiration from shallow groundwater, *Hydrogeology Journal*, *25*(1), 3-23.

Eriksson, E., and V. Khunakasem (1969), Chloride concentration in groundwater, recharge rate and rate of deposition of chloride in the Israel Coastal Plain, *Journal of Hydrology*, *7*(2), 178-197.

Euser, T., H. C. Winsemius, M. Hrachowitz, F. Fenicia, S. Uhlenbrook, and H. H. G. Savenije (2013), A framework to assess the realism of model structures using hydrological signatures, *Hydrol. Earth Syst. Sci.*, *17*(5), 1893-1912.

Ferris, J. G., R. H. Knowles, and R. W. Stallman (1962), *Theory of Aquifer Tests, Geological Survey Water-Supply paper 1536-E*, USGS, Washington.

Freeze, A. R., and J. A. Cherry (1979), *Groundwater*, Prentice Hall, Upper Saddle River, NJ.

Gehrels, J. C., F. C. van Geer, and J. J. de Vries (1994), Decomposition ot groundwater level fluctuations using transfer modelling in an area with shallow to dee unsaturated zones, *Journal of Hydrology*, *157*, 105-138.

Gradshteyn, I. S., and I. M. Ryzhik (1965, equation 3.471-9), *Table of Integrals Series and Products*, Academic Press.
Ha, K., D.-C. Koh, B.-W. Yum, and K.-K. Lee (2007), Estimation of layered aquifer diffusivity and river resistance using flood wave response model, *Journal of Hydrology*, *337*(3–4), 284-293.
Hall, F. R., and A. F. Moench (1972), Application of the convolution equation to stream-aquifer relationships, *Water Resources Research*, *8*(2), 487-493.
Hantush, M. S., and C. E. Jacob (1955), Non-steady radial flow in an infinite leaky aquifer, *Transactions, American Geophysical Union*, *36*, 95-100.
Harbaugh, A. W., E. R. Banta, M. C. Hill, and M. G. McDonald (2000), MODFLOW-2000, the US Geological Survey modular ground-water model - User guide to modularization concepts and the Ground-Water Flow Process, edited, USGS.
Harp, D. R., and V. V. Vesselinov (2011), Identification of pumping influences in long-term water level fluctuations, *Ground Water*, *49*(3), 403-414.
Healy, R., and P. Cook (2002), Using groundwater levels to estimate recharge, *Hydrogeology Journal*, *10*(1), 91-109.
Healy, R. W. (2012), *Estimating groundwater recharge*, Cambridge University Presss, United Kingdom.
Hemker, C. J. (1999), Transient well flow in vertically heterogeneous aquifers, *Journal of Hydrology*, *225*(1–2), 1-18.
Hemker, C. J., and R. G. de Boer (1997), MicroFEM, edited, p. Finite Element Method groundwater flow simulations computer program.
Heppner, C. S., and J. R. Nimmo (2005), A Computer Program for Predicting Recharge with a Master Recession Curve, U.S. Geological Survey.
Hespanha, J. P. (2009), *Linear Systems Theory*.
Hill, M. C. (1998), Methods and guidelines for effective model calibration *Rep. Open-file Rep 98-4005*, USGS.
Hrachowitz, M., O. Fovet, L. Ruiz, T. Euser, S. Gharari, R. Nijzink, J. Freer, H. H. G. Savenije, and C. Gascuel-Odoux (2014), Process consistency in models: The importance of system signatures, expert knowledge, and process complexity, *Water Resources Research*, *50*(9), 7445-7469.
Iman, R. L., J. C. Helton, and J. E. Campbell (1981), An Approach to Sensitivity Analysis of Computer Models: Part I—Introduction, Input Variable Selection and Preliminary Variable Assessment, *Journal of Quality Technology*, *13*(3), 174-183.
Jones, E., E. Oliphant, and P. Peterson (2001), SciPy: Open Source Scientific Tools for Python, edited.
Keating, E. H., J. Doherty, J. A. Vrugt, and Q. Kang (2010), Optimization and uncertainty assessment of strongly nonlinear groundwater models with high parameter dimensionality, *Water Resour. Res.*, *46*(10), W10517.
Knight, J. H., and D. W. Rassam (2007), Groundwater head responses due to random stream stage fluctuations using basis splines, *Water Resources Research*, *43*(6).
KNMI (2018), Royal Netherlands Meteorological Institute, edited.

Koutsoyiannis, D. (2010), One decade of multi-objective calibration approaches in hydrological modelling: a review AU - Efstratiadis, Andreas, *Hydrological Sciences Journal*, *55*(1), 58-78.

Kruseman, G. P., and N. A. de Ridder (1970), *Analysis and evaluation of pumping test data*, International Institute for Land Reclamation and Improvement, Wageningen, The Netherlands.

Lebbe, L., M. Mahauden, and W. De Breuck (1992), Execution of a triple pumping test and interpretation by an inverse numerical model, *Applied hydrogeology*, *4/92*(4/92), 20-34.

Lekahena, E. G. (1983), Groundwater map of the Netherlands, edited, TNO-DGV.

Luo, K., F. Tao, J. P. Moiwo, and D. Xiao (2016), Attribution of hydrological change in Heihe River Basin to climate and land use change in the past three decades, *Scientific Reports*, *6*, 33704.

Maas, C. (1994), On convolutional processes and dispersive groundwater flow, TU Delft, Delft, The Netherlands.

Maas, C. (1995), Modeling natural fluctuations of the groundwater table by mean of the analytical element method (in Dutch), KWR Watercycle Research Institute, Nieuwegein.

Manzione, R., E. Wendland, and D. Tanikawa (2012), Stochastic simulation of time-series models combined with geostatistics to predict water-table scenarios in a Guarani Aquifer System outcrop area, Brazil, *Hydrogeology Journal*, 1-11.

Meinardi, C. R., C. G. J. Schotten, and J. J. de Vries (1998), Groundwater recharge and surtface run-off in the Netherlands (in Dutch), *Stromingen*.

Meinzer, O. E. (1923), The occurrence of ground water in the United States, with a discussion of principles, *Report Rep. 489*, 373 pp, Washington, DC.

Moench, A. F., and P. M. Barlow (2000), Aquifer response to stream-stage and recharge variations. I. Analytical step-response functions, *Journal of Hydrology*, *230*(3–4), 192-210.

Moré, J. J., B. S. Garbow, and K. E. Hillstrom (1980), User guide for MINPACK-1, Argonne National Laboratory Argonne, Illinois, USA.

Narasimhan, T. N. (1999), Boulton's Delayed Yield: A Different Context, *Ground Water*, *37*(3), 323-326.

Nash, J. E. (1957), The Form of the Instantaneous Unit Hydrograph, *International Association of Hydrological Sciences*.

Nash, J. E., and J. V. Sutcliffe (1970), River flow forecasting through conceptual models part I - A discussion of principles, *Journal of Hydrology*, *10*(3), 282-290.

Neuman, S. P. (1975), Analysis of pumping test data from anisotropic unconfined aquifers considering delayed gravity response, *Water Resour. Res.*, *11*(2), 329-342.

Nimmo, J. R., C. Horowitz, and L. Mitchell (2015), Discrete-Storm Water-Table Fluctuation Method to Estimate Episodic Recharge, *Groundwater*, *53*(2), 282-292.

Obergfell, C., M. Bakker, and K. Maas (2016), A time-series analysis framework for the flood-wave method to estimate groundwater model parameters, *Hydrogeology Journal*, *(2016) 24:1807–1819 doi: 10.1007/s10040-016-1436-5*.

Obergfell, C., M. Bakker, W. Zaadnoordijk, and K. Maas (2013), Deriving hydrogeological parameters through time series analysis of groundwater head fluctuations around well fields, *Hydrogeology Journal, Volume 21, Issue 5, pp 987–999 ,doi 10.1007/s10040-013-0973-4*.

Obergfell, C., M. Bakker, and K. Maas (2019), Estimation of Average Diffuse Aquifer Recharge Using Time Series Modeling of Groundwater Heads, Water Resources Research, 55(3), 2194-2210, doi: 10.1029/2018WR024235.

Obergfell, C., M. Bakker, and K. Maas Identification and explanation of a change in the groundwater regime using time series analysis, Groundwater, doi: 10.1111/gwat.12891.

Olsthoorn, T. N. (2008), Do a Bit More with Convolution, *Ground Water*, *46*(1), 13-22.

Peterson, T. J., and A. W. Western (2014), Nonlinear time-series modeling of unconfined groundwater head, *Water Resources Research*, *50*(10), 8330-8355.

Pinder, G. F., J. D. Bredehoeft, and H. H. Cooper, Jr. (1969), Determination of Aquifer Diffusivity from Aquifer Response to Fluctuations in River Stage, *Water Resour. Res.*, *5*(4), 850-855.

Rassam, D. W., D. Pagendam, and H. Hunter (2008), Conceptualisation and application of models for groundwater–surface water interactions and nitrate attenuation potential in riparian zones, *Environmental Modelling & Software*, *23*(7), 859-875.

Ridder, T. B., J. H. Baard, and T. A. Buishand (1984), The influence of sampling methods and analysis techniques on measured chemical concentrations in rain water (in Dutch), De Bilt, The Netherlands.

Rumbaugh, J., and D. Rumbaugh (1996), Groundwater Vistas, edited, Environmental Simulations Inc.

Scanlon, B. R., R. W. Healy, and P. G. Cook (2002), Choosing appropriate techniques for quantifying groundwater recharge, *Hydrogeology Journal*, *10*(1), 18-39.

Schoups, G., and J. A. Vrugt (2010), A formal likelihood function for parameter and predictive inference of hydrologic models with correlated, heteroscedastic, and non-Gaussian errors, *Water Resour. Res.*, *46*(10), W10531.

Schweder, T., and N. Hjort (2016), *Confidence, likelihood, probability: statistical inference with confidence*, Cambridge University Press.

Shapoori, V., T. J. Peterson, A. W. Western, and J. F. Costelloe (2015a), Top-down groundwater hydrograph time-series modeling for climate-pumping decomposition, *Hydrogeology Journal*, *23*(4), 819-836.

Shapoori, V., T. J. Peterson, A. W. Western, and J. F. Costelloe (2015b), Estimating aquifer properties using groundwater hydrograph modelling, *Hydrological Processes*.

Shapoori, V., T. J. Peterson, A. W. Western, and J. F. Costelloe (2015c), Decomposing groundwater head variations into meteorological and pumping components: a synthetic study, *Hydrogeology Journal*, 1-18.

Simmers, I. (1988), *Estimation of Natural Groundwater Recharge*.

Stehfest, H. (1970), Algorithm 368: Numerical inversion of Laplace transforms [D5], *Commun. ACM*, *13*(1), 47-49.

Stoll, S., H. J. Hendricks Franssen, R. Barthel, and W. Kinzelbach (2011), What can we learn from long-term groundwater data to improve climate change impact studies?, *Hydrol. Earth Syst. Sci.*, *15*(12), 3861-3875.

Strack, O. D. L. (1989), *Groundwater Mechanics*, Prentice-Hall.

van Geer, F. C., and A. F. Zuur (1997), An extension of Box-Jenkins transfer/noise models for spatial interpolation of groundwater head series, *Journal of Hydrology*, *192*(1–4), 65-80.

Van Geer, F. C., P. K. Baggelaar, and P. R. Defize (1988), Application of time series analysis to observation records of hydraulic head (in Dutch), *H2O*, *21*, 438-442.

Veling, E. J. M., and C. Maas (2010), Hantush Well Function revisited, *Journal of Hydrology*, *393*(3–4), 381-388.

Venetis, C. (1970), Finite aquifers: Characteristic responses and applications, *Journal of Hydrology*, *12*(1), 53-62.

Von Asmuth, J. R., and M. F. P. Bierkens (2005), Modeling irregularly spaced residual series as a continuous stochastic process, *Water Resour. Res.*, *41*(12), W12404.

Von Asmuth, J. R., K. Maas, and M. F. P. Bierkens (2002), Transfer function-noise modeling in continuous time using predefined impulse response functions, *Water Resour. Res.*, *38*(12), 1287.

Von Asmuth, J. R., K. Maas, M. Bakker, and J. Petersen (2008), Modeling Time Series of Ground Water Head Fluctuations Subjected to Multiple Stresses, *Ground Water*, *46*(1), 30-40.

von Asmuth, J. R., K. Maas, M. Knotters, M. F. P. Bierkens, M. Bakker, T. N. Olsthoorn, D. G. Cirkel, I. Leunk, F. Schaars, and D. C. von Asmuth (2012), Software for hydrogeologic time series analysis, interfacing data with physical insight, *Environmental Modelling & Software*, *38*(0), 178-190.

Vrugt, J. A., and W. Bouten (2002), Validity of First-Order Approximations to Describe Parameter Uncertainty in Soil Hydrologic Models, *Soil Sci. Soc. Am. J.*, *66*(6), 1740-1751.

Vrugt, J. A., H. V. Gupta, W. Bouten, and S. Sorooshian (2003), A Shuffled Complex Evolution Metropolis algorithm for optimization and uncertainty assessment of hydrologic model parameters, *Water Resour. Res.*, *39*(8), 1201.

Wada, Y., M. F. P. Bierkens, A. de Roo, P. A. Dirmeyer, J. S. Famiglietti, N. Hanasaki, M. Konar, J. Liu, H. Müller Schmied, T. Oki, Y. Pokhrel, M. Sivapalan, T. J.

Troy, A. I. J. M. van Dijk, T. van Emmerik, M. H. J. Van Huijgevoort, H. A. J. Van Lanen, C. J. Vörösmarty, N. Wanders, and H. Wheater (2017), Human–water interface in hydrological modelling: current status and future directions, *Hydrol. Earth Syst. Sci.*, *21*(8), 4169-4193.

Weider, K., and D. F. Boutt (2010), Heterogeneous water table response to climate revealed by 60 years of ground water data, *Geophysical Research Letters*, *37*(24).

Weisstein, E. W. (2018a), Central Moment, edited, Mathworld.

Weisstein, E. W. (2018b), Gamma Distribution, edited, Wolfram Web Resource.

Witte, J.-P. M., I. Leunk, D. G. Cirkel, H. F. M. Aarts, and W. Zaadnoordijk (2015), Background groundwater level decrease and groundwater reacharge in North Brabant (in Dutch), *Stromingen*, *24*.

Yuen, K. V. (2010), *Bayesian Methods for Structural Dynamics and Civil Engineering*, John Wiley & Sons (Asia) Pte Ltd, John Wiley & Sons (Asia) Pte Ltd, 2 Clementi Loop, # 02-01,Singapore 129809.

List of publications

Obergfell, C., M. Bakker, and K. Maas Identification and explanation of a change in the groundwater regime using time series analysis, Groundwater, https://doi.org/10.1111/gwat.12891, 2019.

Obergfell, C., M. Bakker, and K. Maas, Estimation of Average Diffuse Aquifer Recharge Using Time Series Modeling of Groundwater Heads, Water Resources Research, 55(3), 2194-2210, https://doi.org/10.1029/2018WR024235, 2019.

Obergfell, C., M. Bakker, and K. Maas, A time-series analysis framework for the flood-wave method to estimate groundwater model parameters, Hydrogeology Journal, 24:1807–1819, https://doi.org/10.1007/s10040-016-1436-5, 2016.

Obergfell, C., M. Bakker, W.J. Zaadnoordijk, and K. Maas, Deriving hydrogeological parameters through time series analysis of groundwater head fluctuations around well fields, Hydrogeology Journal, Volume 21, Issue 5, pp 987–999, https://doi.org/10.1007/s10040-013-0973-4, 2013.

Brad, T., C. Obergfell, B. M. van Breukelen, N. M. van Straalen, and W. F. M. Röling, Spatiotemporal Variations in Microbial Communities in a Landfill Leachate Plume, Groundwater Monitoring & Remediation, 33(4), 69-78. https://doi.org/10.1111/gwmr.12022, 2013.

Acknowledgements

Doing this thesis has been made possible in first instance thanks to my supervisors: my promotor Mark Bakker and Kees Maas.
Mark, the sharpness of your discernments is always impressive, leaving no room for inconsistency. The clarity of your explanations, which from a didactical point of view is exemplary, brought me a lot. I especially enjoyed our work sessions in the café 'Winkel van Sinkel' in Utrecht, together with Kees, rigorous in a relaxed atmosphere. I hope that other opportunities will arise to learn from you in this way!
Kees, what a privilege was it that you continued supervising this research after your official retirement. Your optimism and creativity are exemplary! And of course, I will always remember the occasions when I could join you for an excellent diner, carefully prepared by Adrie, your wife, (thanks Adrie!), forgetting hydrology for a while to talk about history or the music of Bach and Sweelinck!
Universities are extremely stimulating environments, and the years spent doing this thesis offered occasions of inspiring talks at the TU Delft, of course most often around the coffee machine. Conversations with Huub Savenije over any kind of subject in hydrology were inspiring and thought provoking, in particular when invited to take the perspective of the 'giant' instead of that of the 'ant' when considering a hydrological system! Conversations with Theo Olsthoorn were always an occasion to get a valuable tip on groundwater modeling to ponder over the time of the travel back home. And there were all these good talks, stimulating and full of humor with Miriam Coenders, Martijn Westhof, Ruud van der Ent, Gerrit Schoups, Steven Wijs, Koen Hilgersom, Maurits Ertsen, Raoul Collenteur, Joanne van der Spek, Bas Des Tombes, Wim Luxemburg, Thom Bogaard and Rolf Hut. I also remember running to the train station with our department mathematician Ed Velling, who would suddenly stop to watch a rare bird on the top of a chimney with his binoculars, and finally miss the train...
Universities would not function without recurring interventions of secretaries such as Lydia de Hoog and Betty Rothfusz to save students from administrative emergency situations. So many thanks Lydia and Betty!
A lot of thanks also to Flip Witte and Pieter Stuyfzand for their expert comments on the subject of ecohydrology and hydrochemistry, which were insightful for Chapters 4 and 5.
Thanks to Jos von Asmuth, whose publication might be the most cited in this thesis and for tipping me about this research project!
The coffee machine at KWR was another gathering point for good talks with Luit-Jan Sloten, Willem Jan Zaadnoordijk, Ruud Bartholomeus, Gijsberg Cirkel, Yuki Fujima, Diego Bustos Medina, Ruud Bartholomeus, Femke Rambaard, Andreas Antoniou, Kees van Beek, Arnout van Loon, and of course Jan Willem Kooiman.
I am grateful to my family in France. I am lucky to have grown up in a nice home with dear and dedicated parents and nice sisters Véronique and Nathalie (in seniority order). It is so nice to be able to visit you, gathering around an almost unreasonably generous table, together with Alain, Pierrick and Lauranne!

Bart, I discovered a spider web on the frame of my race bike, how is that possible? I hope to find time soon to join you again for a bicycle trip in the Alps! Dirk, the last time we met at café ‘t Smalle in Amsterdam was to talk about your thesis on the history of former mayor of Amsterdam and resistant Gijs van Hall. Next time we will talk about this thesis, quite a different subject!
Finally, I want to thank Katrien my wife. Katrien, you always encouraged me during these thesis years. In particular, the walks along the Kromme-Rijn river near Utrecht have been regenerative. It’s amazing how one of your smiles can make a day a perfect day!

About the author

Christophe Obergfell was born in Strasbourg (France) in 1969 and resides in the Netherlands since 1993. His initial interest for groundwater arose from pollution remediation engineering which motivated his choice for biological and chemical process studies in Strasbourg and Nancy (France). In 1992, Christophe got the opportunity to follow a traineeship in the Netherlands at TNO (Netherlands Organisation for Applied Scientific Research). The Netherlands was at that time renowned for its ambitious soil and groundwater remediation program. Feeling home in the Netherlands, Christophe moved to Utrecht in 1993, and worked 7 years for the Dutch contractor Mourik, at that time one of the leading actors in the soil and groundwater clean-up program. In 2000, Christophe started a new bachelor and master study in hydrology, at the VU university in Amsterdam, combined with freelance groundwater modeling studies. Christophe took the liberty to study things as 'minors' that had nothing to do with hydrology but were just so intriguing, such as quantum physics, statistical mechanics and thermodynamics, and the historical foundations of these disciplines, at the University of Utrecht.In 2009, Christophe started the research project on time series analysis of groundwater level presented in this thesis. From 2014 to 2016, Christophe worked for the Dutch dewatering contractor to experience how hydrogeological works are operated. From 2016 on, Christophe is employed as consultant for Stantec Consultancy. As a groundwater hydrologist, Christophe is particularly interested in understanding the physical meaning of groundwater levels fluctuations and in groundwater flow modeling.